# *Electromagnetic and weak interactions in light exotic nuclei*

**Leonid Grigorenko**

**November XX, 1997**



**Department of Physics**
**Chalmers University of Technology**
**and Göteborg University**
**S-41296, Göteborg, Sweden**

**e-mail: f2blg@vms.fy.chalmers.se**

**ISBN 91-7197-553-5**
**Reproservice, Chalmers Bibliotek**
**Göteborg, 1997**

***Dedicated***
***to my friends –***
***present and lost . . .***

# Abstract

The interest in so-called halo nuclei is a fresh wind in the nuclear physics connected with intensive development of the radioactive nuclear beam technics in the last decade. The discovery of the halo property in some light neutron drip line nuclei was rather unexpected in the sense of the nuclear force saturation concept (formula $r \sim A^{1/3}$). Those nuclei appeared to be a kind of "planetary system" with compact core and 1–4 valence nucleons moving far apart. Generally accepted in the nuclear physics models (Mean Field, Shell model, RPA), treating all the nucleons on the same ground, were unable to predict this phenomenon. Halo properties of the nuclei can be described adequately only in approaches where clusterization is introduced "by hands" (RGM, GCM, Semimicroscopic cluster models ...). It is not exactly clear, why the equivalent treatment for all nucleons is washing out the halo behavior in the calculations, while it is clearly indicated by experiment.

The thesis is based on the series of articles devoted to theoretical investigation of the electromagnetic and weak processes in the light halo nuclei. The purposes of the investigation is: *i*) To develop or/and to improve the few-cluster approaches to the light nuclei A=6-11; *ii*) To find the "area of validity" for these approaches via comprehensive comparison with experiment; *iii*) To extract new material from the experimental data; *iv*) To suggest new experiments, clarifying the aspects of nuclear dynamic, which are questionable nowadays. The special attention is paid to the processes involving continuum of the few-cluster systems. The following reactions were studied:

$^{6}\mathrm{He} \xrightarrow{\beta} \alpha + \mathrm{d}$

$^{6}\mathrm{Li}(0^{+}, T{=}1) \xrightarrow{PV} \alpha{+}\mathrm{d}$ ; $^{6}\mathrm{Li}(0^{+},1) \xrightarrow{\gamma(M1)} {}^{6}\mathrm{Li}(1^{+})$ ; $^{6}\mathrm{Li}(0^{+},1) \xrightarrow{\gamma(M1)} \alpha{+}\mathrm{d}$

$^{8}\mathrm{He} \xrightarrow{\beta} {}^{8}\mathrm{Li}(1^{+})$ ; $^{8}\mathrm{He} \xrightarrow{\beta} {}^{7}\mathrm{Li} + \mathrm{n}$ ; $^{8}\mathrm{He} \xrightarrow{\beta} \alpha{+}\mathrm{T}{+}\mathrm{n}$ ; $^{8}\mathrm{He} \xrightarrow{\beta} {}^{6}\mathrm{Li}{+}\mathrm{n}{+}\mathrm{n}$

$^{9}\mathrm{Li} \xrightarrow{\beta} {}^{8}\mathrm{Be} + \mathrm{n}$ ; $^{9}\mathrm{Li} \xrightarrow{\beta} \alpha + \alpha + \mathrm{n}$

$^{11}\mathrm{Li} \xrightarrow{\beta} {}^{9}\mathrm{Li} + \mathrm{d}$

These studies include semimicroscopic theoretical calculations, estimates using different simplified models and analysis of the experimental data.

# List of publications

[P1] M.V. Zhukov, B.V. Danilin, L.V. Grigorenko and N.B. Shul'gina, "$^6$He $\beta$-decay to the $\alpha$+d channel in a three-body model", Phys. Rev. **C47** (1993) 2937-2940

[P2] L.V. Grigorenko and N.B. Shul'gina, "Parity violating $^6$Li $(0^+1)\rightarrow$ $\alpha$ + d and $^6$Li $(0^+1)\rightarrow$ $\alpha$ + d + $\gamma$ M1 transition", preprint NORDITA - 95/62 N, NBI, 1995.

[P3] M.V. Zhukov, B.V. Danilin, L.V. Grigorenko and J.S. Vaagen, "$\beta$-decay of $^{11}$Li to the deuteron channel and halo analog states in $^{11}$Be", Phys. Rev. **C52** (1995) 2461-2467

[P4] L.V. Grigorenko, N.B. Shul'gina and M.V. Zhukov, "Theoretical studies of $^8$He $\beta$-decay," Nucl.Phys. **A607** (1996) 277-298, erratum Nucl. Phys. **A614** (1997) 567

[P5] M.J.G. Borge et al., "Probing the $^{11}$Li halo structure through $\beta$-decay into the $^{11}$Be$^*$(18 MeV) state", Nucl. Phys. **A613** (1997) 199-208

[P6] N.B. Shul'gina, L.V. Grigorenko, M.V. Zhukov and J.M. Bang, "$^8$He $\beta$-decay to the $^6$Li+n+n channel", Nucl. Phys. **A619** (1997) 143-150.

[P7] L.V. Grigorenko, B.V. Danilin, V.D. Efros, N.B. Shul'gina and M.V. Zhukov, "Discrete spectrum states of the three-body nonborromean nuclei: $^6$Li and $^8$B", preprint CTHSP - 97/11, CTH, 1997.

[P8] L.V. Grigorenko, I.G. Mukha and M.V. Zhukov, "Beta-delayed multi-particle emission: alternative few-body approach", in preparation

# Contents

# Chapter 1

# Introduction

*Each article should contain the answer*
*to the question "what was the reason?"...*
*For this article itself, of course.*

*D.P. Grechukhin*

If we look at the ideas, mainly the following questions are addressed in the thesis: if our theoretical models are adequate for description of structure and reactions of the halo nuclei (if not, what improvement is required), if the experimental information about halo nuclei is sufficient for understanding of the phenomenon (if not, which extra data are desirable to have). If we turn to the structure of the document, it is governed by two facts: Ph. D. thesis is rarely read by anybody except those, who have to read it; Ph. D. thesis is often useful to the author if he continue to work in a similar field. So, in the order of growing importance, this thesis contains a few general discussions, explanations and annotations for the appended articles and vast material concerning the routine work, including the thesaurus of useful formulae in the Appendixes.

The work is divided in five parts, rather distinct in their meaning and volume:

1. The current understanding of science in general and our very special field in particular, is the subject of the **Introduction**. The first two sections contain some general speculations, which are relevant, probably, only to my personality, but which I-in-today would like to keep for me-in-tomorrow. The last section briefly discuss the motivation for the performed studies.

2. The routine calculations are collected in the second chapter **Calculations and Formulae**. I tried to make this chapter useful. It means that one can find a lot of redundant material there; on the other hand it is possible to follow calculations "by eye" and reuse expressions without any "preprocessing" .

3. Material clarifying the "dark places" of the articles and things which are too "trivial" for the refereed literature can be found in the chapter **Physical Processes**.

4. The last chapter contains formulation of **Achievements and Problems** our collaboration and I faced during the studies. Published articles are not considered to belong to the achievements; listed problems are "alive" problems, which are waiting to be resolved. Some of them, I hope, would become a subject for further investigation, both theoretical and experimental.

5. A lot of formulae I found useful during the work are placed in **Appendixes.** Some of them are "standard" or "generally known". But it was important to me to present them in order to keep the uniformity of notations and trace all the derivations. Special cases and redundant variations of formulae are given to decrease the access time and probability of mistakes.

The following Quantum Mechanics and Nuclear science textbooks [48, 37, 25, 30, 72, 73, 22], monographs [74, 67, 79, 57, 20, 28, 104, 99, 27, 54, 65] and mathematical handbooks [1, 64] were useful in the course of the work . The material from these books is used further without references. Publications in which I collaborated are located in the **Publication List**, page vi, and are referred in the text like [P1-8]. Two of them [P2,P7] are not true publications but a preprints. Paper [P5] is not appended to the thesis. It is an experimental article, where I played a minor role in interpretation of the data. Contents of the paper [P7] (binary cluster correlations in the three-body discrete spectrum calculations), though in the main stream of our activities, are falling too apart from the framework of the thesis. They are only briefly touched in the Chapter 4 in the most general words. Paper [P8] is in the course of preparation. Its contents are partly given in the Section 3.6. The purpose of reference in the Publication List is to indicate participants of this work.

The "natural" system of units $\hbar = c = 1$ is used in the thesis.

## 1.1 General (science)

*You can imagine the history of civilization,*
*connected with new technological advances,*
*as a walk through a river during spring flood*
*jumping from one peace of ice to the other.*
*The jumper can be very skillful, but you are never*
*sure, that there is any next peace of ice at all ...*

*S. Lem*

An interesting point of view on the history of science was given more then 150 years ago by Schlosser in his multivolume world's history. At this time the basement of the modern science have already been build, but the fantastic technological prospects of the development of science were far in the future. According to Schlosser the following stages were characteristic to the development of science. First it appear as a sincere movement of the minds and an integral part of the cultural media of the civilization. Then it become too refined, hence esoteric and hence remote from the cultural background, which gave birth to it and was feeding it for some time. After it, the science in this socium disappears in the first serious cataclysm leaving a lot of fragments, often hardly understandable to the future generations.

I think you agree that the modern natural science is too refined and in some aspects really esoteric, requiring many years of patient studies for adepts. Theory of Relativity and Quantum Mechanics imply high knowledge of mathematics for understanding of the philosophical concepts of modern natural science. Methodology of science is highly "inhuman" – nobody can follow the Cartesian "methodological doubt" in his everyday life. People are tired of science and scientists. Science is only multiplying questions, even to understand which you need definite qualification. People need not questions, but answers. The dropdown of people's religiousness is connected not with dying of mythological character of thinking (ready answers), but with predominance of hedonistic concepts over the concepts of destiny and human obligation.

You may tell about it, that the modern civilization is a very special case. May be, it have very little in common with former civilizations and the laws, which governed their development. Nowadays the science is too integrated in the material production and it is a serious reason why the gap between the science and the culture would not become too wide. Such argumentation would be all right if the intellectual reasons were guiding the evolution of the human communities. We do not have a good idea about reasons which are giving birth and giving death to the civilizations, but we can definitely conclude that the benefit of people is not among those reasons. The modern form of the social organization with extremely developed science and technology is very young in the time scale of the civilizations. It is difficult to make any long-range predictions about its stability

in comparison with the civilizations of the past. The horrifying crises in its short history, from some points of view, seem to be overcame more by chance then because of the internal positive and self-stabilizing properties of this new form of organization of the human society. The total, world wide nature of the modern civilization is making any instability very potentially harmful to the humanity in general. In many aspects, the belligerent spreading of the western-type civilization, have a character of simplification of human communities. It is certainly easier to leave in universal simplified social environment. The historical experience and physical intuition tell us that for complicated system simplification is the beginning of the end.

The modern physics appeared in the fantastic synthesis of the first quarter of our century, when it was demonstrated that a widest range of phenomenon, from the structure of the atomic nucleus to the evolution of the universe, can be understood on the same ground. It made most of people to believe that the power of physical science is unlimited and now the nature would be to open the doors to unknown one by one. In reality, after the period of synthesis, when it seem that the new concepts appear as if themselves, without enormous effort, the period of collecting facts and improving technics have came, when a tremendous amount of work is done only to make a minor improvement or clarify some phenomenon, understandable to a few experts in this particular field.

Somehow deeply in their hearts people believed that as far as physics have given freedom to the technological monster, it would answer the question how to deal with it. No, it would not. The physics have provided a new philosophical basement for understanding of the world. But it have done nothing to specify the human's place in this new world. The ability of human society to adopt to the new conditions of the technological environment are often considered questionable. And the fact that the physical science, providing technological base, do not provide ethical solution for the subsequent problems, have caused a kind of disappointment in physics. The new panacea for future troubles people now see in biology, especially the branch of this science dealing with brain and mind. I can scarcely evaluate correctly the prospects for these expectations. The place I expect the most interesting discoveries is the application of methodology (not methods, as it is often done now in biophysics [1]) of "exact" sciences to biological systems. My assurance in existence of the mathematical methods (I do not mean they do exist [2]) suitable to analysis of such system is based on the extreme com-

[1] The success of the modern physics was connected with indeterministic understanding of the nature and application of the methods, which are statistical or are closely connected with the concept of probability. The application of such methods in biology is good only to the analysis of processes close to equilibrium. And the most metaphysical concepts, like "orthogenesis" of Teyar De Sharden — the tendency of the biological system to become more complicated, are often more useful for understanding of life processes, than complicated "exact science-like" calculations modeling some "aspects" of life on the computer, using the framework which was so productive in physics.

[2] I mean that such methods, may be, it would be possible to construct using common methodology of mathematics, introducing the semantical scheme and axiomatic rules for op-

plexity of the biosystems on one hand and on extreme stability of, for example, the processing mechanism of the neural systems or the growth development of organism in ontogenesis, on the other hand. To my opinion it means that the principal laws of such processes does exist and that these laws are rather simple.

In some cases science (certainly aiming the best purposes) is becoming responsible for creation of the new, may be dangerous myths. One of them is a myth about Artificial Intelligence, used as a banner for a branch of the computer science. Human intelligence, in its general meaning, is not so much operation with semantic information, but motivation, what should be done with this information. This "What" is defined by so tiny and unclear biological differences [3], that it is not clear how people can seriously discuss modelling this properties of intelligence [4].

The following few items present the problems discussed above in a brief manner:

- The physics have achieved the "saturation" in the sense of generating new concepts. The new period of synthesis will come when the experimental information will become unexplainable in the terms of existing theories. The last 50 years have not brought such information, probably it would not come soon.

- The technological opportunities supplied by the current development of science are very far from such "saturation". Sometimes it makes feeling that fundamental science is standing, while applied is moving forward.

- It is recognized and sad fact that evolution of relations between people and relations between peoples is much slower (if any at all) then the technical development and subsequent evolution of relations between people and surrounding world. Ethical aspect of the development of science was and is very worrying and unclear.

- The science does not supply any critical understanding of the humanity development perspectives.

- Does not exist any understanding of the processing mechanisms used by neural systems.

The last two items are, to my opinion, closely connected with each other, though sounds very different. And it is related to the eternal problem of the natural science. The problem is that mathematics (semantics of mathematics)

---

eration with concepts. It does not mean that such "mathematics" would have very much in common with the existing one.

[3] Which distinguish textithomo sapience from other animals.

[4] Without having a clear idea what it is.

have demonstrated a mysterious connection with "the nature of the things" [5]. We do know how to use this connection, but its origin is unclear. The belief that the numbers are connected with the real world in a mysterious way is characteristic already to Pifagoreans and then Neoplatonics around two thousand years ago. This belief did not die even in the times of Kepler. And it had really but indirectly recovered in Kobenhavn's interpretation of Quantum Mechanics by Bohr and "positive" understanding of physics of Heizenberg.

It is very possible that our situation in science is similar to that of Neoplatonics. Their mystic science was operating with concepts available for relations concerning integer numbers and geometrical figures (the *Trousers of Pifagor*, the greatest achievement of ancient science). The domain of modern science are the concepts available for functional analysis and group theory (general relativity or Young-Mills like theories supply an example of multidimensional, even multispace Pifagor's Trousers). Everything which is out of this field is probably not only out of our understanding, but is not even understood as being out of our understanding. Today this range of phenomenon simply does not exist.

## 1.2 Particular (nuclear science)

For many years the serious part of the nuclear science was flowering on the marginal wastes of the military offices. The limitation of the arms race after the disintegration of the Soviet Union and the decay of the Soviet Union scientific media were most harmful for the nuclear science. The use of the nuclear science development is not so evident as, say, from the development of the solid state physics. In the sense of purely fundamental investigations the subject of the nuclear science is not so winning as a subject of particle science (at least to amateurs). In the eyes of common people "nuclear scientist" is ordinary associated with "gunsmith".

In my opinion the nuclear science is a wonderful alloy of two opposite things. One is opportunity and necessity to apply a wide variety of the theoretical methods. The other is impossibility to apply them in an arbitrary way, strong limitations for groundless "theoretical dreams" connected with the deep investigations of the former times and serious amounts of experimental material you can not contradict. Existence of the serious problems, concerning just the basement of the nuclear science, still unresolved after many years of investigations, tells us that principal discoveries are possible in this field (it is a pity we do not know

[5] If you remember the history of science, its development was mainly inductive, always encouraged by the new experimental facts. But sometimes it was making a "deductive jumps", introducing in purely mathematical form generalizing concepts meaningless to human "common sense". Wonderful examples of such concepts are extremal action principle and Schrödinger equation. The philosophy of science have had a lot of troubles trying to explain those concepts in the terms of the ordinary human language. Such explanations would be rather interesting to one, well acquainted with mathematics and physics, but unfortunately practically useless to amateur.

tomorrow or in 50 years). This aspect is not the last if you wish to follow the fine path, where the routine application of the well-known principles to the routine problems once is transforming to understanding of some fragment of the real world.

Syndrome of Chernobil' and irresponsible behavior of the "green" movement are a serious threat also to the nuclear energetics. For today, the nuclear energetics is the only realistic[6] alternative to the use of the organic fuel. The "green" organizations are carefully keeping silence about the fact that organic fuel is ordinary more ecologically dirty then nuclear fuel and that the transmission of the huge volumes of complicated organic in the heat is irreversible robbery of the future generations.

## 1.3 Very special: electroweak interaction in light exotic (halo) nuclei

As always in the nuclear science electromagnetic and weak interaction can be used in two ways: to clarify the nuclear structure if the interaction is well-known and reliably theoretically estimated or to extract some knowledge about the exotic aspects of interaction if the nuclear structure can be reliably obtained by the calculations

**What is halo nuclei?** It was shown in the series of genuine experiments that properties of some light neutron rich nuclei can be understood supposing "planetary system"-like structure with compact "core" and 1–4 "valence" nucleons moving far apart (see current reviews [106, 66, 90]). The evidence for it was provided by the following experiments:

1. The interaction radii measurements for the nuclei like $^{6}$He, $^{8}$He, $^{9}$Li, $^{11}$Li, $^{11}$Be, $^{12}$Be (see [91] and summary in [90]). Those radii were found abnormally large.

2. Interaction cross sections and particle removal cross sections for halo nuclei. It was shown that these cross-sections can be presented as a sum (see, for example, [68])

$$\sigma(interaction) = \sigma_{core}(interaction) + \sigma_{valence}(removal)$$

which can be interpreted like follows: the probability of valence nucleons to be inside core is very low, so, processes involving valence and core nucleons are practically not coherent.

[6] Realistic here means working today, not in some quite unclear perspective. Alternative energy sourses are actively developed, but in current technological and economical conditions they can not be more than auxiliary, like for the countryside.

3. Coulomb dissociation cross sections for halo nuclei (especially for $^{11}$Li) are much higher (like an order of magnitude), than it could be expected from systematics.

4. Quadrupole moment measurements for $^{9}$Li and $^{11}$Li have close values. It means that the difference between there interaction cross-sections can not be explained by large deformation of $^{11}$Li.

**What is new?** For many years the approach treating nucleus very much as peace of "nuclear matter" was known to be valid in the wide areas of the "stability valley", where formula $r \sim A^{1/3}$ is working well. The discovery of the halo structures was unexpected because they do not manifest itself in such widely used models the nuclear structure calculations such as shell-model of Hartrey-Fock method. Until now the halo nuclei properties are well obtained in the models where the clusterization is introduced more or less "by hands", like in different versions of RGM or only "by hands" like for example in different three-body approaches applied to nuclei heavier then A=3.

**What is interesting?** Why did these few nuclei caused such a great interest?

1. Reactions with halo nuclei important for the astrophysical applications. Though of decades of active studies the understanding of nucleosynthesis processes is limited with "bottleneck" in the nuclear sector of the problem.

2. Fundamental interactions: sometimes halo nuclei allows accurate theoretical treatment making it a perspective tool for investigations of the fundamental interactions.

3. The valence nucleons in the halo nuclei are loosely bound and hence are forming the "nuclear matter" with extremely low density. The investigation of halos may shed a light on the off-shell behavior of the nucleons in such conditions.

4. Excess of "exotics" (you can always find what you need) make the radioactive beams perspective instrument for technical and medical applications.

**Why electroweak processes?** Nuclear reactions is the main source of information about nuclei. You have a widest choice of projectiles, targets and conditions of experiment, defining the reaction mechanism. In the observable future there is no opportunity to investigate the radioactive nuclei with electron beams. So, we have in our disposal very few electroweak processes, generously supplied by nature. However, this processes give a unique opportunity of "direct access" to the wave function (WF), not distorted by guesses about reaction mechanism and necessity to use the models having limited reliability and applicability for the analysis.

**What is interesting in the continuum?** Together with bound states the eigenstates of the nuclear Hamiltonian in the continuum form a complete set of functions. Hence the quantities lacking in the discrete spectrum should be found in the continuum. That is the idea of the sum rule approaches, which allow to cross-check the consistency of measurements for many observables.

Exact microscopic methods to deal with continuum of more then binary systems are:

1. Faddeev equations (two-body and three-body continuum of the three-body system).
2. Hyperspherical Harmonics method (three-body continuum of the three-body system).
3. Different forms of RGM (2-continuum of nuclei up till A=12).

Continuum studies are more complicated than studies of the discrete spectrum and for that reason are dominated with approaches which are not exact. The main are

1. Potential models (Optical models, DWBA,...), which implies *existence* of potential between scattered subsystems.
2. Parametrization using properties of the Green's function (R-matrix approach)
3. Discretezation of continuum (Shell-model, RPA,...). It is suggested that incorrect boundary conditions would, nevertheless, allow the system to preserve important aspects of internal dynamic.

All the listed flavours of the approximate continuum treatment were used to some extent in the course of my work, as well as exact three-body calculations, if we need that.

**Why we like Hyperspherical Harmonics?** Hyperspherical Harmonic (HH) method is a native domain of our collaboration. Using methods and computer codes developed by M.V. Zhukov, V.D. Efros, B.V. Danilin, L.V. Chulkov, A.A. Korsheninnikov and I.J. Thompson it was possible to perform bound state studies of $^{4}$He [55], $^{6}$He, $^{6}$Li [106] $^{8}$Li [88], $^{8}$B [P7], $^{11}$Li [106], $^{12}$Be, $^{14}$Be [93], $^{17}$Ne [108] and three-body continuum studies of $^{5}$He [55] (two-body continuum), $^{6}$He, $^{6}$Li, $^{6}$Be [47, 45], $^{8}$Li [P6], $^{10}$He [69]. Huge calculations supply precise nuclear structure information. However, utilizing the hidden symmetry of the few-body nuclear Hamiltonian (see Appendix 7), the method also allows to pick up the essential dynamics of a system using very few terms (say, one) of the hyperspherical expansion. The HH method equations are taken in the form, which automatically incorporate the correct asymptotical behavior of the WF at large

distances [78]. These two properties are very helpful for estimates and stimulate analytics in favor of numerics (like in [107]).

The HH method is very suitable for application in "democratic" (or "Borromean") systems – systems with no bound binary subsystems (see review paper [106]). The examples of such systems are $^{6}$He, $^{11}$Li, $^{14}$Be, $^{17}$Ne. If there is a bound subsystem, then the asymptotics of the HH method WF is incorrect in some region of space. To deal with the problem, the special method, called Interpolation Approach was developed [103, 105, 55] and implemented [55, 98]. The idea of the method is that the binary WF is subtracted from the total WF with some variational coefficient and the resulting WF have predominantly three-body asymptotics (hence it is easily expandable over HH basis). New implementation of the method was done in [P7] for the discrete spectrum states of the nonborromean systems ($^{6}$Li, $^{8}$Li, $^{8}$B), where the two-body threshold is situated lower than a three-body one.

Extension of the three-body HH method to the binary continuum is the main prospect for my future work.

# Chapter 2

# Calculations and Formulae

*Science does not consist of formulae.*
*Science does consist of statements.*

*D.P. Grechukhin*

This chapter practically completely consists of formulae. The idea was to create as extended and easy-to-use handbook material as possible. The sad experience I have is that some of the calculations are done several times, because previous attempts are either lost or were not detailed enough to be understood afterwards. I tried to make most of the calculations so detailed, that it is possible to follow them "by eye", without papers. Though general definitions are given in the Appendixes, somewhere I am giving them once more in the text. I hope none of the values or expressions are undefined in the work as "generally known".

## 2.1 Wave functions

### 2.1.1 HH method wave function; discrete spectrum

The three-body discrete spectrum WF in (LS) coupling are constructed as

$$\Psi^{JM}_{TT_3} = \rho^{-5/2} \sum_{Kl_xl_y} \chi_{Kl_xl_y}(\rho)\ \mathcal{J}^{JM}_{Kl_xl_y}(\Omega\rho)\ \Phi_{TT_3}$$

$$\Psi^{JM}_{TT_3} = \rho^{-5/2} \sum_{KLSl_xl_y} \chi_{KLSl_xl_y}(\rho)\ \mathcal{L}^{JM}_{KLSl_xl_y}(\Omega\rho)\ \Phi_{TT_3}$$

for the case of spinless particles and particles with spin, respectively. Functions $\mathcal{L}$ and $\mathcal{J}$ are defined in (7.1). The normalization conditions for the functions

$\Psi^{JM}_{TT_3}$ are:

$$\int d\Omega_x\, d\Omega_y \int_0^\infty d\rho\ \rho^5 \int_0^{\pi/2} \sin^2\theta\, \cos^2\theta\, d\theta\ \left(\Psi^{J'M'}_{T'T'_3}\right)^+ \Psi^{JM}_{TT_3} = \delta^{MM'}_{JJ'}\,\delta^{T_3T'_3}_{TT'}$$

### 2.1.2 Two-body continuum WF

The problems constructing the continuum WFs are the following. In the "open space" we have a state vector with definite momentum:

$$|\mathbf{k}\rangle = \frac{\exp\{i\mathbf{kr}\}}{\sqrt{V}} = \frac{4\pi}{\sqrt{V}} \sum_{lm} i^l\, j_l(kr)\ Y_{lm}(\hat{r}) Y^*_{lm}(\hat{k})$$

Around the point, where particles are meeting, the basis with definite angular momentum is more natural:

$$|lm\rangle = j_l(kr) Y_{lm}(\hat{r})$$

To make scattering calculations[1] we need decomposition coefficients $\langle lm|\,|\mathbf{k}\rangle$ for plane wave over functions with definite angular momentum. For spinless not interacting particles it is trivial:

$$|\mathbf{k}\rangle = \sum_{lm} |lm\rangle\,\langle lm|\,|\mathbf{k}\rangle \quad \Rightarrow \quad \langle lm|\,|\mathbf{k}\rangle = \frac{4\pi}{\sqrt{V}}\, i^l\, Y^*_{lm}(\hat{k})$$

If an interaction is introduced, then function $j_l(kr)$ should be replaced with the solution of the two-body Schrödinger equation $F_l(kr)$ :

$$|\mathbf{k}\rangle = \frac{1}{k}\sum_{lm} \Psi_{lm}(E;\mathbf{r})\,\langle lm|\,|\mathbf{k}\rangle = \sum_{lm} F_l(kr) Y_{lm}(\hat{r}) \cdot \frac{4\pi}{\sqrt{V}}\, i^l\, Y^*_{lm}(\hat{k})$$

The normalization condition for function $F_l(kr)$ is

$$F_l(kr) \overset{kr\to\infty}{\to} \frac{\sin(kr + \delta_l + l\pi/4)}{kr}$$

Note that function

$$\Psi_{lm}(E;\mathbf{r}) = k\, F_l(kr) Y_{lm}(\hat{r})$$

has the same formal structure as discrete spectrum WF.

Now we make very formal calculations, showing how to deal with more complicated cases. For this purpose we should construct a unity operator using functions $|lm\rangle$

[1] In reality to calculate matrix elements in a standard way, see Appendix 9 .

$$1 = A\sum_{l'm'}\int k'^2 dk'\ |k'l'm'\rangle\langle k'l'm'|$$

The easiest way to define the coefficient $A$ is to expand function $|\mathbf{k}\rangle$ itself:

$$|\mathbf{k}\rangle = A\sum_{l'm'}\int k'^2 dk'\ |k'l'm'\rangle\langle k'l'm'|\,|\mathbf{k}\rangle =$$

$$= A\sum_{l'm'}\int k'^2 dk' F_{l'}(k'r)Y_{l'm'}(\hat{r})\int d\mathbf{r}' F_{l'}(k'r')Y^*_{l'm'}(\hat{r}')\sum_{lm}F_l(kr')Y_{lm}(\hat{r}')\times$$

$$\times\tfrac{4\pi}{\sqrt{V}}\,i^l\,Y^*_{lm}(\hat{k}) = A\sum_{lm}\int k'^2 dk' F_l(k'r)Y_{lm}(\hat{r})\cdot\tfrac{4\pi}{\sqrt{V}}\,i^l\,Y^*_{lm}(\hat{k})\cdot\int r'^2 dr' F_{l'}(k'r')F_l(kr')$$

The expression $\int r'^2 dr' F_{l'}(k'r')F_l(kr')$ can not depend neither on the quantum number $l$ nor on the short-range interaction, hence it is sufficient to calculate $\int r^2 dr j_0(k'r)j_0(kr)$

$$\int r^2 dr\, j_0(k'r)j_0(kr) = \frac{1}{kk'}\int\frac{e^{ik'r}-e^{ik'r}}{2i}\frac{e^{ikr}-e^{ikr}}{2i}dr =$$

$$= \frac{1}{kk'}\left\{\frac{\pi}{2}\delta(k'-k)-\frac{\pi}{2}\delta(k'+k)\right\} = \langle k,k'>0\Rightarrow\rangle = \frac{1}{kk'}\,\frac{\pi}{2}\,\delta(k'-k)$$

$$\int_0^\infty r^2 dr F_l(k'r)F_l(kr) = \frac{\pi}{2kk'}\,\delta(k'-k)$$

$$|\mathbf{k}\rangle = A\frac{4\pi}{\sqrt{V}}\sum_{lm}\int k'^2 dk'\,\frac{\pi}{2kk'}\,\delta(k'-k)\ i^l F_l(k'r)\ Y_{lm}(\hat{r})Y^*_{lm}(\hat{k})$$

After this the unity operator is obtained

$$A = \frac{2}{\pi}\quad ;\qquad 1 = \sum_{l'm'}\int\frac{2}{\pi}\,k'^2 dk'\ |k'l'm'\rangle\langle k'l'm'| \tag{2.1}$$

**Particles with spin**

Let us assume that the total spin $S$ (with projection $\lambda$) of two particles is defined. Then

$$|\mathbf{k},S\lambda\rangle = \chi_{S\lambda}\sum_{lm}F_l(kr)Y_{lm}(\hat{r})\cdot\frac{4\pi}{\sqrt{V}}\,i^l\,Y^*_{lm}(\hat{k})$$

$$|JMl',k'\rangle = F_{l'}(k'r)\ [Y_{l'}(\hat{r})\otimes\chi_{S'}]_{JM}$$

$$\langle JMl',k'|\,|\mathbf{k},S\lambda\rangle = \frac{4\pi}{\sqrt{V}}\int d\mathbf{r}\sum_{lmm'S'M'_S} i^l F_{l'}(k'r)F_l(kr)\ Y^*_{l'm'}(\hat{r})Y_{lm}(\hat{r})\,Y^*_{lm}(\hat{k})\ \times$$

$$\times C^{JM}_{l'm'S'M'_S}\ \chi^+_{S'M'_S}\chi_{S\lambda} = \sum_m\frac{2\pi^2}{\sqrt{V}}\,\frac{\delta(k-k')}{kk'}\ i^{l_y}Y^*_{lm}(\hat{k})\ C^{JM}_{lmS\lambda}$$

And using the definition (2.1) one can obtain

$$|\mathbf{k},S\lambda\rangle = \sum_{lm}\left(\frac{4\pi}{\sqrt{V}}\, i^l Y^*_{lm}(\hat{k})\; C^{JM}_{lmS\lambda}\right) F_l(kr)\; [Y_l(\hat{r})\otimes\chi_S]_{JM}$$

And decomposition coefficients of functions with definite momentum and spin over functions with definite total angular momentum and its projection are

$$\langle JMl|\,|\mathbf{k},S\lambda\rangle = \sum_{m}\frac{4\pi}{\sqrt{V}}\, i^l Y^*_{lm}(\hat{k})\; C^{JM}_{lmS\lambda}$$

**Alpha+d continuum**

Now a more complicated task: to construct the three-body, two-cluster continuum $\alpha$+d WF. The distorted waves of deuterons in respect with $\alpha$-cluster is given by ($\lambda$ is the projection of the deuteron spin)

$$|\mathbf{k},1\lambda\rangle = \sum_{l_x} F_{l_x}(X)\left[Y_{l_x}(\hat{X})\otimes\chi_S\right]_{1\lambda}\sum_{l_y m_y} F_{l_y}(kY)Y_{l_y m_y}(\hat{Y})\cdot\frac{4\pi}{\sqrt{V}}\, i^{l_y}\, Y^*_{l_y m_y}(\hat{k})$$

while the form of this WF, suited for the calculations, is

$$\left|JML l'_x l'_y, k'\right\rangle = F_{l'_x l'_y}(X,k'Y)\;\left[\left[Y_{l'_x}(\hat{X})\otimes Y_{l'_y}(\hat{Y})\right]_L\otimes\chi_{S'}\right]_{JM}$$

The expansion coefficient is

$$\left\langle JML l'_x l'_y, k'\right|\,|\mathbf{k},1\lambda\rangle = \frac{4\pi}{\sqrt{V}}\int d\mathbf{Y}d\mathbf{X}\sum_{\substack{l'_x m'_x l'_y m'_y m_x m_y\\ M_S M_{S'} M_L}} i^{l_y} F_{l'_x l'_y}(X,k'Y)F_{l_x}(X)F_{l_y}(kY)\times$$

$$\times\, C^{1\lambda}_{l_x m_x S M_S} C^{JM}_{L M_L S' M'_S} C^{L M_L}_{l'_x m'_x l'_y m'_y}\; Y^*_{l'_x m'_x}(\hat{X})Y_{l_x m_x}(\hat{X})\; Y^*_{l'_y m'_y}(\hat{Y})Y_{l_y m_y}(\hat{Y})\; Y^*_{l_y m_y}(\hat{k})\times$$

$$\times\chi^+_{S'}\chi_S = \frac{4\pi}{\sqrt{V}}\sum_{m_x M_L M_S}\frac{\pi}{2kk'}\,\delta(k-k')\; i^{l_y}Y^*_{l_y m_y}(\hat{k})\; C^{1\lambda}_{l_x m_x S M_S} C^{JM}_{L M_L S M_S} C^{L M_L}_{l_x m_x l_y m_y}$$

Integration over $X^2dX$ used the fact that starting from some large $Y = Y_{\min}$ the function $F_{l_x l_y}(X,kY)$ can be factorized $F_{l_y}(kY)\cdot F_{l_x}(X)$ and normalization $\delta(k-k')$ is not influenced by the range $0 < Y < Y_{\min}$ , where such factorization is impossible. By means of formula (9.3) we obtain (for deuteron $S=1$)

$$\langle JML l_x l_y, k'|\,|\mathbf{k},1\lambda\rangle = \frac{2\pi^2}{\sqrt{V}}\,\frac{\delta(k-k')}{kk'}\,(-)^{J+L+S}\,\hat{1}\hat{L}\begin{Bmatrix} 1 & S & l_x\\ L & l_y & J\end{Bmatrix}$$

$$\sum_{m_y} i^{l_y}Y^*_{l_y m_y}(\hat{k})C^{JM}_{l_y m_y 1\lambda}$$

Using the definition of the unity operator (2.1) the continuum WF can be obtained

$$|\mathbf{k},1\lambda\rangle = \sum_{JMl_xl_y}\left(\sum_{m_y}\frac{4\pi}{\sqrt{V}}i^{l_y}Y^*_{l_ym_y}(\hat{k})(-)^{J+L+S}\hat{1}\hat{L}\left\{\begin{array}{ccc}1 & S & l_x\\ L & l_y & J\end{array}\right\}C^{JM}_{l_ym_y1\lambda}\right)\times$$

$$\times\, F_{l_xl_y}(X,kY)\ \left[\left[Y_{l'_x}(\hat{X})\otimes Y_{l'_y}(\hat{Y})\right]_L\otimes\chi_S\right]_{JM}$$

$$\langle JM|\,|\mathbf{k},1\lambda\rangle = \sum_{m_y}\left(\frac{4\pi}{\sqrt{V}}\,i^{l_y}Y^*_{l_ym_y}(\hat{k})\,(-)^{J+L+S}\,\hat{1}\hat{L}\left\{\begin{array}{ccc}1 & S & l_x\\ L & l_y & J\end{array}\right\}C^{JM}_{l_ym_y1\lambda}\right)$$

This procedure can be understood also as recoupling of $\alpha$-d WF from (LS) scheme suitable for the three-body calculations to (jj) coupling characteristic to the continuum.

### 2.1.3 HH method wave function; continuum

Similar to the two-body case we begin to construct the three-body continuum WF defining the 6-dimensional plane wave

$$|\mathbf{p}_x\mathbf{p}_y\rangle = \frac{1}{V}\exp\{i\mathbf{P}_x\mathbf{X}+i\mathbf{P}_y\mathbf{Y}\} = \frac{1}{V}\exp\{i\mathbf{p}_x\mathbf{x}+i\mathbf{p}_y\mathbf{y}\} =$$

$$= \frac{(2\pi)^3}{V(\varkappa\rho)^2}\sum_{KLM_Ll_xl_y} i^K J_{K+2}(\varkappa\rho)\mathcal{J}^{LM_L}_{Kl_xl_y}(\Omega\rho)\mathcal{J}^{LM_L}_{Kl_xl_y}(\Omega_\varkappa) \qquad (2.2)$$

$$\Omega_\varkappa = \{\theta_\varkappa,\hat{p}_x,\hat{p}_y\}\quad ;\qquad \Omega\rho = \{\theta\rho,\hat{x},\hat{y}\}$$

where $\mathbf{X}$, $\mathbf{Y}$ and $\mathbf{P}_x$, $\mathbf{P}_y$ are Jacobi coordinates and momenta; $\mathbf{x}$, $\mathbf{y}$ and $\mathbf{p}_x$, $\mathbf{p}_y$ are normalized Jacobi coordinates and momenta. So, for a plane wave of spinless particles we have

$$|LM_Ll_xl_y,K\rangle = \frac{(2\pi)^3}{V(\varkappa\rho)^2}i^K J_{K+2}(\varkappa\rho)\mathcal{J}^{LM_L}_{Kl_xl_y}(\Omega\rho)$$

$$\langle LM_Ll_xl_y,K\,\|\mathbf{p}_x\mathbf{p}_y\rangle = \sqrt{\frac{2}{\pi}}\frac{(2\pi)^3}{V}i^K\mathcal{J}^{LM_L}_{Kl_xl_y}(\Omega_\varkappa)$$

After this we replace $J_{K+2}(\varkappa\rho)$ with solution of the hyperradial equation (now spins of constituents are coupled in total spin $S$ ) $\sqrt{\frac{2}{\pi\varkappa\rho}}\chi^{K'L'S'l'_xl'_y}_{KLSl_xl_y}(\varkappa\rho)$ — see for example [47] — and find the coefficients of the expansion in a similar manner as in Section 2.1.2 (functions $\mathcal{J}$ and $\mathcal{L}$ are defined in (7.1) ):

$$|\mathbf{p}_x\mathbf{p}_y,SM_S\rangle = \sqrt{\frac{2}{\pi}}\frac{(2\pi)^3}{V(\varkappa\rho)^{5/2}}\sum_{\substack{KLSl_xl_y\\JM}} i^K\times$$

$$\times \left( \sum_{K'L'S'l'_x l'_y} \chi^{K'L'S'l'_x l'_y}_{KLSl_x l_y}(\varkappa\rho)\ \mathcal{L}^{JM}_{K'L'S'l'_x l'_y}(\Omega\rho) \right) \sum_{M_L} C^{JM}_{LM_L SM_S} \mathcal{J}^{LM_L}_{Kl_x l_y}(\Omega_\varkappa)$$

$$\langle JMLl_x l_y, K \,\|\mathbf{p}_x \mathbf{p}_y, SM_S\rangle = \sqrt{\frac{2}{\pi}} \frac{(2\pi)^3}{V} i^K \sum_{M_L} \mathcal{J}^{LM_L}_{Kl_x l_y}(\Omega_\varkappa)\ C^{JM}_{LM_L SM_S}$$

The normalization of the function $\chi(\varkappa\rho)$ is given by the asymptotic relation

$$\chi^{K'L'S'l'_x l'_y}_{KLSl_x l_y}(\varkappa\rho) \overset{\varkappa\rho\to\infty}{\sim} \sin(\varkappa\rho + (K+2)\pi/4 + \delta^{K'L'S'l'_x l'_y}_{KLSl_x l_y})$$

### 2.1.4 COSMA WF. $^6$He, $^6$Li; GT matrix element

The first $p$-shell oscillator function coupled with the spin of nucleon in total spin $j$ is

$$|0,1,j\rangle = \sqrt{\frac{8}{3\sqrt{\pi}}} \frac{r}{r_0^{5/2}} \exp\left\{-\frac{r^2}{2r_0^2}\right\}\ C^{jm_j}_{1m1/2\nu} Y_{1m}(\hat{r})\chi\nu$$

If we assume that nucleons in $^6$He and $^6$Li are occupying only $p_{3/2}$ shells, then after recoupling to (LS) scheme and transformation to Jacobi coordinates, the WFs of the nuclei can be obtained as follows (isospin part and L=2 component of $^6$Li are omitted):

$$\Psi_{JM} = \frac{8}{3\sqrt{\pi} r_0^5} \exp\left\{-\tfrac{Y^2 - X^2/4}{r_0^2}\right\} \cdot \left\{ A\sqrt{3}\left(Y^2 - \tfrac{X^2}{4}\right) \left[\left[Y_0(\hat{X}) \otimes Y_0(\hat{Y})\right]_0 \otimes \chi_J\right]_{JM} + \right.$$

$$\left. +\ B\ XY \left[\left[Y_1(\hat{X}) \otimes Y_1(\hat{Y})\right]_J \otimes \chi_0\right]_{JM} \right\}$$

where

| | $J\pi$ | $R_{mat}$ | $r_0$ | $A$ | $B$ |
|---|---|---|---|---|---|
| $^6$He | $0^+$ | $2.57 \pm 0.1$ | $2.73 \pm 0.13$ | $\sqrt{2/3}$ | $-\sqrt{1/3}$ |
| $^6$Li | $1^+$ | $2.35 \pm 0.08$ | $2.43 \pm 0.1$ | $\sqrt{10/27}$ | $\sqrt{15/27}$ |

Let us construct the same WFs now as the Slater determinants. So we have to construct the determinants with definite angular momenta. For this purpose we use the following operators

$$L_+ = l_1^+ + l_2^+$$

$$l^+\psi_{lm} = \sqrt{(l-m)(l+m+1)}\psi_{lm+1}$$
$$l^-\psi_{lm} = \sqrt{(l+m)(l-m+1)}\psi_{lm-1}$$

The ME of operator $l^+$ are

$$\begin{cases} l^+ \left|3/2, 3/2\right\rangle & = \left|0\right\rangle \\ l^+ \left|3/2, 1/2\right\rangle & = \sqrt{3}\left|3/2, 3/2\right\rangle \\ l^+ \left|3/2, -1/2\right\rangle & = 2\left|3/2, 1/2\right\rangle \\ l^+ \left|3/2, -3/2\right\rangle & = \sqrt{3}\left|3/2, -1/2\right\rangle \end{cases}$$

The WF is constructed as a sum of all the possible determinants

$$\Psi_{00}^{He} = \frac{1}{\sqrt{2}}\left(\alpha \left| \begin{array}{c} 3/2\uparrow \\ -3/2\downarrow \end{array} \right| + \beta \left| \begin{array}{c} 1/2\uparrow \\ -1/2\downarrow \end{array} \right|\right) \quad ; \qquad \alpha^2 + \beta^2 = 1$$

Function $L_+\Psi_{00}^{He}$ should be 0, giving us the second condition

$$L_+\Psi_{00}^{He} = \frac{1}{\sqrt{2}}\left(\alpha\sqrt{3} \left| \begin{array}{c} 3/2\uparrow \\ -1/2\downarrow \end{array} \right| + \beta\sqrt{3} \left| \begin{array}{c} 3/2\uparrow \\ -1/2\downarrow \end{array} \right|\right) = 0 \quad ; \qquad \alpha + \beta = 0$$

And as a result $^6$He function is

$$\Psi_{00}^{He} = \frac{1}{\sqrt{2}}\left(\frac{1}{\sqrt{2}} \left| \begin{array}{c} 3/2\uparrow \\ -3/2\downarrow \end{array} \right| - \frac{1}{\sqrt{2}} \left| \begin{array}{c} 1/2\uparrow \\ -1/2\downarrow \end{array} \right|\right)$$

This procedure is a bit more complicated for $^6$Li. Here we have to apply also operator $T_+ = \tau_1^+ + \tau_2^+$ using the fact that $^6$Li g.s. is an isospin singlet.

$$\Psi_{11}^{Li} = \frac{1}{\sqrt{2}}\left(\alpha \left| \begin{array}{c} 3/2\uparrow \\ -1/2\downarrow \end{array} \right| + \beta \left| \begin{array}{c} 1/2\uparrow \\ 1/2\downarrow \end{array} \right| + \gamma \left| \begin{array}{c} 3/2\downarrow \\ -1/2\uparrow \end{array} \right|\right) \quad ; \qquad \alpha^2 + \beta^2 + \gamma^2 = 1$$

$$\begin{cases} L_+\Psi_{11}^{Li} = \frac{1}{\sqrt{2}}\left(2\alpha \left| \begin{array}{c} 3/2\uparrow \\ 1/2\downarrow \end{array} \right| + \beta\sqrt{3} \left| \begin{array}{c} 3/2\uparrow \\ 1/2\downarrow \end{array} \right| + \beta\sqrt{3} \left| \begin{array}{c} 1/2\uparrow \\ 3/2\downarrow \end{array} \right| + \gamma \left| \begin{array}{c} 3/2\downarrow \\ 1/2\uparrow \end{array} \right|\right) \\ T_+\Psi_{11}^{Li} = \frac{1}{\sqrt{2}}\left(\alpha\sqrt{2} \left| \begin{array}{c} 3/2\uparrow \\ -1/2\uparrow \end{array} \right| + \gamma\sqrt{2} \left| \begin{array}{c} 3/2\uparrow \\ -1/2\uparrow \end{array} \right|\right) \end{cases}$$

$$\begin{cases} 2\alpha + \sqrt{3}\beta = 0 \\ 2\gamma - \sqrt{3}\beta = 0 \\ \alpha + \gamma = 0 \end{cases} \Rightarrow \quad \alpha = \sqrt{\frac{3}{10}} \quad \beta = -\sqrt{\frac{2}{5}} \quad \gamma = -\sqrt{\frac{3}{10}}$$

The calculations of ME of the GT operator $\sigma_1^+\tau_1^- + \sigma_2^+\tau_2^-$ between two determinants are trivial. It should be noted only that each determinant has $n!$ terms, which provide $n!$ equal terms in the $B_{GT}$ value; this coefficient is canceled out by normalization coefficient $1/\sqrt{n!}$ in the WFs.

$$\tau^- \left|\uparrow\right\rangle = \left|\downarrow\right\rangle$$

$$\begin{cases} \left\langle 3/2, 3/2\right| \sigma^+ \left|3/2, 1/2\right\rangle = -\sqrt{2/3} \\ \left\langle 3/2, 1/2\right| \sigma^+ \left|3/2, -1/2\right\rangle = -\sqrt{8/9} \\ \left\langle 3/2, -1/2\right| \sigma^+ \left|3/2, -3/2\right\rangle = -\sqrt{2/3} \end{cases}$$

$$B_{GT} = \frac{2J'+1}{2J+1}\left(\Psi_{11}^{Li}\left|\sigma_1^+\tau_1^- + \sigma_2^+\tau_2^-\right|\Psi_{00}^{He}\right) = 3\left(-\sqrt{\frac{10}{9}}\right)^2 \mathbf{J}^4 = 6\frac{5}{9}\mathbf{J}^4 \qquad (2.3)$$

The same value can also be found in equation (3.3). Here **J** is an overlap of the radial parts of one-particle oscillator functions:

$$\mathbf{J} = \left(\frac{2r_0^{He}r_0^{Li}}{\left(r_0^{He}\right)^2 + \left(r_0^{Li}\right)^2}\right)^{5/2}$$

### 2.1.5 COSMA WF. $^8$He, $^8$Li; GT matrix element

To construct $^8$He WF in "$p_{3/2}$ approximation" is very simple

$$\Psi_{00}^{He} = \frac{1}{\sqrt{24}}\begin{vmatrix} 3/2\uparrow \\ 1/2\uparrow \\ -1/2\downarrow \\ -3/2\downarrow \end{vmatrix}$$

The $^8$Li WF is given by a sum of three determinants

$$\Psi_{11}^{Li} = \frac{1}{\sqrt{2}4}\left(\alpha\begin{vmatrix} 3/2\uparrow \\ 1/2\uparrow \\ -1/2\uparrow \\ -1/2\downarrow \end{vmatrix} + \beta\begin{vmatrix} 3/2\uparrow \\ 1/2\uparrow \\ -3/2\uparrow \\ 1/2\downarrow \end{vmatrix} + \gamma\begin{vmatrix} 3/2\uparrow \\ -1/2\uparrow \\ -3/2\uparrow \\ 3/2\downarrow \end{vmatrix}\right)$$

The zero component of angular momentum is $J_0 = 1$ in this WF. It means that for the general set of coefficients $(\alpha, \beta, \gamma)$ it is a sum of $\Psi_{11}^{Li}$, $\Psi_{21}^{Li}$. Hence formally we should satisfy the condition: $L_+\Psi^{Li} = 0$ to avoid functions with J=2.

$$L_+\Psi_{11}^{Li} = \frac{1}{\sqrt{24}}\times$$

$$\times\left(2\alpha\begin{vmatrix} 3/2\uparrow \\ 1/2\uparrow \\ -1/2\uparrow \\ 1/2\downarrow \end{vmatrix} + \sqrt{3}\beta\begin{vmatrix} 3/2\uparrow \\ 1/2\uparrow \\ -1/2\uparrow \\ 1/2\downarrow \end{vmatrix} + \sqrt{3}\beta\begin{vmatrix} 3/2\uparrow \\ 1/2\uparrow \\ -3/2\uparrow \\ 3/2\downarrow \end{vmatrix} + 2\gamma\begin{vmatrix} 3/2\uparrow \\ 1/2\uparrow \\ -3/2\uparrow \\ 3/2\downarrow \end{vmatrix}\right)$$

$$\begin{cases} 2\alpha + \sqrt{3}\beta = 0 \\ 2\gamma + \sqrt{3}\beta = 0 \\ \alpha^2 + \beta^2 + \gamma^2 = 1 \end{cases} \Rightarrow \quad \alpha = \sqrt{\frac{3}{10}} \quad \beta = -\sqrt{\frac{2}{5}} \quad \gamma = \sqrt{\frac{3}{10}}$$

And using the formulae of the previous section the $B_{GT}$ value is obtained

$$B_{GT} = \frac{2J'+1}{2J+1}\left(\Psi_{11}^{Li}\left|\sum_{i=1}^{4}\sigma_i^+\tau_i^-\right|\Psi_{00}^{He}\right) = 3\left(-\frac{10}{3\sqrt{5}}\right)^2 \mathbf{J}^8 = \frac{20}{3}\mathbf{J}^8$$

This is the mysterious "20/3" value, which appears in the Section 4 of [P4].

## 2.2 Beta-decay

### 2.2.1 Beta-decay preliminaries

Here are presented some constants for $\beta$-decay and simple formulae connecting $\beta$-decay variables for the allowed Gamow-Teller (GT) transitions.

**Probability of the decay**

$$W = \frac{\ln 2}{t_{1/2}} = \frac{G_V^2 \lambda^2 m_e^5}{2\pi^3} \cdot B_{GT} \cdot f\left(A, Z, Q\right)$$

where $\lambda = G_A/G_V = -1.268 \pm 0.002$ ($\lambda^2 = 1.608 \pm 0.004$) [53]. $B_{GT}$ is Gamow-Teller strength of the transition and $f\left(A, Z, Q\right)$ is phase volume of leptons in the final state. $Q = E - m_e$ is the energy release in the reaction (energy available to leptons and recoil).

**Gamow-Teller strength of the transition** between states with definite total spin $J$, total isotopic spin $T$ and its third component $T_3$ can be expressed as

$$B_{GT} = \frac{2J'+1}{2J+1} \left| \sum_{k=1}^{N} \left\langle J' \left\| \sigma_k \right\| J \right\rangle \left\langle T' T_3' \left| \tau_k^- \right| T T_3 \right\rangle \right|^2$$

**Phase volume of leptons**

$$f\left(A, Z, Q\right) = \int_1^{Q/m_e} \left(Q/m_e - \varepsilon\right)^2 \varepsilon \sqrt{\varepsilon^2 - 1}\, F\left(A, Z, Q\right) d\varepsilon$$

where $f\left(A, Z, Q\right)$ is the Fermi function (can be found for example in [57])correcting for the density of the lepton states on the surface of the nucleus

**$ft_{1/2}$ values**

$$ft_{1/2} = 2 \cdot \frac{\pi^3 \ln 2}{G_V^2 m_e^5} \cdot \frac{1}{\lambda^2 B_{GT}} = \frac{2ft(0^+ \to 0^+)}{\lambda^2 B_{GT}}$$

where

$$ft(0^+ \to 0^+) = \frac{\pi^3 \ln 2}{G_V^2 m_e^5} = 3072.4 \pm 1.6 \text{ sec}$$

The following formulae present some simple relations between the values given above

$$ft_{1/2} = \frac{3821.9 \pm 2.0}{B_{GT}}$$

$$\frac{G_V^2 \lambda^2 m_e^5}{2\pi^3} = \frac{\lambda^2 \ln 2}{2ft(0^+ \to 0^+)} \qquad \frac{1}{B_{GT} f} = \frac{\lambda^2 t_{1/2}}{2ft(0^+ \to 0^+)}$$

### 2.2.2 Nuclear Hamiltonian for the beta$^-$-decay

The matrix element of the weak interaction Hamiltonian after nonrelativistic reduction in the space of nucleons can be written as

$$H_{fi} = (2\pi)\delta\left(E_f - E_i\right) \int \prod_{k=1}^{N} d^3\mathbf{r}_k \Psi_f^*\left(\mathbf{r}_1 \ldots \mathbf{r}_N\right) \widehat{H}_\beta\left(\mathbf{r}_1 \ldots \mathbf{r}_N\right) \Psi_i\left(\mathbf{r}_1 \ldots \mathbf{r}_N\right)$$

where

$$\widehat{H}_\beta\left(\mathbf{r}_1, \ldots, \mathbf{r}_N\right) = -\frac{G_V}{\sqrt{2}} \sum_{k=1}^{N} \left\{L_0^*\left(\mathbf{r}_k\right) + \lambda\left(\mathbf{L}^*\left(\mathbf{r}_k\right), \boldsymbol{\sigma}_k\right)\right\} \tau_k^-$$

$$L_\mu^*\left(\mathbf{r}_k\right) = \overline{\Psi}_e\left(\mathbf{r}_k\right) \gamma_\mu \left(1 + \gamma_5\right) \Psi_\nu\left(\mathbf{r}_k\right) = \frac{\overline{u}_e \gamma_\mu \left(1 + \gamma_5\right) \overline{u}_\nu}{\sqrt{2E_e 2E_\nu}\, V} \exp\left(i\mathbf{q}\mathbf{r}_k\right)$$

$$\mathbf{q} = \mathbf{p}_e - \mathbf{p}_\nu \quad ; \qquad \gamma_5 = \begin{pmatrix} 0 & -1 \\ -1 & 0 \end{pmatrix}$$

$N$ is a number of nucleons in the system. Note, that the $\sigma$-matrices have standard definition, while operators $\tau^\pm$ are "normalized" (see definition in Appendix 9.2). The time dependence of the lepton currents and nuclei wave function (WF) appears in the matrix element as a $\delta$-function of energy.

### 2.2.3 Discrete spectrum of daughter states.

1. We are going to study here only GT transitions to the discrete spectrum of states in the daughter nuclei.

2. In the case of the allowed transitions we are restricted to the long-wave approximation of the lepton current

$$\exp\left(i\mathbf{q}\mathbf{r}\right) \sim 1$$

3. The nuclear WF can be written in a factorized form:

$$\Psi_{JM}^{TT_3} = \left|JM\right\rangle \left|TT_3\right\rangle$$

Within these assumptions the matrix element is given by

$$H_{fi} = -\frac{G_V \lambda}{\sqrt{2}} \left(2\pi\right) \delta\left(E_f - E_i\right) \sum_{\mu=-1}^{1} \frac{\overline{u}_e \gamma_\mu \left(1 + \gamma_5\right) \overline{u}_\nu}{\sqrt{2E_e 2E_\nu} V} \sum_{k=1}^{N} C_{JM1\mu}^{J'M'} \left\langle J' \left\| \sigma_k \right\| J \right\rangle \times$$

$$\times \left\langle T'T_3' \left| \tau_k^- \right| TT_3 \right\rangle$$

The probability of the decay can be obtained in an ordinary manner using the Fermi rule

$$dW = \frac{1}{\Delta t} \sum_f \overline{\left|H_{fi}\right|^2} d\rho_f$$

where $f$ is the index containing quantum numbers of the possible final states. Overline denote averaging over available initial states. A more compact notation for isospin ME is used $\left\langle \tau_k^- \right\rangle = \left\langle T'T'_3 \left| \tau_k^- \right| TT_3 \right\rangle$

$$\sum_f \overline{|H_{fi}|^2} = \frac{1}{2J+1} \frac{G_V^2 \lambda^2}{2} (2\pi)\, \delta(E_f - E_i)\, \Delta t \sum_{MM'\mu\upsilon} C^{J'M'}_{JM1\upsilon} C^{J'M'}_{JM1\mu} \times$$

$$\times \frac{(\overline{u}_e \gamma_\mu (1+\gamma_5) u_\nu)\, (u_\nu^+ (1+\gamma_5) \gamma_\upsilon^+ \gamma_0 u_e)}{2E_e 2E_\nu V^2} \left| \sum_{k=1}^{N} \langle J' \| \sigma_k \| J \rangle \left\langle \tau_k^- \right\rangle \right|^2$$

The following expressions are used: $\gamma_0^+ = \gamma_0$, $\overline{\gamma}^+ = -\overline{\gamma}$, $\gamma_5^+ = \gamma_5$. The sum over the spin states of leptons is implicitly meant here. It allows to replace lepton bispinors by the projection operators

$$\sum_{Spin} u_e u_e^+ = p_e^\alpha \gamma_\alpha - m_e \qquad\qquad \sum_{Spin} u_\nu u_\nu^+ = p_\nu^\beta \gamma_\beta$$

$$\sum_{Spin} (\overline{u}_e \gamma_\mu (1+\gamma_5) u_\nu) \left(u_\nu^+ (1+\gamma_5) \gamma_\upsilon^+ \gamma_0 u_e\right) =$$

$$= p_\nu^\beta Sp\left[(p_e^\alpha \gamma_\alpha - m_e) \gamma_\mu (1+\gamma_5) \gamma_\beta \gamma_0 (1+\gamma_5) \gamma_\upsilon^+ \gamma_0\right] =$$

- $\{\gamma_\mu \gamma_5\} = 0 \;\Rightarrow\; \gamma_\beta \gamma_0 (1+\gamma_5) = (1+\gamma_5) \gamma_\beta \gamma_0$
- $\gamma_5^2 = 1 \qquad \Rightarrow\; (1+\gamma_5)^2 = 2(1+\gamma_5)$

$$= 2\, p_\nu^\beta\, Sp\left[(p_e^\alpha \gamma_\alpha - m_e) \gamma_\mu (1+\gamma_5) \gamma_\beta \gamma_0 \gamma_\upsilon^+ \gamma_0\right] =$$

- $\{\gamma_\mu \gamma_\upsilon\} = 2\eta_{\mu\upsilon}$, $\upsilon = 1,2,3 \;\Rightarrow\; \gamma_\upsilon^+ \gamma_0 = \gamma_0 \gamma_\upsilon$
- $\gamma_0^2 = 1$, $\quad Sp$ taken from any three $\gamma$-matrix is zero

$$= 2\, p_e^\alpha p_\nu^\beta\, Sp\left[(1+\gamma_5) \gamma_\alpha \gamma_\mu \gamma_\beta \gamma_\upsilon\right] = 2\, p_e^\alpha p_\nu^\beta\, 4\left[\eta_{\alpha\mu}\eta_{\beta\upsilon} + \eta_{\alpha\upsilon}\eta_{\mu\beta} - \eta_{\alpha\mu}\eta_{\beta\upsilon} + i\varepsilon_{\alpha\mu\beta\upsilon}\right] =$$

$$= 8\left[p_e^\mu p_\nu^\upsilon + p_e^\mu p_\nu^\upsilon - (E_e E_\nu - \mathbf{p}_e \mathbf{p}_\nu)\, \eta^{\mu\upsilon}\right]$$

As far as

$$\sum_{MM'} C^{J'M'}_{JM1\mu} C^{J'M'}_{JM1\upsilon} = \frac{2J'+1}{3}\, \delta_{\mu\upsilon} \tag{2.4}$$

and $(\mu, \upsilon = 1,2,3\ )$, we finally obtain

$$\sum_{MM'\mu\upsilon} C^{J'M'}_{JM1\mu} C^{J'M'}_{JM1\upsilon}\ (\overline{u}_e \gamma_\mu (1+\gamma_5) u_\nu) \left(u_\nu^+ (1+\gamma_5) \gamma_\upsilon^+ \gamma_0 u_e\right) =$$

$$= \frac{2J'+1}{3} 8\left[\, 2\mathbf{p}_e \mathbf{p}_\nu + 3\,(E_e E_\nu - \mathbf{p}_e \mathbf{p}_\nu)\,\right] = \frac{2J'+1}{3} 6 \cdot 4\, E_e E_\nu \left(1 - \frac{\mathbf{p}_e \mathbf{p}_\nu}{3\, E_e E_\nu}\right)$$

The expression for summed and averaged (over the discrete sets of quantum numbers) ME of the weak Hamiltonian is

$$\sum_f \overline{|H_{fi}|^2} = \frac{1}{2J+1} \frac{G_V^2 \lambda^2}{2} (2\pi)\, \delta(E_f - E_i)\, \Delta t\, \frac{6}{V^2} \left(1 - \frac{\mathbf{p}_e \mathbf{p}_\nu}{3\, E_e E_\nu}\right) \times$$

$$\times \frac{2J'+1}{3} \left| \sum_{k=1}^{N} \langle J' \| \sigma_k \| J \rangle \left\langle \tau_k^- \right\rangle \right|^2$$

and the differential probability of the decay

$$dW = \frac{1}{2J+1} \frac{G_V^2 \lambda^2}{2} (2\pi)\, \delta(E_e + E_\nu - Q) \frac{6}{V^2} \left(1 - \frac{\mathbf{p}_e \mathbf{p}_\nu}{3\, E_e E_\nu}\right) \times$$

$$\times \frac{2J'+1}{3} \left| \sum_{k=1}^{N} \langle J' \| \sigma_k \| J \rangle \left\langle \tau_k^- \right\rangle \right|^2 \frac{V^2 \mathbf{dp}_e \mathbf{dp}_\nu}{(2\pi)^6} \tag{2.5}$$

where $Q$ is the energy available to leptons (recoil is neglected): $Q = E - m_e$. After integration over angular variables of the leptons we obtain:

$$dW = \frac{G_V^2 \lambda^2}{2\pi^3} \cdot \left( \frac{2J'+1}{2J+1} \left| \sum_{k=1}^{N} \langle J' \| \sigma_k \| J \rangle \left\langle \tau_k^- \right\rangle \right|^2 \right) \cdot \left( \delta \left( E_e + E_\nu - Q \right) p_e^2 dp_e p_\nu^2 dp_\nu \right)$$

This equation shows how the expression for probability can be split into one part connected with nucleon current and one part connected with leptons in a natural way. The convenient expression for the probability of the $\beta$-decay is:

$$W = \frac{G_V^2 \lambda^2 m_e^5}{2\pi^3} \cdot B_{GT} \cdot f\left(A, Z, Q\right)$$

where

$$B_{GT} = \frac{2J'+1}{2J+1} \left| \sum_{k=1}^{N} \langle J' \| \sigma_k \| J \rangle \left\langle T' T_3' \left| \tau_k^- \right| T T_3 \right\rangle \right|^2$$

$$f\left(A, Z, Q\right) = \int_1^{Q/m_e} \left(Q/m_e - \varepsilon\right)^2 \varepsilon \sqrt{\varepsilon^2 - 1} F\left(A, Z, Q\right) d\varepsilon$$

The Fermi function $F\left(A, Z, Q\right)$ is introduced here to take into account the distortion of an electron WF in a Coulomb field of a nucleus. Normally it is defined as sum of the $s_{1/2}$ and $p_{1/2}$ electron densities in the point-like Coulomb potential on a surface of a nucleus.

### 2.2.4 Two-body continuum daughter state

#### Spin 0 particles in the final state

In this section we are interested in the formal structure of the $\beta$-decay matrix elements and expressions for the probability of the decay in the case of a two-body continuum daughter state. For simplicity we assume that clusters (particles) in

the final state are spinless and initial state have the same two-body structure. The two-body continuum WF of two spinless particles is given by

$$\Psi_{lm} = \frac{1}{k}\sum_{lm}\Psi_{lm}\left(E;\mathbf{r}\right)\cdot Y^{*}_{lm}\left(\widehat{k}\right)\frac{4\pi i^{l}}{\sqrt{V}} = \sum_{lm}F_{l}\left(kr\right)Y_{lm}\left(\widehat{r}\right)Y^{*}_{lm}\left(\widehat{k}\right)\frac{4\pi i^{l}}{\sqrt{V}} \quad (2.6)$$

The terms expressing internal degrees of freedom of the particles are omitted. Note that the cluster relative motion WF $\Psi_{lm}\left(k,\mathbf{r}\right) = F_{l}\left(kr\right)Y_{lm}\left(\widehat{r}\right)$ have a formal structure of the continuum WF (except asymptotic) as far as:

$$F_{l}\left(kr\right) \overset{kr\to\infty}{\sim} \frac{\sin(kr+\delta_{l}+l\pi/4)}{kr} \quad (2.7)$$

Normalization of the WF is discussed in more details in Appendix, Section 12.2

**Matrix elements.** The matrix elements between states of the discrete spectrum and the continuum in the spinless approximation have the formal structure:

$$\frac{1}{k}\sum_{l'm'}\left\langle l'm',\gamma'\left|\hat{O}\right|lm,\gamma\right\rangle Y^{*}_{l'm'}\left(\widehat{k}\right)\frac{4\pi i^{l}}{\sqrt{V}}$$

the multiindex $\gamma$ includes here the rest of the possible quantum numbers belonging to the internal degrees of freedom. Expression in the brackets includes a coefficient, which depends on the angular momenta of the constituents, and overlap integrals of the radial parts of WFs. It is calculated formally identically to the case of the discrete spectrum. The difference from the discrete spectrum ME arises only in the coefficient after brackets, containing angular dependence in the momentum space.

**Density of the final states.** To make the calculations self consistent the density of the final states should be taken as

$$d\rho_{f} = \frac{Vd^{3}k}{(2\pi)^{3}}$$

we prefer to keep the normalization volume $V$ in our calculations because it simplify the dimension analysis of the expressions: the density of the final states is dimensionless and "discrete spectrum" matrix element in brackets have the dimension of operator $\hat{O}$ — energy, if it is a Hamiltonian.

Similar to the equation (2.5), the expression for the differential probability of the $\beta$-decay is obtained

$$dW = \frac{1}{2l+1}\frac{G_{V}^{2}\lambda^{2}}{2}\frac{2}{V^{2}E_{e}E_{v}}\left[p_{e}^{\mu}p_{\nu}^{v}+p_{e}^{\mu}p_{\nu}^{v}-\left(E_{e}E_{\nu}-\mathbf{p}_{e}\mathbf{p}_{\nu}\right)\eta^{\mu v}\right]\times$$

$$\times\sum_{l'm'\tilde{l}'\tilde{m}'}\left(\frac{1}{k}\sum_{k=1}^{N}\left\langle l'\left\|\sigma_{k}\right\|l\right\rangle\left\langle\tau_{k}^{-}\right\rangle\right)^{*}\left(\frac{1}{k}\sum_{\tilde{k}=1}^{N}\left\langle\tilde{l}'\left\|\sigma_{\tilde{k}}\right\|l\right\rangle\left\langle\tau_{k}^{-}\right\rangle\right)\times$$

$$\times C^{l'm'}_{lm1\mu} C^{\tilde{l}'\tilde{m}'}_{lm1\upsilon} \frac{(4\pi)^2}{V} Y^*_{l'm'}\left(\widehat{k}\right) Y_{\tilde{l}'\tilde{m}'}\left(\widehat{k}\right) (2\pi)\,\delta(E_f - E_i)\,\frac{V^3 \mathbf{dp}_e \mathbf{dp}_\nu \mathbf{dk}}{(2\pi)^9} \quad (2.8)$$

In this expression the momenta of leptons and fragments of mother nucleus are correlated. We have to integrate over the angles $d\Omega_k$, before we are able to treat them independently:

$$dW = \frac{1}{2l+1}\frac{G_V^2\lambda^2}{2}(2\pi)\delta(E_e + E_\nu + E - Q)\frac{6}{V^2}\left(1 - \frac{\mathbf{p}_e\mathbf{p}_\nu}{3\,E_e E_\nu}\right)\times$$

$$\times \frac{2l'+1}{3}\left|\frac{1}{k}\sum_{k=1}^{N}\langle l'\,\|\sigma_k\|\,l\rangle\left\langle\tau_k^-\right\rangle\right|^2 \frac{2}{\pi}\,k^2 dk\,\frac{V^2\mathbf{dp}_e\mathbf{dp}_\nu}{(2\pi)^6}$$

$$dW = \frac{G_V^2\lambda^2}{2\pi^3}\left(\frac{2l'+1}{2l+1}\left|\frac{1}{k}\sum_{k=1}^{N}\langle l'\,\|\sigma_k\|\,l\rangle\left\langle\tau_k^-\right\rangle\right|^2 \frac{2}{\pi}\,k^2 dk\right)\times$$

$$\times\left(\delta\left(E_e + E_\nu + E - Q\right)p_e^2 dp_e p_\nu^2 dp_\nu\right)$$

Now, as it has already been done for the $\beta$-decay to the discrete spectrum state, the expression for the probability is split into one part connected with nucleon current and one part connected with the lepton current:

$$W = \int_0^Q \frac{G_V^2\lambda^2 m_e^5}{\pi^4\upsilon}\cdot B_{GT}(E)\cdot f\left(A,Z,Q-E\right)\,dE \quad (2.9)$$

where $\upsilon = \sqrt{2M_R E}$ is a relative velocity of the daughter fragments. Here we present some alternative notations for this formula, which may be more suitable for some purposes. These notations use the definition of the coefficients through the $ft(0^+ \to 0^+)$ value or express the probability in terms of branching ratio to some other $\beta$-decay process with characteristics $E(main)$, $B_{GT}(main)$, $t_{1/2}(main)$ — which are considered to be known.

$$W = \int_0^Q \frac{\lambda^2 \ln 2}{\pi\upsilon\, ft(0^+ \to 0^+)}\cdot B_{GT}(E)\cdot f\left(A,Z,Q-E\right)\,dE$$

$$Br = \int_0^Q \frac{2}{\pi\upsilon}\cdot\frac{B_{GT}(E)}{B_{GT}(main)}\cdot\frac{f\left(A,Z,Q-E\right)}{f\left(A,Z,E(main)\right)}\;dE$$

$$Br = \int_0^Q \frac{\lambda^2 t_{1/2}(main)}{\pi\upsilon\, ft(0^+ \to 0^+)}\cdot B_{GT}(E)\cdot f\left(A,Z,Q-E\right)\,dE$$

In all these formulae

$$B_{GT}(E) = \frac{2J'+1}{2J+1} \left| \sum_{k=1}^{N} \langle l' \left\| \sigma_k \right\| l \rangle \left\langle T'T'_3 \left| \tau_k^- \right| TT_3 \right\rangle \right|^2$$

The reduced ME $\langle l' \left\| \sigma_k \right\| l \rangle$ contains the final state WF $\Psi_{lm}(k, \mathbf{r})$, which is defined by equations (2.6), (2.7).

$$\Psi_{lm}(k, \mathbf{r}) \overset{kr \to \infty}{\sim} \frac{\sin(kr + l\pi/4 + \delta_l)}{r} Y_{lm}(\hat{r})$$

The integral $B_{GT}$ value (which is the subject of the GT sum rule) is

$$B_{GT}(int) = \int_0^\infty \frac{2}{\pi \upsilon} B_{GT}(E)\, dE$$

**Realistic case of nonzero spin particles in the final state**

In the realistic case of particles with a spin and an internal structure, the continuum WF, suitable for calculations of the ME, will be more complicated:

$$\begin{gathered} \Psi_{JM} = \frac{1}{k} \sum_{lm} \Psi_{lS}^{JM}(E; \mathbf{r}) \cdot Y_{lm}^* \left( \widehat{k} \right) \frac{4\pi i^l}{\sqrt{V}} C_{lmSm_s}^{JM} = \\ = \sum_{lmS} \left[ [\psi(1)_{S_1} \otimes \psi(2)_{S_2}]_{SM_S} \otimes \psi_{lM_l}^{JS}(k; \mathbf{r}) \right]_{JM} \cdot Y_{lm}^* \left( \widehat{k} \right) \frac{4\pi i^l}{\sqrt{V}} C_{lmSm_s}^{JM} \end{gathered} \tag{2.10}$$

This expression is derived in Section 2.1.2. The reason for its rather complicated form is that we have to expand the continuum WF with definite relative momentum and spins of the constituents over the eigenfunctions of the same Hamiltonian, but with definite total momenta. The term after the square brackets in equation (2.10) is nothing but coefficients of this decomposition. So, magnetic quantum numbers $M_S, M_l$ belong to the coupling "inside"— they are "blind", while $m_S, m$ are describing the asymptotic region — they are "observable". "Observable" in our context means the following. If we put WF (2.10) in the equation (2.8) instead of simplified spin zero WF we get

$$dW = \frac{1}{2J+1} \frac{G_V^2 \lambda^2}{V^2 E_e E_v} \left[ p_e^\mu p_\nu^\upsilon + p_e^\mu p_\nu^\upsilon - (E_e E_\nu - \mathbf{p}_e \mathbf{p}_\nu) \eta^{\mu\upsilon} \right] C_{JM1\mu}^{J'M'} C_{JM1\upsilon}^{J'\tilde{M}'} \times$$

$$\times \sum_{l'm'\tilde{l}'\tilde{m}'} \left( \frac{1}{k} \sum_{k=1}^{N} \langle J', l' \left\| \sigma_k \right\| J, l \rangle \left\langle \tau_k^- \right\rangle \right)^* \left( \frac{1}{k} \sum_{\tilde{k}=1}^{N} \left\langle J', \tilde{l}' \left\| \sigma_{\tilde{k}} \right\| J, l \right\rangle \left\langle \tau_{\tilde{k}}^- \right\rangle \right) \times$$

$$\times \frac{(4\pi)^2}{V} Y_{l'm'}^* \left( \widehat{k} \right) Y_{\tilde{l}'\tilde{m}'} \left( \widehat{k} \right) C_{l'm'S'm'_s}^{J'M'} C_{\tilde{l}'\tilde{m}'S'm'_s}^{J'\tilde{M}'} (2\pi)\, \delta(E_f - E_i) \frac{V^3 \mathbf{dp}_e \mathbf{dp}_\nu \mathbf{dk}}{(2\pi)^9}$$

If the spin dependence of the $\beta$-decay probability and the angular distributions are not measured, then we can integrate over $d\Omega_k$ and then sum it up over $m', m'_s$. This puts the product $C^{J'M'}_{l'm'S'm'_s} C^{J'\tilde{M}'}_{\tilde{l}'\tilde{m}'S'm'_s}$ to unity due to the orthogonality of the Clebsch-Gordon coefficients. And the expression for the probability, we get after it, is absolutely the same as equation (2.9) in the previous section (of course, the reduced matrix element is more complicated here).

### 2.2.5 Three-body continuum daughter state

In this section we will discuss the following model calculation: the initial state is represented by a three-cluster discrete spectrum WF and the daughter state belongs to the three-body continuum of the same clusters. It is not the case for the nuclei, like $^8$He, $^9$Li, $^{11}$Li where this type of $\beta$-decay (three-body continuum daughter state) really occurs. How we shall deal with such systems is shown in the example of the $^8$He $\beta$-decay in [P4] (Section 6). Here we do not repeat these speculations, but present a detailed derivation of the expressions for the probability for the simple case mentioned above.

Let us construct the WF of the initial state as a *hyperspherical harmonic* method WF in (LS) coupling (for details see Section 2.1.3 ).

$$\Psi^{JM}_{TT_3} = \rho^{-5/2} \sum_{KLSl_xl_y} \chi_{KLSl_xl_y}(\rho)\ \mathcal{L}^{JM}_{KLSl_xl_y}(\Omega\rho)\ \Phi_{TT_3}$$

Function $\mathcal{L}^{JM}_{KLSl_xl_y}(\Omega_5)$ contains not only hyperangular dependence, but also internal functions of the clusters, coupled in total angular momentum $S$.

$$\mathcal{L}^{JM}_{KLSl_xl_y}(\Omega\rho) = \psi^{l_xl_y}_K(\theta)\left[\left[Y_{l_x}\otimes Y_{l_y}\right]_L \otimes \Psi_S(clusters)\right]_{JM}$$

Factorization of function $\Psi^{JM}_{TT_3}$ for spin-angular-radial and isotopic spin parts, suggested above is not obligatory in reality, but was accounted here not to make derivations too detailed.

To construct the three-body continuum WF, in a close analogy to the two-body case we begin with plane wave. The expansion of the 6-dimensional plane wave over the hyperspherical harmonics is given by

$$\frac{1}{V}\exp\{i\mathbf{P}_x\mathbf{X} + i\mathbf{P}_y\mathbf{Y}\} = \frac{1}{V}\exp\{i\mathbf{p}_x\mathbf{x} + i\mathbf{p}_y\mathbf{y}\} =$$

$$= \frac{(2\pi)^3}{V(\varkappa\rho)^2} \sum_{KLM_Ll_xl_y} i^K J_{K+2}(\varkappa\rho)\, \mathcal{J}^{LM_L}_{Kl_xl_y}(\Omega\rho)\, \mathcal{J}^{LM_L}_{Kl_xl_y}(\Omega_\varkappa) \qquad (2.11)$$

$$\mathcal{J}^{LM_L}_{Kl_xl_y}(\Omega) = \psi^{l_xl_y}_K(\theta)\ \left[Y_{l_x}(\hat{x})\otimes Y_{l_y}(\hat{y})\right]_{LM_L}$$

$$\Omega_\varkappa = \{\theta_\varkappa, \hat{p}_x, \hat{p}_y\} \quad ; \qquad \varkappa = \sqrt{2ME} = \sqrt{2M\left(E_x + E_y\right)} = \sqrt{p_x^2 + p_y^2}$$

$$\theta_\varkappa = \arctan\left(\sqrt{E_x/E_y}\right) = \arctan\left(p_x/p_y\right)$$

$$\Omega_\rho = \{\theta_\rho, \hat{x}, \hat{y}\} \quad ; \qquad \rho = \sqrt{x^2+y^2} \quad ; \qquad \theta_\rho = \arctan(x/y)$$

where $\mathbf{X}$, $\mathbf{Y}$ and $\mathbf{P}_x$, $\mathbf{P}_y$ are Jacobi coordinates and momenta; $\mathbf{x}$, $\mathbf{y}$ and $\mathbf{p}_x$, $\mathbf{p}_y$ are normalized Jacobi coordinates and momenta (for definition see Section 7.2 of the Appendix). Note that momentum $\mathbf{p}_y$ is connected with momentum $P_3$ of the "third" particle in a simple way:

$$\mathbf{P}_3 = -\sqrt{\frac{(A_1+A_2)A_3}{A_1+A_2+A_3}}\,\mathbf{p}_y$$

After it we incorporate total spin of the clusters in equation (2.11) and replace $J_{K+2}(\varkappa\rho)$ with solution of the hyperradial equation $\sqrt{\frac{2}{\pi\varkappa\rho}}\chi^{K'L'S'l'_x l'_y}_{KLSl_x l_y}(\varkappa\rho)$ (see for example [47])

$$\Psi^{JM}_{TT_3} = \sqrt{\frac{2}{\pi}}\,\frac{(2\pi)^3}{V(\varkappa\rho)^{5/2}} \sum_{KLl_x l_y} i^K \left( \sum_{K'L'S'l'_x l'_y} \chi^{K'L'S'l'_x l'_y}_{KLSl_x l_y}(\varkappa\rho)\; \mathcal{L}^{JM}_{K'L'S'l'_x l'_y}(\Omega\rho) \right) \times$$

$$\times \sum_{M_L} C^{JM}_{LM_L SM_S}\, \mathcal{J}^{LM_L}_{Kl_x l_y}(\Omega_\varkappa)\; \Phi_{TT_3}$$

There is no sum over quantum numbers $S$ and $M_S$ — the wave function have definite total spin and its projection in the outgoing channel. The normalization of the function $\chi(\varkappa\rho)$ is given by the asymptotic relation

$$\chi^{K'L'S'l'_x l'_y}_{KLSl_x l_y}(\varkappa\rho) \overset{\varkappa\rho\to\infty}{\sim} \sin(\varkappa\rho + (K+2)\pi/4 + \delta^{K'L'S'l'_x l'_y}_{KLSl_x l_y})$$

We see, that like in the two-body case (2.6), the three-body continuum WF can be split into two parts. Notation of one is identical to the notation of the discrete spectrum WF; it depends on all the coordinates and only on *total* energy of the system. The other is coefficient of the expansion of the continuum functions (hence with definite momenta and total spin of constituents) over the hyperspherical harmonics (functions with definite total angular momentum). In the three-body case this part is also responsible for the description of the correlations in momentum space (the distribution of energy between subsystems).

$$\Psi^{JM}_{TT_3} = \frac{1}{\varkappa^{5/2}} \sum_{KLl_x l_y} \Psi_{KLSl_x l_y}(E;\rho,\Omega\rho)\cdot i^K \sqrt{\frac{2}{\pi}}\,\frac{(2\pi)^3}{V} \sum_{M_L} C^{JM}_{LM_L SM_S}\, \mathcal{J}^{LM_L}_{Kl_x l_y}(\Omega_\varkappa)$$

$$\Psi_{KLSl_x l_y}(E;\rho,\Omega\rho) = \rho^{-5/2} \sum_{K'L'S'l'_x l'_y} \chi^{K'L'S'l'_x l'_y}_{KLSl_x l_y}(\varkappa\rho)\; \mathcal{L}^{JM}_{K'L'S'l'_x l'_y}(\Omega\rho)\; \Phi_{TT_3}$$

For differential probability of the $\beta$-decay we get the expression (it is written for one component $\{KLSl_xl_y\}$ in the initial state)

$$dW = \frac{1}{2J+1}\frac{G_V^2\lambda^2}{V^2E_eE_v}\left[p_e^\mu p_\nu^\upsilon + p_e^\mu p_\nu^\upsilon - (E_eE_\nu - \mathbf{p}_e\mathbf{p}_\nu)\,\eta^{\mu\upsilon}\right]\sum_{MM'\tilde{M}'} C^{J'M'}_{JM1\mu}C^{J'\tilde{M}'}_{JM1\upsilon}\times$$

$$\times\sum_{S'M'_S}\sum_{K'L'M'_Ll'_xl'_y}\left(\frac{1}{\varkappa^{5/2}}\sum_{k=1}^{N}\left\langle J',K'L'S'l'_xl'_y\,\|\sigma_k\|\,J,KLSl_xl_y\right\rangle\left\langle\tau_k^-\right\rangle\right)^*\times$$

$$\times\sum_{\tilde{K}'\tilde{L}'\tilde{M}'_L\tilde{l}'_x\tilde{l}'_y}\left(\frac{1}{\varkappa^{5/2}}\sum_{\tilde{k}=1}^{N}\left\langle J',\tilde{K}'\tilde{L}'S'\tilde{l}'_x\tilde{l}'_y\,\|\sigma_{\tilde{k}}\|\,J,KLSl_xl_y\right\rangle\left\langle\tau_k^-\right\rangle\right)\frac{2(2\pi)^6}{\pi V^2}\times$$

$$\times\sum_{\tilde{M}'_LM'_L}\mathcal{J}^{L'M'_L*}_{K'l'_xl'_y}(\Omega_\varkappa)\mathcal{J}^{\tilde{L}'\tilde{M}'_L}_{\tilde{K}'\tilde{l}'_x\tilde{l}'_y}(\Omega_\varkappa)\;C^{J'M'}_{L'M'_LS'M'_S}C^{J'\tilde{M}'}_{\tilde{L}'\tilde{M}'_LS'M'_S}\times$$

$$\times\;(2\pi)\;\delta\left(E_f-E_i\right)\;\frac{V^4\mathbf{dp}_e\mathbf{dp}_\nu\mathbf{dp}_x\mathbf{dp}_y}{(2\pi)^{12}}$$

After integration over $d\Omega_x d\Omega_y$ and summation over magnetic quantum numbers

$$dW = \frac{1}{2J+1}\frac{G_V^2\lambda^2}{2}\,(2\pi)\,\delta\left(E_e{+}E_\nu+E_x+E_y-Q\right)\frac{6}{V^2}\left(1-\frac{\mathbf{p}_e\mathbf{p}_\nu}{3E_eE_\nu}\right)\times$$

$$\times\frac{2J'+1}{3}\left|\sum_{K'l'_xl'_y}\left(\sum_{L'S'}\sum_{k=1}^{N}\left\langle J',K'L'S'l'_xl'_y\,\|\sigma_k\|\,J,KLSl_xl_y\right\rangle\left\langle\tau_k^-\right\rangle\right)\psi^{K'}_{l'_xl'_y}(\theta_\varkappa)\right|^2\times$$

$$\times\;\frac{2}{\pi}\,\frac{p_x^2dp_xp_y^2dp_y}{\varkappa^5}\,\frac{V^2\mathbf{dp}_e\mathbf{dp}_\nu}{(2\pi)^6}$$

$$dW = \frac{G_V^2\lambda^2}{2\pi^3}\left(\delta\left(E_e+E\nu+E_x+E_y-Q\right)p_e^2dp_epu^2dp\nu\right)\times$$

$$\times\frac{2J'+1}{2J+1}\left|\sum_{K'l'_xl'_y}\left(\sum_{L'S'}\sum_{k=1}^{N}\left\langle J',K'L'S'l'_xl'_y\,\|\sigma_k\|\,J,KLSl_xl_y\right\rangle\left\langle\tau_k^-\right\rangle\right)\psi^{K'}_{l'_xl'_y}(\theta_\varkappa)\right|^2\times$$

$$\times\;\frac{\sqrt{2M}}{2\pi}\,\frac{\sqrt{E_xE_y}dE_xdE_y}{E^{5/2}}$$

Introducing the $B_{GT}$ value, which now depends on the distribution of energy between the subsystems, we can write expression for the $\beta$-decay probability:

$$W = \frac{G_V^2\lambda^2m_e^5}{2\pi^3}\,\frac{\sqrt{2M}}{2\pi}\int_0^Q\frac{dE_y}{\sqrt{E_y}}\int_0^{Q-E_y}\frac{dE_x}{\sqrt{E_x}}\,B_{GT}(E_x,E_y)\,f\left(A,Z,Q-E_x-E_y\right) \tag{2.12}$$

Here we present few alternative notations for this formula. These notations use the definition of coefficients through the $ft(0^+\to0^+)$ value or express the

probability in the terms of branching ratio to some other $\beta$-decay process with known half-life time $t_{1/2}(main)$.

$$W = \frac{\lambda^2 \ln 2\sqrt{2M}}{4\pi\, ft(0^+ \to 0^+)} \int\limits_0^Q \frac{dE_y}{\sqrt{E_y}} \int\limits_0^{Q-E_y} \frac{dE_x}{\sqrt{E_x}}\, B_{GT}(E_x, E_y)\, f\,(A, Z, Q - E_x - E_y)$$

$$Br = \frac{\lambda^2 t_{1/2}(main)\sqrt{2M}}{4\pi\, ft(0^+ \to 0^+)} \int\limits_0^Q \frac{dE_y}{\sqrt{E_y}} \int\limits_0^{Q-E_y} \frac{dE_x}{\sqrt{E_x}}\, B_{GT}(E_x, E_y)\, f\,(A, Z, Q - E_x - E_y)$$

In the particular case of the $\beta$-decay, which operator is diagonal in respect with $K$ and angular quantum numbers (it is not displayed in the formulae above, where we keep different indexes for all the initial and final state quantum numbers), then

$$B_{GT}(E_x, E_y) = \frac{2J'+1}{2J+1} \frac{E_x E_y}{E^{5/2}} \times$$

$$\times \sum_{LS' l'_x l'_y} \left| \sum_K \left( \sum_{k=1}^N \left\langle J', KLS' l'_x l'_y \right\| \sigma_k \left\| J, KLS l_x l_y \right\rangle \left\langle \tau_k^- \right\rangle \right) \psi^K_{l'_x l'_y}(\theta_\varkappa) \right|^2 \qquad (2.13)$$

The reduced ME have the following structure:

$$M_{K',\gamma'}(E) = \left\langle J', K'L'S'l'_x l'_y \right\| \sigma_k \left\| J, KLS l_x l_y \right\rangle =$$

$$= \sum_{S''} A^{J',K'L'S'l'_x l'_y}_{J,KLSS'' l_x l_y} \int\limits_0^\infty \chi^{K'L'S'l'_x l'_y}_{KLS'' l_x l_y}(\varkappa\rho)\; \chi_{KLS l_x l_y}(\rho)\, d\rho \qquad (2.14)$$

and hence depend only on the total energy $E = E_x + E_y$. Coefficient $A$, having numerous indexes includes angular momentum algebra term and overlap integrals of internal WFs of constituent clusters.

The integrated over the energy value of $B_{GT}$ (which is the subject of the GT sum rule) is given by

$$B_{GT}(int) = \frac{\sqrt{2M}}{2\pi} \int\limits_0^Q \frac{dE_y}{\sqrt{E_y}} \int\limits_0^{Q-E_y} \frac{dE_x}{\sqrt{E_x}} \cdot B_{GT}(E_x, E_y)$$

Expression (2.12) give us a $\beta$-delayed spectrum of the "third" particle, if we remove integration over $dE_y$. We can obtain the spectra of the other particles using the formalism of Raynal-Revai unitary transformation [84]. This transformation converts hyperspherical harmonics between different Jacobi systems.

$$\mathcal{J}^{LM_L}_{Kl_x l_y}(i;\Omega) = \sum_{l'_x l'_y} R^{l'_x l'_y}_{l_x l_y}(j \to i; KL)\, \mathcal{J}^{LM_L}_{Kl'_x l'_y}(j;\Omega) \qquad (2.15)$$

In the case of the $\beta$-decay, the reduced matrix elements are transformed in a simple manner:

$$\langle J', KLS' l_x l_y \| \sigma_k \| J, KLS l_x l_y \rangle (i) =$$
$$= \sum_{l'_x l'_y} \left( R^{l'_x l'_y}_{l_x l_y} (j \to i; KL) \right)^2 \langle J', KLS' l'_x l'_y \| \sigma_k \| J, KLS l'_x l'_y \rangle (j)$$

## 2.3 Probability of M1 transition

The operator of M1 transition is ordinary obtained using the following assumptions:

- the density of the transition Hamiltonian is $H(\mathbf{r}) = -(\mathbf{A}(\mathbf{r}) \cdot \mathbf{j}(\mathbf{r}))$ for the transverse calibration of the electromagnetic field.
- For the long-wave approximation of the electromagnetic field $qr \gg 1$, only the M1 multipole is taken into account in the expansion of the field.
- A simple form of the nucleon current including orbital and spin parts is

  $$\langle f | \mathbf{j}(\mathbf{r}) | i \rangle = e \sum_{k=1}^{N} \int \prod_{t=1}^{N} \mathbf{dr}_t \delta(\mathbf{r} - \mathbf{r}_k) \left\{ \Psi_f^* \frac{\vec{\nabla}_k - \overleftarrow{\nabla}_k}{2M} \Psi_i + K_k \left[ \vec{\nabla}_k \times \left( \Psi_f^* \frac{\boldsymbol{\sigma}_k}{2M} \Psi_i \right) \right] \right\}$$

  where the functions $\Psi_f$ and $\Psi_i$ depend on all the coordinates $\mathbf{r}_t, t = 1 \ldots N$, $K_k$ is magnetic moment of the nucleon number $k$, $M$ is a nucleon mass

After this, the operator giving matrix element of the transition Hamiltonian (it depends on $\lambda$ – the magnetic quantum number connected with the polarization of the produced photon) is obtained

$$\hat{H}_\lambda = -\sqrt{\frac{2\pi}{qV}} \frac{\lambda q e}{2M} \sum_{k=1}^{N} \left[ \left( \frac{1 + \tau_k^0}{2} \right) \mathbf{L}_k + K_p \left( \frac{1 + \tau_k^0}{2} \right) \boldsymbol{\sigma}_k + K_n \left( \frac{1 - \tau_k^0}{2} \right) \boldsymbol{\sigma}_k \right]_\lambda$$

This formula already includes the normalization of the photon WF ($V$ is normalization volume). The density of the final states for photons should be taken in the ordinary form

$$d\rho_f = \frac{V d^3 q}{(2\pi)^3}$$

Using the fact, that M1 transition occurs between orthogonal states, and operator of the total angular momentum $\mathbf{J} = \sum_{k=1}^{N} (\mathbf{L}_k + \boldsymbol{\sigma}_k / 2)$ would not have nonzero matrix elements between them, the expression above can be rewritten

$$H^\lambda = -\sqrt{\frac{2\pi}{qV}} \frac{\lambda q e}{4M} \sum_{k=1}^{N} \left[ (K_p + K_n - 1/2) \sigma_k^\lambda + \left\{ L_k^\lambda + (K_p - K_n) \sigma_k^\lambda \right\} \tau_k^0 \right] \quad (2.16)$$

$$K_p = 2.79 \quad ; \qquad K_n = -1.91 \quad ; \qquad e^2 = 1/137$$

The reduced matrix element of the operator (2.16), assuming orthogonality in the isospin space, the WFs of initial and final nuclei, is given by

$$M_{M1} = -\sqrt{\frac{2\pi}{qV}} \frac{\lambda q e}{4M} \left(K_p - K_n\right) \sum_{k=1}^{2} \left\langle J' \left\| \sigma_k \right\| J \right\rangle \left\langle T' T'_3 \left| \tau_k^0 \right| T T_3 \right\rangle$$

Which produce using Fermi rule the following equation for the probability:

$$dW = 2\pi\, \delta\left(E_f - E_i\right) \sum_{\lambda,\lambda'=-1}^{1} \frac{1}{2J+1} \sum_{MM'} \left|M_{M1}\right|^2 C^{J'M'}_{JM1\lambda'} C^{J'M'}_{JM1\lambda} \frac{V d^3 q}{(2\pi)^3}$$

Summing up over $M$, $M'$ (see formula (2.4) ) and integrating over the angles of the photon

$$dW = 2\pi\, \delta\left(q - E\right) \sum_{\lambda,\lambda'=-1}^{1} \frac{1}{2J+1} \left| \sum_{k=1}^{2} \left\langle J' \left\| \{\ldots\}_k \right\| J \right\rangle \left\langle T' T'_3 \left| \tau_k^0 \right| T T_3 \right\rangle \right|^2 \times$$

$$\times \frac{2J'+1}{3} \lambda^2 \delta_{\lambda\lambda'} \frac{2\pi}{qV} \frac{q^2 e^2}{16M^2} \frac{V 4\pi q^2 dq}{(2\pi)^3} \tag{2.17}$$

where $\Delta E$ is the energy release of the reaction and $\{\ldots\}_k = \{L_k + \left(K_p - K_n\right)\sigma_k\}$

$$W = \left( \frac{2J'+1}{2J+1} \left| \sum_{k=1}^{2} \left\langle J' \left\| \{\ldots\}_k \right\| J \right\rangle \left\langle T' T'_3 \left| \tau_k^0 \right| T T_3 \right\rangle \right|^2 \right) \frac{e^2 \Delta E^3}{12M^2}$$

Expression in the brackets looks very much like the definition of the $B_{GT}$ for the $\beta$-decay and we will refer it as $B_{M1}$.

$$W = \frac{e^2 \Delta E^3}{12M^2} B_{M1} \quad ; \quad B_{M1} = \left( \frac{2J'+1}{2J+1} \left| \sum_{k=1}^{2} \left\langle J' \left\| \{\ldots\}_k \right\| J \right\rangle \left\langle T' T'_3 \left| \tau_k^0 \right| T T_3 \right\rangle \right|^2 \right)$$

# Chapter 3

# Physical processes

*There is no Science of nuclei.*
*There are Sciences of each individual nucleus.*

*D.P. Grechukhin*

The discussion of different processes in this chapter aims to fill omissions and complement places in our articles not detailed enough. Some questions are also not suited to be described in the refereed literature, because they are too "trivial". So, here I try to "shed more light" on some **fragments** of our work which are not advertised enough in the articles, omitted for triviality or "hidden" in the old works. The brief but **overall** view of the field is given in the next chapter.

## 3.1 Nucleons RMS radii and halo concept

It is often possible to find in the current literature, dedicated to the nuclei close to the neutron (proton) drip line, discussion about if this or that nucleus has a *halo* or only *skin* or neither of them. I would like to participate in this discussion, making a little exercise introducing the numerical gauge for the halo property of the nuclei. The *haloism coefficient*[1] is defined as a ratio of mean radii for nucleons from halo and from core (considered from the system center of mass)

$$\mathcal{H} = \frac{r_n(halo)}{r_n(core)}$$

For one nucleon halo systems (with mass number $A$) it can be obtained from the experimental RMS matter radii values for the whole system $R_{(A)}$ and the

[1] If we believe in the existence of halos, this coefficient should be of fundamental importance for our field.

core nucleus $R_{(A-1)}$ in a model independent way[2]

$$r_n(halo) = \sqrt{\frac{A-1}{A}\left(AR^2_{(A)} - (A-1)R^2_{(A-1)}\right)}$$
$$r_n(core) = \sqrt{\frac{1}{A-1}R^2_{(A)} + \frac{A-1}{A}R^2_{(A-1)}}$$

It can easily be obtained from the definition of the RMS matter radius for the system mass number $A$ :

$$AR^2_{(A)} = \sum_{i=1..A} < R^2_i >$$

For two-nucleon halos the relation is not so simple, because the average distance from the CM to the core $r(core)$ depends on the correlations between valence nucleons; it should be calculated. Three-body codes give as values $r_n(halo)$ and $r(core)$ and

$$r_n(core) = \sqrt{r(core)^2 + R^2_{(A-2)}}$$

Values of *haloism coefficients* together with radii, they are based on, are given in the following table.

| Nucleus | Model | $R_{(A)}$ | $R_{(A-i)}$ | $r_n(halo)$ | $r(core)$ | $r_n(core)$ | $\mathcal{H}$ |
|---|---|---|---|---|---|---|---|
| $^{11}$Be | $^{10}$Be+n | 2.73 | 2.3 | 5.72 | 0.57 | 2.37 | 2.41 |
| $^{11}$Li | $^{9}$Li+n+n | 3.12 | 2.32 | 5.65 | 0.91 | 2.49 | 2.27 |
| $^{6}$He | $\alpha$+n+n | 2.57 | 1.46 | 3.46 | 1.24 | 1.92 | 1.81 |
| $^{8}$B | "$^{7}$Be"+p | 2.52$^{\dagger}$ | 2.09$^{\dagger}$ | 3.82 | 0.55 | 2.16 | 1.77 |
| $^{6}$Li | $\alpha$+n+p | 2.35$^{\dagger}$ | 1.46 | 3.06 | 1.20 | 1.89 | 1.62 |
| $^{8}$Li | "$^{7}$Li"+n | 2.37 | 2.05$^{\dagger}$ | 3.25 | 0.46 | 2.10 | 1.55 |
| $^{17}$Ne | $^{15}$O+p+p | 2.75 | 2.59 | 3.74 | 0.35 | 2.62 | 1.43 |

**Table 1.** $^{\dagger}$Theoretical values. Wave functions of $^{8}$Li and $^{8}$B were obtained in the three-body model $\alpha$+$t$($^{3}$He)+n(p). In these calculations "$^{7}$Li" and "$^{7}$Be" clusters appear to be contracted in comparison with free nuclei: $R_{^7Li} = 2.32$ and $R_{^7Be} = 2.35$ fm. Most of the radii included in columns 2 and 3 can be found in [3, 91, 4, 5, 6].

One can see that after introduction of coefficient $\mathcal{H}$ we have to revise our understanding about which nuclei have halo. The most studied halo nuclei $^{11}$Li and $^{11}$Be are certainly out of any competition. But we find that $^{8}$B has practically as developed halo as the "classical" halo nucleus $^{6}$He (inspite of strong Coulomb interaction). And what is quite unexpected even in $^{8}$Li, considered to be normal

[2]Problem is that the RMS radii values can be model dependent themselves. See discussion and reexamination of radii for $^{8}$B, $^{11}$Li, $^{11}$Be in [8].

"compact" nucleus, one neutron is leaving in average more then 1.5 times further from the center of mass then the rest of nucleons. Of course when one speaks about "neutron skin", the radial excess connected with only one (or two) valence neutrons, is "shared" among all of them. And you we not feel the full scale of the halo property, demonstrated here by a very simple calculations.

## 3.2 The beta-decay of $^6$He to $^6$Li g.s.

The reasons why this process is interesting and instructive are the following:

- The process is well studied experimentally. The half life of $^6$He is known with a great precision $t_{1/2} = 806.7 \pm 1.5$ ms [4]. Because of low energy release (3.504 MeV) there is no doubt that it is entirely allowed Gamow-Teller decay.
- The value of $B_{GT} = 4.745 \pm 0.02$ deduced from experimental half life time is a champion in the sense of the Gamow-Teller sum rule. In this nucleus 79% of the sum rule is exhausted by the GT resonance (which is the ground state of $^6$Li). We remind that in heavy nuclei the lack of the GT sum rule is ordinary about 60% in the whole spectrum (real measurements up to a hundred MeV) [62, 63].
- There is a lot of experimental information about $^6$He and $^6$Li, which are the initial and final nuclear states for this reaction. A few successful theoretical models, explaining many observables for these systems have recently been developed [71, 58, 94, 24, 44, 14, 43, 106, 41, 95, 19], [61, 59, 60, 12, 70, 49, 101].

Within our collaboration $^6$He $\beta$-decay to $^6$Li g.s. was studied in [44], and in details in [46]. $B_{GT} = 4.923 \pm 0.05$ was found in these calculations. Here we follow mainly the results of the last reference, but we will also give some formulae which we need for the discussions later. We use for this calculation the hyperspherical harmonic method WF (for details see Sections 2.1.1, 7.3 ).

$$\Psi^{JM}_{TT_3} = \rho^{-5/2} \sum_{KLSl_xl_y} \chi_{KLSl_xl_y}(\rho)\ \mathcal{L}^{JM}_{KLSl_xl_y}(\Omega_5)\, \Phi_{TT_3}$$

The $\alpha$-core is a spectator in the $\beta$-decay. One-particle reduced matrix element between coordinate parts of $^6$He ($0^+1$) and $^6$Li ($1^+0$) WFs for valence nucleons is given by

$$\langle J' \| \sigma_k \| J \rangle = \sum_{LSS'} \begin{bmatrix} (-)^S, k=1 \\ (-)^{S'}, k=2 \end{bmatrix} \hat{J}\hat{S}' \begin{Bmatrix} J & L & S \\ S' & 1 & J' \end{Bmatrix} \hat{S}\frac{\hat{1}}{2} \begin{Bmatrix} S & 1/2 & 1/2 \\ 1/2 & 1 & S' \end{Bmatrix} \times$$

$$\times (-)^{J'+L+1} \langle 1/2 \| \sigma \| 1/2 \rangle \sum_{Kl_xl_y} \int \chi^{Li}_{KLS'l_xl_y}(\rho)\, \chi^{He}_{KLSl_xl_y}(\rho)\, d\rho \qquad (3.1)$$

The formula (9.7) for the reduced ME of operator $\sigma$ between states of two nucleons with total spins was used here. Together with the matrix element of the isospin operator $\tau$

$$\left\langle T'T'_3 \left| \tau_k^- \right| TT_3 \right\rangle = \left\langle 00 \left| \tau_k^- \right| 11 \right\rangle = \left\langle \frac{\uparrow\downarrow - \downarrow\uparrow}{\sqrt{2}} \left| \tau_k^- \right| \uparrow\uparrow \right\rangle = (-)^{k+1}/\sqrt{2}$$

it gives for $B_{GT}$ (the definitions of operators and some reduced ME are given in the Section 9.2 ):

$$B_{GT} = 6 \left( \sum_{\substack{K=0,2,... \\ l=even}} \int \chi^{Li}_{K01l} \chi^{He}_{K00l} d\rho - \frac{1}{\sqrt{3}} \sum_{\substack{K=2,4,... \\ l=odd}} \int \chi^{Li}_{K10l} \chi^{He}_{K11l} d\rho \right)^2 \qquad (3.2)$$

The coefficient 6=3(N-Z) arises also in the GT sum rule as an upper limit for the $B_{GT}$ value. A very large $B_{GT}$ value is obtained in our calculations due to the fact that dominating "admixture" components in $^6$Li ($\chi^{Li}_{21011}$) and in $^6$He ($\chi^{He}_{21111}$) have different signs, and hence the second term increases the matrix element. To get better feeling for the machinery, let us calculate this matrix element using shell-model one-particle WFs in (jj) coupling (with some unknown coefficients).

$$\Psi_{He} = A_H[s_{1/2}s_{1/2}]_0 + B_H[p_{3/2}p_{3/2}]_0 + C_H[p_{1/2}p_{1/2}]_0$$

$$\Psi_{Li} = A_L[s_{1/2}s_{1/2}]_1 + B_L[p_{3/2}p_{3/2}]_1 + C_L[p_{1/2}p_{1/2}]_1$$

Assuming equal oscillator radii for He and for Li the reduced ME is obtained

$$\langle J', j'l' \| \sigma_k \| J, jl \rangle = (-)^{k+1} \hat{J}\hat{j} \left\{ \begin{array}{ccc} J & j & j \\ j & 1 & J' \end{array} \right\} \hat{j}\frac{\hat{1}}{2} \left\{ \begin{array}{ccc} j & l & 1/2 \\ 1/2 & 1 & j \end{array} \right\} \delta_{jj'}\delta_{ll'} \times$$

$$\times (-)^J \langle 1/2 \| \sigma \| 1/2 \rangle \; D_L(j'l') D_H(jl)$$

The coefficient $D$ in this formula is $A$, $B$ or $C$ depending on $j$ and $l$. The $B_{GT}$ value is obtained in this approach as

$$B_{GT} = 6 \left( A_L A_H + \frac{\sqrt{5}}{3} B_L B_H + \frac{1}{3} C_L C_H \right)^2 \qquad (3.3)$$

To reproduce the experimental value of the $B_{GT}(\text{exp}) = 4.70 \pm 0.02$ with minimal weight of $s$-wave component we have to put the weight of $[p_{1/2}p_{1/2}]$ about zero and weight of the $[s_{1/2}s_{1/2}]$ on the level of 17–20%. This evaluation is pointing the drastic difference between the HH method collective WF and the COSMA WF, combined from one-particle WFs.

## 3.3 The beta-decay of $^6$He to alpha+d continuum

This decay is studied in [P1]. The details of experimental and theoretical status of the problem, as well as references can be found in the Section 4.2.2 "$\beta$-decay and M1 transition to $\alpha$+d continuum" in the next Chapter of the thesis. The investigation given in [P1] is now not the most advanced of those, which have been performed to understand the process. Nevertheless it is giving an instructive example, how the most intimate features of the nuclear structure may become observable in some circumstances. We would like to discuss this once again, since it was done in a rather brief manner in the article.

The drawback of our approach was, that while for the $^6$He ground state the exact three-body WFs were used, the $\alpha$+d continuum was constructed as a product of the $s$-wave deuteron WF and the optical $\alpha$+d relative motion WF. As this WF was not an eigen state of the three-body Hamiltonian, we orthogonalized it to the $^6$Li ground state WF, obtained in a three-body approach. Then the $B_{GT}$ value for the process can be written as follows (brackets here denote **only** overlap of **coordinate** parts of corresponding WFs ! )

$$B_{GT}(E) = 6 \left\{ \left\langle \alpha + d \right| - \frac{\left\langle \alpha + d \right| \left| {}^6Li \right\rangle}{\left\langle {}^6Li \right| \left| {}^6Li \right\rangle} \left\langle {}^6Li \right| \right\} \left| {}^6He \right\rangle^2 =$$

$$= 6 \left\{ \left\langle \alpha + d \right| \left| {}^6He \right\rangle - \left\langle \alpha + d \right| \left| {}^6Li \right\rangle \frac{\left\langle {}^6Li \right| \left| {}^6He \right\rangle}{\left\langle {}^6Li \right| \left| {}^6Li \right\rangle} \right\}^2 = \tag{3.4}$$

$$= 6 \left\langle \alpha + d \right| \left\{ \left| {}^6He \right\rangle - \left| {}^6Li \right\rangle \frac{\left\langle {}^6Li \right| \left| {}^6He \right\rangle}{\left\langle {}^6Li \right| \left| {}^6Li \right\rangle} \right\}^2$$

We see that effectively we can deal not with the continuum WF orthogonalized to the g.s. WF, but with the coordinate part of the $^6$He g.s. WF orthogonalized to the $^6$Li g.s. WF. This is much better from a presentation point of view, because in the latter case we have not only the functions of the same nature (discrete spectrum), but also spatially very similar functions (it can be found, for example, in [44]).

In the Figures 3.1 the WF of $^6$He is plotted in the plane of the Jacobi coordinates. The WF in Figure 3.1a is an exact three-body WF obtained in the calculations [44]. WF in Figure 3.1b is the COSMA method WF (see Section 2.1.4), which was proved to be good enough at least in some cases (see [106], Section 5). Asymptotic of this WF at large distances is absolutely incorrect, but it is difficult to see on this kind of plot. WFs of $^6$Li are not given because of its high spatial identity with $^6$He WF: one can scarcely see a difference.

But the spatial part of the $^6$He WF, orthogonalized to the spatial part of the $^6$Li WF (curled brackets in the last line of expression (3.4) ) is displaying this differences immediately. It is plotted in Figures 3.2, again for the exact

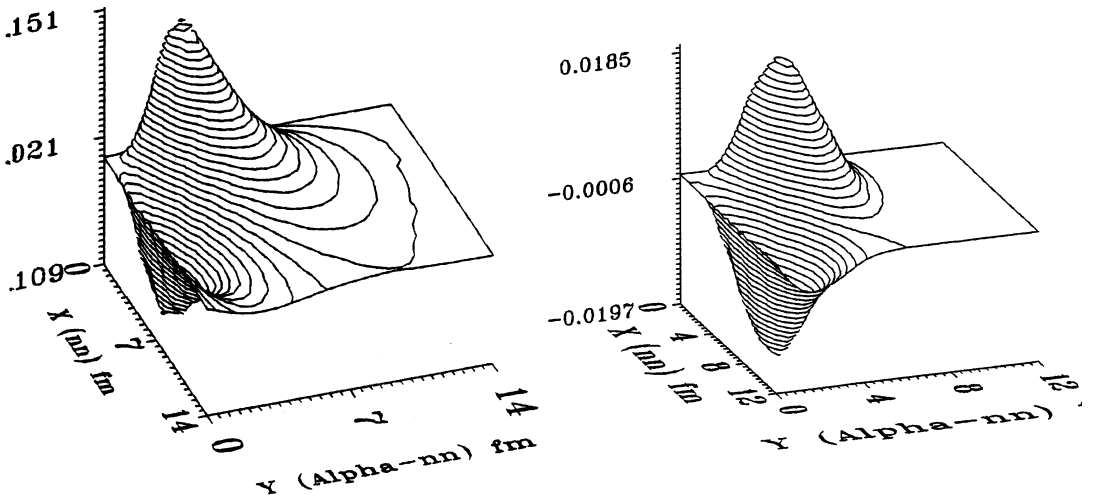


Figure 3.1: (a) Component with L=0, S=0, $l_x$=$l_y$=0 of the HH method WF of $^6$He. X is distance between neutrons; Y — between center of mass of two neutrons and $\alpha$. (b) Component with L=0, S=0, $l_x$=$l_y$=0 of the COSMA method WF of $^6$He.

WF (Figure 3.2a) and WF with incorrect asymptotic behavior (Figure 3.2b). Now it is evident that sensitivity to the asymptotic behavior is large and results obtained using WFs with incorrect asymptotic have no big sense. To obtain a $B_{GT}$ value from the WF presented in Fig. 3.2a it should be overlapped with the $\alpha$-d continuum WF. Figures 3.3 are giving the examples of such WFs at fixed energies. The $\alpha$-d relative motion WF plotted in Figure 3.3a, was obtained at $E_d$ = 450 keV in a deep potential; WF in Figure 3.3b was obtained at $E_d$ = 600 keV in a potential with $s$-wave repulsive core. Comparing Figures 3.2a and 3.2b–3.3a it is easy to understand that

1. The model for $\alpha$-d WF is not very essential for these calculations. This is confirmed by the results of calculations presented in [P1], Table 1. Difference in probabilities obtained with "opposite" (totally attractive and totally repulsive), but the phase equivalent potentials, is not more then 25%. Probably even exact dynamical calculations for the $\alpha$-d WF would not change the situation.

2. The most important region for overlap is between 9 and 14 fm in the coordinate Y. In Figure 1 we can see that the value of WF itself at such distances is very low, hence any slight deviation in the shape of the asymptotic would influence drastically the probability of the reaction.

According to the item 2, it should be pointed out that WF of $^6$He, used in the calculations [P1], have analytically truthful asymptotic. While the asymptotic of the $^6$Li WF can not be established that reliably. The methods of dealing with

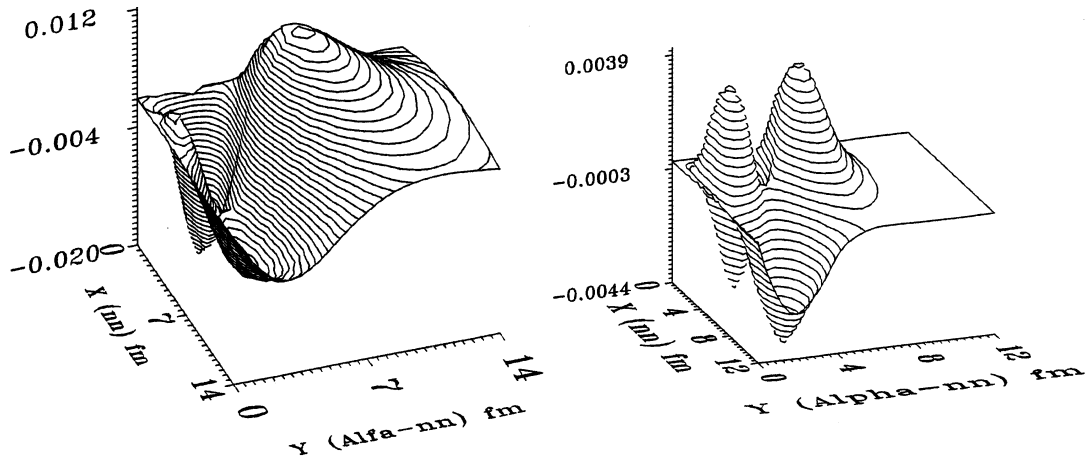


Figure 3.2: (a) Component with L=0, S=0, $l_x$=$l_y$=0 of the HH method WF of $^6$He after orthogonalization to $^6$Li ground state WF with the same quantum numbers. (b) Component with L=0, S=0, $l_x$=$l_y$=0 of the COSMA method WF of $^6$He after orthogonalization to $^6$Li ground state WF.

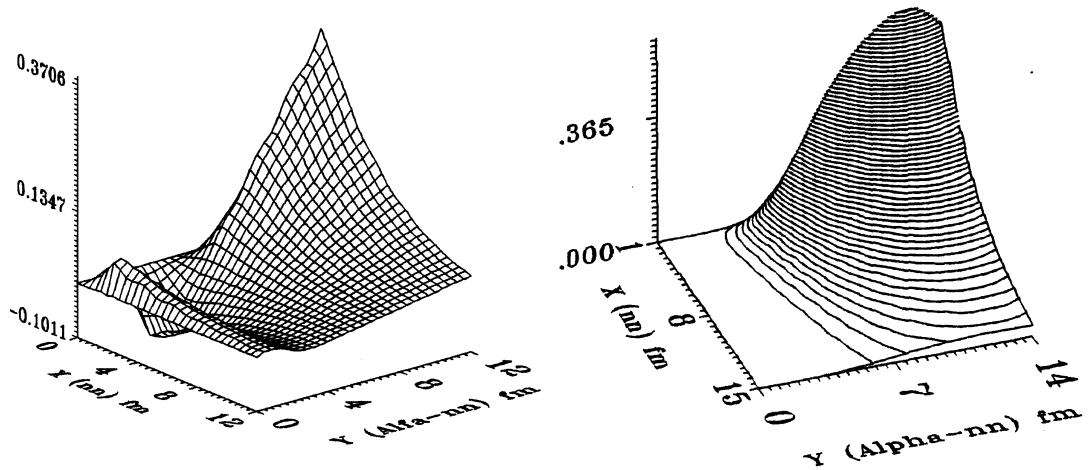


Figure 3.3: (a) The $\alpha$+d continuum WF at $E_d$=450 keV. This WF was obtained in a deep potential with forbidden states. (b) The $\alpha$+d continuum WF at $E_d$=600 keV. This WF was obtained with a purely repulsive potential.

the problem have already been developed [P7], but its application to the process, belongs to the future.

So this decay appears to be extremely sensitive to very fine details of nuclear structure. According to the results of the theoretical investigation of the process (not only by us), we can conclude that this level of precision have not yet been achieved by the theory of nuclear structure and reactions.

## 3.4 $^6$He: what about Gamow-Teller sum rule?

As we have seen in the Section 3.2, the Gamow-Teller transition to the ground state of $^6$Li exhaust about 82% of GT sum rule[3]. We know that $\beta$-decay in $\alpha$+d continuum is responsible for negligible part $\sim 10^{-5}$ of sum rule (See [85], [P1] and Sections 3.3, 4.2.2). So, where are the rest 18% ?

Following the results , expression (3.2) for $B_{GT}$ value can be written a symbolic form:

$$B_{GT} = 6\left(\left\langle {}^6Li, main\right| \left|{}^6He, main\right\rangle - \frac{1}{\sqrt{3}}\left\langle {}^6Li, adm\right| \left|{}^6He, adm\right\rangle\right)^2$$

where *main* and *adm* stand for dominating $L = 0$ and admixture $L = 1$ components of $^6$He, $^6$Li wave functions. It is clear, that, even if we insert instead of one final state a complete set of functions, the $B_{GT}$ value would never achieve the sum rule value 6 due to coefficient $\frac{1}{\sqrt{3}}$ at admixture ME. This lack of the sum rule is compensated, due to the transitions in the three-body continuum with $T = 1$ (certainly $T_3 = 0$ ).

The energy dependences of $B_{GT}$ values with normal $T = 0$ and opposite $T = 1$ total isospins are shown in Figure 3.4. The sum rule is exhausted (within 1% precision) by 15 MeV (over three-body threshold). About 11% are connected with $T = 0$ channel and about 5% with $T = 1$. We see that GT strength is very smoothly distributed in the continuum — no $1^+$ resonances; wide peaks at 2.7 and 5.0 MeV are connected with three-body kinematics more, then with some special dynamics of the continuum.

In the experimental studies of GT strength distribution (see for example [62, 63]), inelastic scattering of high-energy protons is measured under the lowest possible angle. A smooth background is subtracted. It should be noted that for heavy nuclei, with a lot of multiparticle emission channels opened, the GT strength associated with many-body continuum exit channels would be even smoother then in Figure 3.4. Can it happen so, that widely discussed deficit of the GT sum rule (which achieve 60% in some nuclei) is connected with subtraction of GT strength together with background ?

[3]That corresponds to our theoretical value $B_{GT} = 4.923$ .

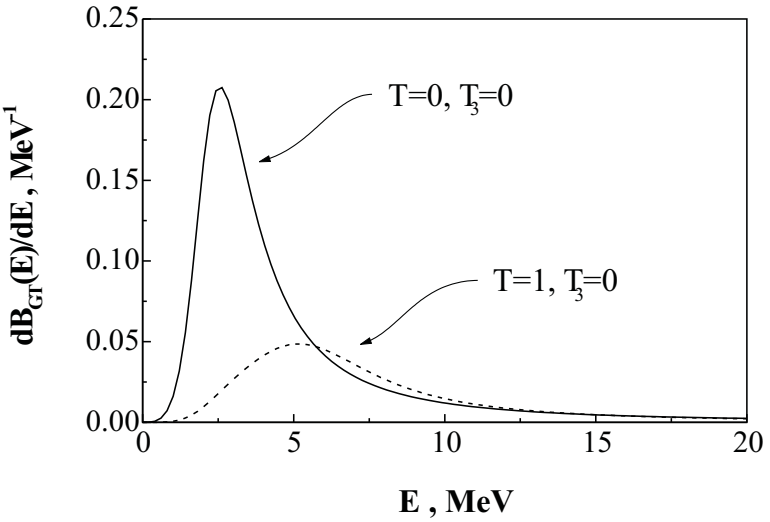


Figure 3.4: $B_{GT}$ strength as a function of energy. $E$ is the energy from the three-body breakup threshold. Solid curve is associated with transition in $J = 1$, $T = 0$, $T_3 = 0$ continuum; dashed curve — $J = 1$, $T = 1$, $T_3 = 0$ continuum.

## 3.5 The beta-decay of $^8$He to alpha+T+n continuum

**Why R-matrix sequential decay formalism** [17, 18, 82, 33] **is not adequate** for the analysis of few particle emission $\beta$-delayed spectra? In this section we address only this question, which was not emphasized enough in the [P4]. R-matrix theory is a powerful instrument in the theory of nuclear reactions and it has been successfully applied for many years. In some cases it was the only tool available for analysis of experimental data, which justify to some extent its application to the cases, where it is formally not applicable. Let us give the reasons why it is not suited for the analysis of experimental spectra (now only three-body) yielding from the highly excited states of the daughter nuclei.

1. R-matrix theory is based on the assumption about the behavior of the WF's logarithmic derivative on the surface of the nucleus. One of the conditions preceding this assumption is the short-range character of the nuclear interaction. It is not the case for the three-body continuum: effective potentials of the three-body problem are decaying as $\rho^{-3}$

2. Assumption of item 1 leads to the conclusion that close to the resonance two-body continuum WF is not changing the shape in the internal region of interaction, but only amplitude. This allows to predict easily the energy behavior of any ME including two-body continuum near resonance: well-known Breit-Wigner shape.

3. The statement of item 2 is perfectly correct for the narrow resonances: for

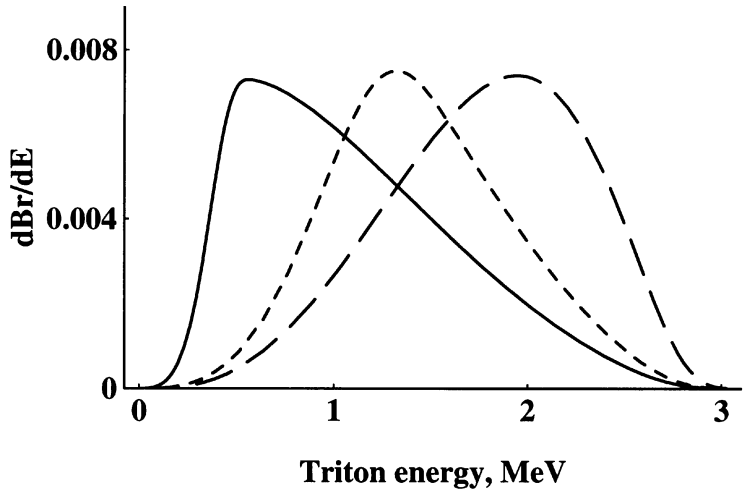


Figure 3.5: Possible R-matrix spectra demonstrating what kind of spectra can be obtained playing with radius of channel in the case of highly situated resonance. If the excitation energy is high enough the resonance itself is masked and you see only peak, connected with the phase volume of leptons, tail of the Breit-Wigner bell and penetrability. Resonance position is 10.4 MeV, width — 1.5 MeV. Radius of channel is: solid line — 5 fm; short dashed — 1.8 fm; long dashed — 0.9 fm.

example if the width of resonance is about 100 keV then the region of validity would be $\sim$ 2–7 MeV over the resonance. In the case of broad resonance this statement is violated within the width of resonance (corrections are introduced in R-matrix theory to improve the situation).

4. In the cases when the $\beta$-decay takes place through the highly excited states of $^8$He, $^9$Li or $^{11}$Li the resonance peak itself is masked by the phase volume of the leptons. And what is see on the fit is product of Breit-Wigner slope ($\sim (E - E_R)^{-2}$), phase volume of leptons ($\sim (Q - E)^5$) and two-body penetrability (which depends on charges and angular momenta).

   **Two-body penetrability** have nothing in common with the three-body system. It is used in [P4], Section 6 only to demonstrate possible form of a small Coulomb correction to the three-body spectrum. In the R-matrix fitting is completely defining the shape of spectrum.

   Resonance, situated 5-11 MeV above the first particle emission threshold is expected to be wide (at least $\sim$1 MeV). Hence the tail of the Breit-Wigner bell can not (at least may not) have anything in common with real energy profile of the ME.

Possible shapes of spectra easily obtained in such approach (and all prob-

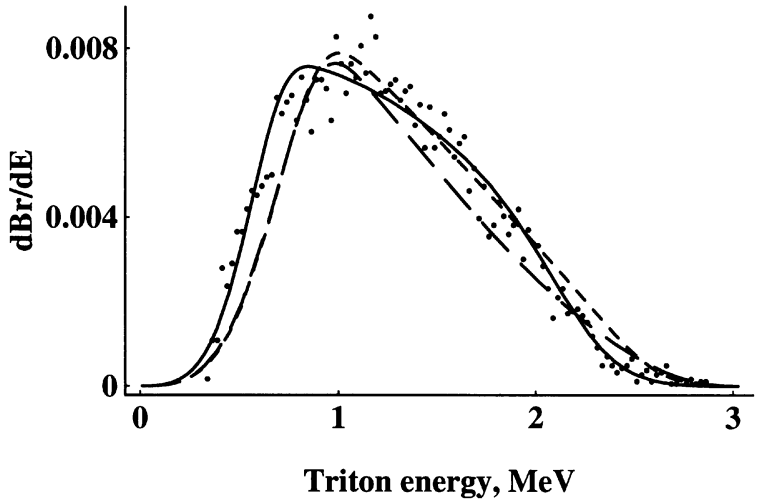


Figure 3.6: R-matrix fits demonstrating sensitivity of the $\beta$-delayed triton spectrum shape to the position of resonance (if resonance energy is high and close to the mother nucleus energy). Values specifying each curve are {Resonance position, Resonance width, Radius of channel, $B_{GT}$ value for the resonance}. Solid line — {9.3, 1.8, 3.2, 3.07}; Short dashed — {9.85, 1.6, 2.5, 6.35}; Long dashed — {10.4, 1.4, 2.5, 10.96}. If the position of resonance is taken higher then this, the shape of the spectrum is not changing any more.

ably meaningless) are shown in Figure 3.5 [4].

5. Introduction of the strong correlations in the momentum space is obligatory using R-matrix approach in the analysis of the three-body spectra from highly situated resonances. Existence of resonances in the subsystems (like $^5$He$^*$ in $^8$He) to my opinion can not be responsible for such correlations far in the continuum. In more details the question is discussed in [P4].

Ordinary the results of R-matrix fits are presented in the form of "best fit". Figures 3.6 and 3.7 are given to demonstrate the available freedom. If you allow "chi-squared", more than one, then you can see that interval where we may find $B_{GT}$ value is between 3 and $\infty$ and width of resonance between 1.7 and 6 MeV.

The penetrability $P_l(E)$ is defined in this calculations not in standard, but reasonable way, using the quasiclassical expression for probability of tunneling through the barrier:

$$P_l(E) = \exp\left\{-2\int_{R_c}^{r_+}\sqrt{2M_R(U_l(r)-E)}dr\right\}$$

[4]The energy of resonance in all the Figures is calculated in respect with $^8$Li g.s. Three-body threshold $\alpha$+T+n is 4.501 MeV and "two-body threshold" $^5$He$^*$+T is 5.651 MeV. All the presented R-matrix calculations are one channel and one level. Radius of channel here is defined nonstandardly.

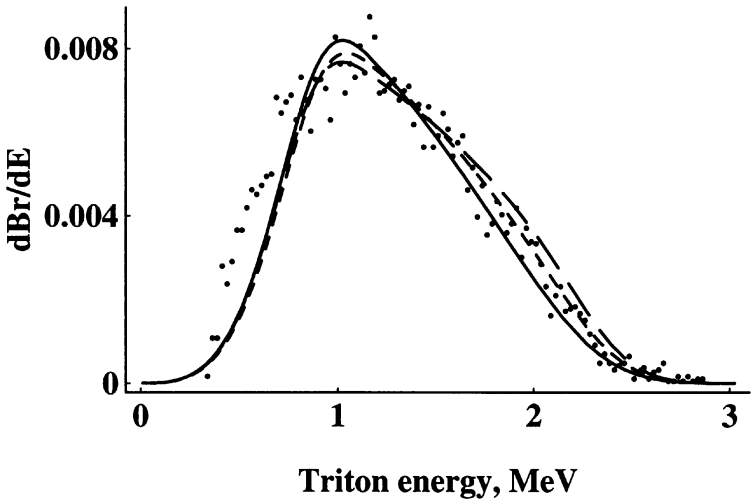


Figure 3.7: R-matrix fits demonstrating sensitivity of the $\beta$-delayed triton spectrum shape to the width of resonance (if resonance energy is high and close to the mother nucleus energy). Values specifying each curve are {Resonance position, Resonance width, Radius of channel, $B_{GT}$ value for the resonance}. Solid line — {9.5, 2.5, 2.4, 3.13}; Short dashed — {9.5, 2.0, 2.4, 3.73}; Long dashed — {9.5, 1.7, 2.5, 4.21}. If the width of resonance is taken greater then 2.5 MeV, the shape of the spectrum is not changing any more.

where $R_c$ is radius of channel, $r_+$ is the classical stopping point of the potential $U_l(r)$, which is sum of Coulomb and centrifugal energies, and $M_R$ is the reduced mass of the channel. So my results may deviate from the completely standard calculations. But for evaluation purposes they are sufficient.

## 3.6 The beta-decay of $^9$Li to alpha+alpha+n continuum

This Section is based on the work done in collaboration with I. Mukha and M. Zhukov. The complete results of analysis would be published elsewhere ([P8], in preparation).

A beta-decay of the lithium isotope $^9$Li gives an excellent opportunity to test the theoretical approach to analysis of the three-body $\beta$-decays proposed in paper [P4]. In $^8$He case we were studying the three-body decay of the state ($\sim$8.8 MeV) which we suspect to be a kind of compound state (Halo Analog state). In contrast, for $^9$Li $\beta$-decay all the excited states in the daughter, $^9$Be, break up into two alpha particles and one neutron and have internal structure dominated by three-cluster component. This decay is one of the most pure examples of the $\beta$-decay followed by the three-particle emission to continuum states. The system $\alpha + \alpha + n$ has only one really strong final state interaction channel (a resonance

$^8$Be($0^+$) between two $\alpha$'s ), which is not destroying the three-particle emission picture for most of states accessible in the $\beta$-decay.

The idea of the "generalized R-matrix approach" is following. If we know about the existence of the three-body decaying states in the spectrum we can simulate the energy behavior of the ME $M_{K,\gamma}$ in (2.14) by the expression similar to ordinary R-matrix formula. The "replacement" rule for the ME (neglecting the shift of the level) is:

$$M_{K,\gamma}(E) \to \sqrt{3(N_{nuc}-Z)\,\Phi_{K\gamma}}\,\frac{\Gamma^{1/2}_{K\gamma}(E)}{(E_R-E)-i\Gamma_{K\gamma}(E)/2} \tag{3.5}$$

Here $\Phi_{K\gamma}$ is a dimensionless value characterizing the overlap of the coordinate WFs of the mother and daughter states. This replacement is justified by the form of equations used in HH method:

$$\left[\frac{d^2}{d\rho^2}+\frac{\mathcal{M}(\mathcal{M}+1)}{\rho^2}+\{\,2ME-V_{K\gamma,K\gamma}(\rho)\,\}\right]\chi_{K\gamma}(\varkappa\rho)=$$

$$=\sum_{K'\gamma'\neq K\gamma} V_{K'\gamma',K\gamma}(\rho)\,\chi_{K'\gamma'}(\varkappa\rho) \tag{3.6}$$

$$\mathcal{M}=K+\frac{3}{2}\quad;\qquad V_{K'\gamma',K\gamma}(\rho)=\,2M\left(\mathcal{J}_{K\gamma}(\Omega\rho)\mid\sum_{j\neq i=1}^{N}V_{ij}(\rho,\Omega\rho)\mid\mathcal{J}_{K'\gamma'}(\Omega\rho)\right)$$

They are equivalent to one effective particle motion in a deformed field. In one channel approximation the energy dependence of the width, obtained by using HH equation, is practically the same as in R-matrix approach:

$$\Gamma_{K\gamma}(E)=2\,P_{\mathcal{M}}(E)\,\boldsymbol{\gamma}^2_{K\gamma}\quad;\qquad P_{\mathcal{M}}(E)=\frac{\varkappa\rho_c}{F^2_{\mathcal{M}}(\varkappa\rho_c)+G^2_{\mathcal{M}}(\varkappa\rho_c)}$$

The reduced width of the channel is denoted with bold letter $\boldsymbol{\gamma}$ to distinguish from multiindex $\gamma$. The physical meaning of the reduced width $\boldsymbol{\gamma}_{K\gamma}$ is the same, as in the two-body case, characterizing the spectroscopic factor for the three-body outgoing channel. The problem here is to choose radii of channels properly. This problem is resolved, may be not in the best, but in self-consistent way using the systematics of the known three-body decaying states properties.

Functions $F_{\mathcal{M}}$ , $G_{\mathcal{M}}$ are regular and irregular solutions of equation (3.6) for the case $V_{K'\gamma',K\gamma}(\rho)\equiv 0$ . In the absence of Coulomb interaction (systems like *core+n+n*) they can be written in terms of Bessel functions:

$$\begin{aligned} F_{\mathcal{M}}(\varkappa\rho) &= \sqrt{\pi\varkappa\rho/2}\;J_{\mathcal{M}+1/2}(\varkappa\rho)\\ G_{\mathcal{M}}(\varkappa\rho) &= \sqrt{\pi\varkappa\rho/2}\;Y_{\mathcal{M}+1/2}(\varkappa\rho)\end{aligned}$$

### 3.6.1 Available experimental data

To make a sound conclusions on the basis of the formalism discussed above we need a self-consistent set of the $\alpha$-particle and neutron data in the whole $\beta$-decay window. The complicated job of putting all the data together was done by I. Mukha and with permanent assistance of G. Nyman, using their experience from [82, 80]. One may find some aspects of the synthesized spectra dubious, but it displays the best level of experimental knowledge for today.

The decay scheme of $^9$Li was constructed mainly through the measurements of $\beta-$delayed neutrons and alpha particles, which have been studied in several experiments [9, 39, 76, 26, 75, 82]. In particular, the absolute value of a $^9$Li neutron branching ratio $P_n$ was evaluated of 50(3)% [26, 75, 82].

The measured $\alpha-$spectra displayed the clear evidence for the $\beta$-transitions to the highly excited states in $^9$Be at the excitation energy 11.28 MeV and/or 11.8 MeV. For the 11.28 MeV state the branching ratio (Br) was evaluated of 4.0(5)% in the [75] using the simplest phase volume assumption in analysis of the measured spectra of the $\beta$-delayed particles for both single $\alpha$-particles and $\alpha$-$\alpha$-coincidences. This branching gives $B_{GT}$=7(1) without correction for the width of the level[5]. The authors have claimed no $\beta-$feeding through the 11.81 MeV state with the upper limit Br$\leq$ 0.1%. Very interesting $E_1$+$E_2$ spectrum was constructed for the events suggested to originate from the 11.28 MeV state decay. Unfortunately this spectrum, clearly showing the strong energy correlations (deviation from the pure phase volume), was obtained using assumption about phase volume, and hence it is not very useful for our purposes.

In the work [82] the neutron and the alpha particle spectra were re-measured and a more sophisticated analysis was applied. The neutron energy spectrum was measured by the $^3$He spectrometer up to 3 MeV. But only the part of spectrum under 2 MeV was considered as reliable, due to the drastic drop of the spectrometer efficiency at higher energies. This spectrum is shown in Figure 3.8 by diamonds. The characteristic feature of the neutron spectrum is a sharp peak at about 682 keV, interpreted in [82] as the evidence of the decay via the narrow $^9$Be($5/2^-$) state to the binary channel $^8$Be(g.s.)+n. The width of the peak is defined mainly by the recoil effect due to a beta emission. The alpha spectrum was measured with a Si-detector telescope operated both in inclusive mode, which supplied a high statistics and in anti-coincidence mode, which suppressed the beta background contribution at low energies. The data were interpreted with a sequential emission mechanism for decay of the daughter $^9$Be states using R-matrix approach (applied to $\beta$-decays by Barker and Warburton, [18]), and corrections for a $\beta$-transition to broad level have been applied for the extracted $B_{GT}$ values. The analysis, sensitive mainly to a high energy part of the alpha spectrum, established the branching ratios of 1.1(2)% and of 2.7(2)% to the 11.28 MeV and 11.81 MeV states, respectively. This conclusion leads to surprisingly high values of the reduced transition probabilities $B_{GT}$=0.9(3) and $B_{GT}$=5.6(12),

[5]For some reason enormous $B_{GT}$ value (sum rule is 9) did not cause any questions in [75].

respectively, that one corrects the results of the [75]. But one should mention as well that the shapes of the measured $\alpha$-spectra in [82] do not agree internally at low energies. In particular, the "kink" in two $\alpha$-spectra in Figure 4 in [82] appears at different energies. In the present work we used the combination of those two spectra smoothly connected at about 1.2 MeV and normalized for known total branching to $2\alpha$+n continuum $P_n = 50(3)\%$.

Recently, an experimental study of $\beta$-delayed charged particles neutrons and $\gamma$-rays that follow the $^{11}$Li decay has been reported [34, 80, 35]. During this experiment, the $\beta$-delayed alpha and neutron spectra from the $^{9}$Li decay have been carefully measured as well. The charged particles were registered by a $\Delta$E-E telescope detector consisting of a thin gas $\Delta$E detector placed in front of a Si E-detector that allowed the discrimination of low-energy $\alpha$-particles from the $\beta$-background. The measured alpha spectrum for $^{9}$Li (see Fig. 3 in [80]) coincides with the previously published one in [82], which was measured in the inclusive mode, see the inset in Fig. 4 there. The only difference is that at energies below 500 keV the contribution of the $\beta$-background dominates in the $\alpha$-spectrum measured in [82], but at higher energies this spectrum has larger statistics. In the present work we have decided to include into analysis a combination of the two mentioned $\alpha$-spectra. Namely, the low energy part of the $\alpha$-spectrum from [80] (between a detection threshold of 350 keV and 700 keV) is more reliable then [82]. Spectrum [80] can be easily normalized, because it exactly overlaps with spectrum [82] in a wide energy range. The resulting spectra are shown in Figure 3.10.

A spectrum of $\beta$-delayed neutrons from $^{9}$Li, measured by scintillator detectors using a time-of-flight method, is shown in Figure 3.8 by dots with error-bars (see a description of the BC501 liquid-scintillator detector in [10]; the measurements will be reported in [36] in details). A threshold of neutron registration was of 0.8 MeV, so the neutron spectrum should be reliable at energies above 1.5 MeV. This spectrum was considered as an addition to the spectrum measured with the $^{3}$He spectrometer. Both n-spectra were normalized in the energy region 1.5–1.8 MeV for the known $P_n$ value.

### 3.6.2 Experimental data analysis

Analysis procedure was the following: a set of quantum numbers (QN) and other parameters fitting the neutron spectrum was found for the Jacobi system (($\alpha$-$\alpha$)-n), then the spectrum was converted to ($\alpha$-n)-$\alpha$) system to check the consistency of the whole picture. We can not simply fit $\alpha$ spectrum because of technical difficulties: we can not work in the system ($\alpha$-n)-$\alpha$) with pure harmonics but only with a specific mixtures of harmonics. These mixtures after conversion to (($\alpha$-$\alpha$)-n) system should not give odd waves in the $\alpha$-$\alpha$ relative motion. That is the reason making attempts to analyze the $\alpha$ spectrum from the $^{9}$Li $\beta$-decay as a sequential decay via the states of $^{5}$He (for example [18, 82]) are formally erroneous. The amplitudes with definite quantum numbers in the $\alpha$-n channel

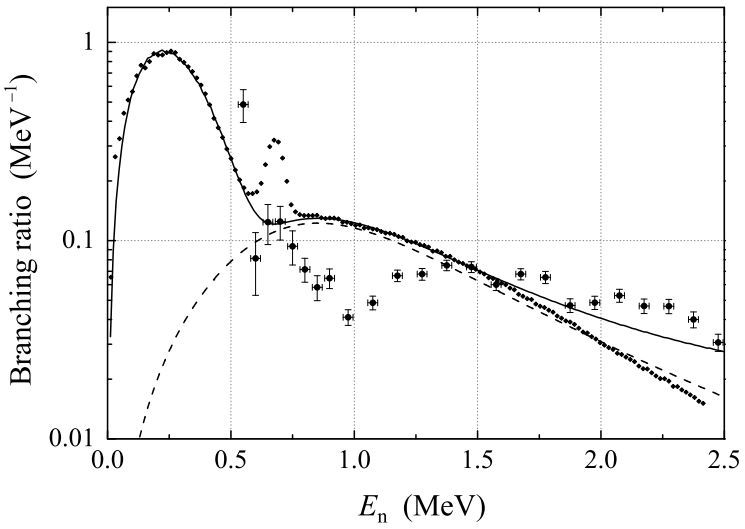


Figure 3.8: Diamonds gives the neutron spectrum from $^9$Li $\beta$-decay [82], measured with $^3$He spectrometer. Dots with error bars – time of flight spectrum from [36]. Spectra are adjusted to cross at about 1.5 MeV, where both of them are more or less reliable, and normalized to total branching ratio Br=0.5. Solid curve is full fit involving three-body contributions from 2.43, 11.28 MeV states and binary (channel $^8$Be+n) contribution from 2.7 MeV state. The later spectrum is shown also separately by dashed line.

usually have a significant Pauli forbidden components[6].

**Low energies ( $E^* < 3$ MeV)**

It was shown in papers [29, 82] that the wide bump in the neutron spectrum under 0.7 MeV is connected with the democratic decay (in terms of [82] it is decay via the tail of $2^+$ state in $^8$Be) of 2.43 MeV $5/2^-$ state. Our analysis of the neutron spectrum (Figs. 3.8, 3.9) nicely confirm the results of [29], where the QN $L = 2, l_x = 2, l_y = 1$ were assigned to the continuum WF of this state. We have to take into account not only the lowest $K$, but also the next. Relative weights of harmonics, totally normalized to unity, are (percentage in brackets come from analysis [29]):

$$\begin{array}{l} K = 3, L = 2, l_x = 2, l_y = 1 - 95\% \ (90\%) \\ K = 5, L = 2, l_x = 2, l_y = 1 - 5\% \ (10\%). \end{array} \tag{3.7}$$

The admixture of $K = 5$ is essential to shift the spectrum to lower energies. So it can be qualitatively understood as an admixture caused by Coulomb interaction:

[6]For negative parity states the exceptions are following hyperspherical harmonics ( in $\{K, L, l_x, l_y\}$ notation for (($\alpha$-$\alpha$)-n) Jacobi system): {1 1 0 1} – dominates in the ground state, {3 2 2 1} – dominates in $5/2^-$ state (see below in text). Both have 90% $p$-wave in $\alpha$-n subsystems. See next section for more detailed discussion.

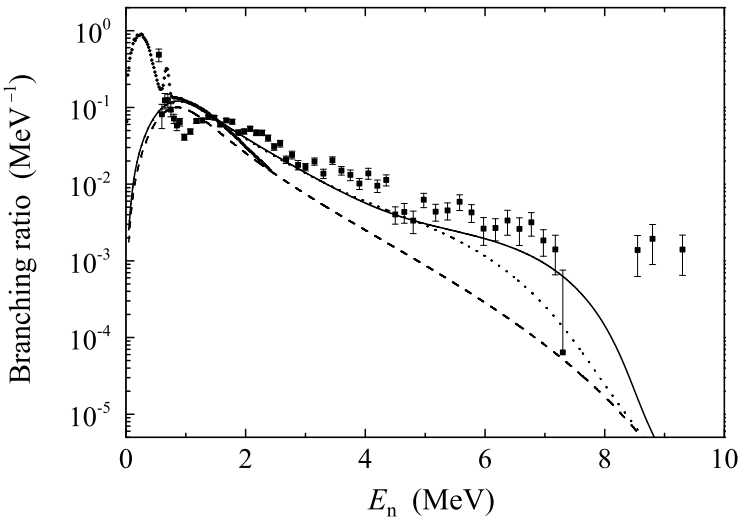


Figure 3.9: Different alpha spectra correspond to the neutron spectrum (3.7), shown in Fig. 3.8, depending on the total angular momentum $L$ of the system: solid curve – $L = 1$, dashed curve – $L = 2$, dotted curve – $L = 3$. Case $L = 1$ is not consistent with $5/2^-$ spin assignment for this state and is given only to demonstrate sensitivity to the $L$ value. Experimental data points [80] are reliable over 350 keV. Case $L = 2$ seems slightly more favorable, but the data is too poor to draw a definite conclusion.

Coulomb is shifting $\alpha$ spectrum to higher energies, hence neutron spectrum to lower. The assignment $l_x = 2$, $l_y = 1$ is very reliable: if we take any other reasonable set of QN it gives enormous and slowly converging decomposition over $K$. QN $L$ do not influence the fit in the eigen Jacobi system, but it is important when we convert the amplitudes to the other Jacobi systems. In Fig. 3.9 the low-energy $\alpha$ spectra are shown originating from one and the same neutron spectrum[7]. One can see that $L = 2$ is slightly more preferable, but generally the data is too poor to make a reliable conclusion. On the other hand, if we trust the formalism, then cases $L = 2$ and $L = 3$ are clearly distinguishable in this type of experiment. The quenching of component with $L = 3$ can be connected with properties of Raynal-Revai coefficients, as it was pointed out in [97]. For $L = 2$ the weight of $p$-wave in $\alpha$-n subsystem is 90% while for $L = 3$ only 24%.

Comparatively sharp peak in the neutron spectrum at 0.68 MeV was prescribed in [82] to the binary decay of the 2.43 MeV state in $^8$Be+n continuum, widened by the beta-recoil and the energy resolution. If we take this point of view, this peak is not in the scope of our studies.

It was found that the wide structure in the neutron spectrum between 0.5 –

[7]Certainly, $L = 1$ is not valid for $5/2^-$ and is given only to demonstrate the sensitivity to this QN.

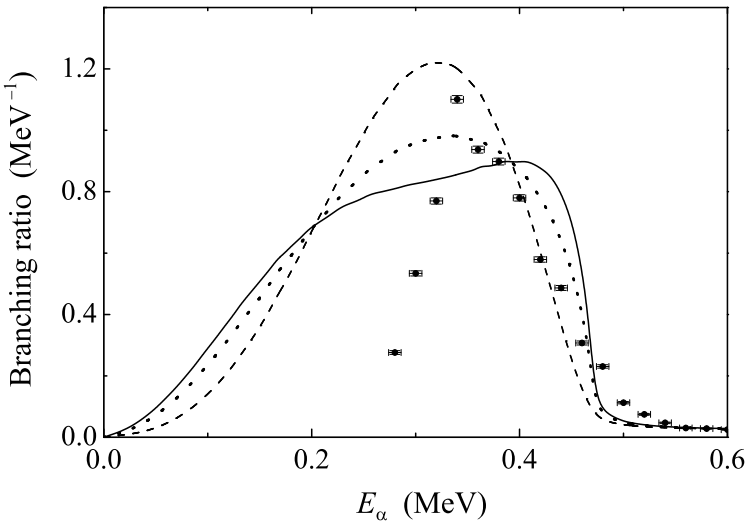


Figure 3.10: Diamonds gives the alpha spectrum from $^9$Li $\beta$-decay, combined from the $\beta$-particle anticoincidence events (under 1.2 MeV) and "singles" (after 1.2 MeV) spectra given in [82]. Spectrum is normalized to total Branching ratio 0.335. Dots with error bars is the spectrum from [80], also shown in Fig. 3.9; it has an experimental cut-off at 350 keV. Drastic difference between these spectra for energies 0.5–0.8 MeV is attributed to the detector wide solid angle in [82] causing "double-hits" for low-energy alphas. Spectrum is normalized to coincide with previous after 0.8 MeV. Solid curve is full fit involving three-body contributions from 2.43 (dashed curve), 11.28 (dotted curve) MeV states. 2.43 MeV state contribution was calculated with $L = 2$ (see Fig. 12 caption for details).

1.4 MeV can not be associated with three-body decay of *any* state in the $^9$Be continuum. It unavoidably gives too high intensity in the $\alpha$ spectrum over 0.5 MeV. The whole picture can be naturally explained if we assume that these neutrons are coming from the decay to the $^8$Be+n continuum. Then $\alpha$-particles from $^8$Be decay have energies mainly under 0.1 MeV, where available $\alpha$ spectra are not reliable at all (or do not exist). Binary $\beta$-delayed spectrum shown by dashed curve in Fig. 3.8 was obtained in a potential formalism ([P4], Section 5) taking into account, simply speaking, size of mother system and continuum properties $^8$Be+n. Potential used in this channel for p-wave was a Gaussian shape with $U_0 = -18.85$ MeV, $r_0 = 3.3$ fm. It gives a wide resonance about 1.3 MeV over $^8$Be+n threshold, $\Gamma \sim 1. - 1.6$ MeV. That corresponds well with $1/2^-$ state at 2.8 MeV. Branchings and $B_{GT}$ values of different states and channels are summarized in Table 2.

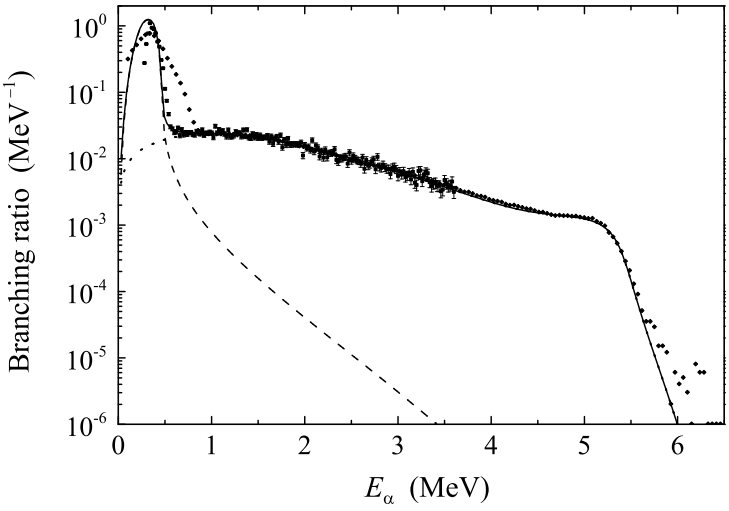


Figure 3.11: Experimental data points are described in caption Fig. 13. Solid curve shows the fit of the high-energy part of alpha spectrum from $^9$Li $\beta$-decay involving 11.28 MeV state (one component fit, $K = 5, L = 1, l_x = 2, l_y = 1$) and plane wave three-body continuum. Dashed curve gives the plane wave contribution. Dash-dots and dots show the one component spectra from 11.28 MeV state connected with $K = 5, L = 1, l_x = 2, l_y = 1$ and $K = 7, L = 3, l_x = 4, l_y = 1$ sets of QN correspondingly.

**High energy ( $E^* > 10$ MeV)**

Now let us turn to the high energy part of spectra. Should be noted that the spectra over 1 MeV of the total energy can be described by the decay of only one level (11.23 MeV) if we suggest quite exotic mode:

$$\begin{cases} K = 1, L = 1, l_x = 0, l_y = 1 \\ K = 5, L = 1, l_x = 2, l_y = 1 \end{cases} \tag{3.8}$$

The obtained values of branching and $B_{GT}$ are 5.6% and 2.29 correspondingly; they are listed in Table 2 in columns "Variant 1". Spectrum of $\alpha$-particles for such configuration (Fig. 3.10) looks more than satisfying but the sound physical interpretation of such a mode is complicated. We would like to try to stick to one channel approximation. The admixture of the higher $K = 5$ which was necessary to take into account for the 2.43 MeV state, as we understand is due to the Coulomb interaction and higher in the continuum its effect should become weaker.

It was found that the expressive "step" in the $\alpha$ spectrum after 4.6 MeV can be reproduced by *one* harmonic only using following sets of QN (Fig. 3.11):

$$K = 5, L = 1, l_x = 2, l_y = 1 \tag{3.9}$$

$$K = 7, L = 3, l_x = 4, l_y = 1 \tag{3.10}$$

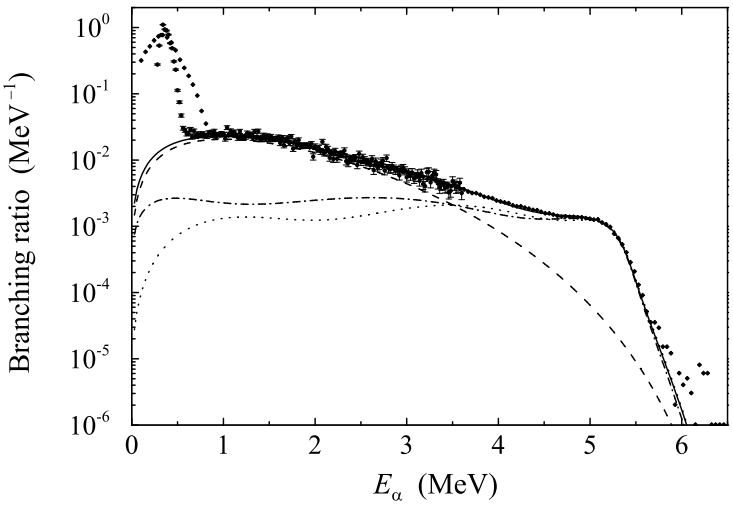


Figure 3.12: Experimental data points are described in caption Fig. 11. Solid curve corresponds to solid curve Fig. 3.11 plus binary 2.7 MeV state continuum. Dashed curve describe the binary channel contribution. Dotted curve gives the full fit for the case with 11.28 MeV state represented with harmonic $K = 7, L = 3, l_x = 4, l_y = 1$. The binary spectrum was fitted under 1.6 MeV and three-body contributions were fitted in the alpha sector: no real fitting was done for high energies. Three data points around 9 MeV give a sign of the binary $^8$Be+n decay mode of 11.28 MeV state, but this information is too poor to discuss it further.

taken for the state 11.23 MeV (harmonics with $K \leq 9$ and $l_i \leq 4$ were accounted). 11.81 MeV state does not fit the spectrum in such approximation[8]. This conclusion is nor very sensitive to the width of the state: width influence mainly the spectrum slope close to the end point. Width values between 400 and 600 keV are acceptable.

We prefer the first set of QN (3.9); fitting results are given in Table 2 in columns "Variant 2". The second possible set of QN (3.10) is quite natural if we recall that wide $g$-wave state in $^8$Be is situated just in that energy region. On the other hand it is not favorable because *i*) it is comparatively "highly excited" ( $K = 7$ ) *ii*) there is no direct $\beta$-decay to this harmonic (no $L = 3$ component in $^9$Li WF) *iii*) $\beta$-feeding is possible to $L = 2$ component (and then the state decays through $L = 3$ component), but the lowest excitations of the $L = 2$ components ($K = 3, 5$ ) are already occupied in the continuum (see (3.7)).

What we get for neutrons converting spectra "Variant 1" (Fig. 13) and "Variant 2" (Fig. 3.11) is shown in Fig 15. It should be noted that no fitting was done for the high-energy part of spectrum: it was obtained from $\alpha$ spectrum automatically. The normalization of the experimental neutron spectrum is not

[8]If we use 11.81 MeV state, the slope in the end of spectrum ($\sim$5.5 MeV in experiment) occur $\sim$300 keV later, which is clearly distinguishable. We certainly can not reject an admixture on a level of 10%.

so reliable in that energy region.

### Medium energies ( $3 < E^* < 10$ MeV)

In one channel calculations "Variant 2" we can reproduce only the highest part of $\alpha$-spectrum using contribution of the 11.28 MeV state (Fig. 3.11). Spectrum between 0.7 and 4.6 MeV require separate interpretation. It was found that a reasonable result (dashed curve in Fig. 3.11) can be obtain in the simplest plane wave approximation. Of cause it was not the complete plane wave WF (2.2), but one term from it, we found suitable: $K = 3, L = 1, l_x = 2, l_y = 1$. Somehow this choice is justified by the fact that it gives qualitative explanation why the is no $K = 3$ in the decay mode (3.9): continuum with this set of QN is already occupied.

| E, MeV | Notes | Br, % | $B_{GT}$ |
|---|---|---|---|
| | **Variant 1** | | |
| 11.28 | two component fit | 5.6 | 2.29 |
| 2.7 | binary, $^8$Be+n, $l = 1$ | 15.1 | 0.018 |
| 2.43 | binary, $^8$Be+n, $l = 3$ | 1.4 | 0.0014 |
| | three-body | 27.9 | 0.026 |
| | **Variant 2** | | |
| 11.28 | $K = 5, L = 1$ | 2.5 | 1.09 |
| $\sim$7 | 3-body plane wave$^\dagger$ | 5. | 0.2 |
| 2.7 | binary, $^8$Be+n, $l = 1$ | 13.4 | 0.015 |
| 2.43 | binary, $^8$Be+n, $l = 3$ | 1.4 | 0.0014 |
| | three-body | 27.9 | 0.026 |

**Table 2.** Branchings and $B_{GT}$ values extracted from experimental data. "Variant 1" – decay of 11.28 MeV state via exotic mode, expression (3.8). "Variant 2" – one component decay mode for 11.28 MeV state, expression (3.9) plus direct decay in three-body continuum. $^\dagger$7 MeV here is not a state energy, but the energy, where kinematical enhancement occurs in the $B_{GT} \cdot f$ value.

### Possible structure of 11.28 and 11.81 MeV (doublet?)

These states were observed in numerous reactions [7, 4, and refs. therein]. Nevertheless there is no clear spin assignment for them and there are two different points of view on their structure:

i In analysis [82] the "super-allowed" Gamow-Teller $\beta$-feedings to these states were found to be in relation $Br_{11.81}$:$Br_{11.28}$=70:30, which immediately suggest similar structure and spin-parity in the interval $1/2^-$-$5/2^-$ for both.

ii The other point of view, somehow supported by [4, and refs. therein] (basing on the shell-model calculations [16]), is that one of these states is a "high-spin" state ($\sim 9/2$) possibly "built on" the $4^+$ excitation in $^8$Be.

Our analysis do not require the $\beta$-feeding to the upper state, but following of the Halo Analogue state ideology [P3], we would like to give some arguments in the support of the first point of view.

The center of the doublet (11.28, 11.81) is shifted 2.56 MeV down from $^9$Li g.s. and splitting is 0.53 MeV. If we assume the simplest model for $^9$Li g.s. as consisting of $^7$Li g.s. and two neutrons in $0^+$ state[9], then we can connect the energy shift of the doublet with deuteron energy and splitting with the splitting between $^7$Li g.s. and $^7$Li $1/2^-$, which is 0.478 MeV. The simplified picture, where the *internal* WF of these states is more or less $^7$Li($3/2^-$ or $1/2^-$)+d easily explain why these states may have large $B_{GT}$ value and *how* this large $B_{GT}$ *can* be connected only with lower 11.28 MeV state.

Real situation is more complicated. We know, for example from the calculations [96], that "$^7$Li $3/2^-$" is dominating in the $^9$Li g.s. WF, but there is significant weight of "$^7$Li $1/2^-$". Hence the $^7$Li clusters in the 11.28 and 11.81 MeV state's WFs are, probably, the orthogonal mixtures of "$^7$Li $3/2^-$" and "$^7$Li $1/2^-$". So our simple way of thinking about these states provides only a hint how it can be that states, which are very close in energy (and probably have similar structure), have quite different $B_{GT}$ values. Detailed studies of their structure should be performed to confirm or reject this approach.

The validity of these speculations is diminished, however, by the complexity and even inconsistency of the experimental data concerning the 11.28 and 11.81 MeV states.

### 3.6.3 Precision of sequential decay formalism for $^9$Li

Here I would like to continue the discussion of the Section 3.5 about the necessity of more accurate treatment of the many-body $\beta$-delayed decays than it can be done within the R-matrix sequential decay formalism (see sections dedicated to the $^9$Li $\beta$-decay in [82, 32]). I would like to repeat once again that the criticism against the R-matrix formalism is only concerning a very narrow field of a few-body decay analysis. In that field I think we can suggest something more suited to the basic physics of the system — "generalization" of R-matrix analysis for the few-body case [P4, P8].

An additional difficulty, which arises during the analysis of $^9$Li $\beta$-decay to $\alpha$+$\alpha$+n continuum, is a proper treatment of the symmetry between two equivalent $\alpha$-clusters. If we take system $^5$He+$\alpha$ and convert its WF to the Jacobi system where there is definite angular momentum between two alphas, we will find both negative and positive parity components in $\alpha$-$\alpha$ relative motion. This means that assumption about $^5$He+$\alpha$ character of the decay would be reasonable only in some special cases, when the "forbidden" part of $^5$He+$\alpha$ WF is small enough. Using a hyperspherical basis we can easily find out what is the $p$-wave

[9] Unfortunately, decompositions given in theoretical calculations [96] do not allow to confirm or reject this assumption.

contents of different configurations in $^9$Be WF (see end of Section 2.2.5 ). Table 3 lists the lowest HH possibly dominating the negative parity states in $^9$Be. The quantum numbers $\{K, L, l_x, l_y\}$ stand for the hyperspherical amplitudes in the (($\alpha$-$\alpha$)-n) Jacobi system; the third column contains weights of components with $l_x = 1$ in (($\alpha$-n)-$\alpha$) Jacobi system for these amplitudes.

| States | Possible structure | Weight of $l = 1$ in $\alpha$-n, % |
|---|---|---|
| $1/2^-$, $3/2^-$ | 1 1 0 1 | 90 |
| | 3 1 0 1 | 52 |
| | 5 1 0 1 | 25 |
| | 3 1 2 1 | 71 |
| | 5 1 2 1 | 23 |
| $3/2^-$, $5/2^-$ | 3 2 2 1 | 90 |
| | 5 2 2 1 | 52 |
| $5/2^-$, $7/2^-$ | 3 3 2 1 | 44 |
| | 5 3 2 1 | 18 |
| | 7 3 4 1 | 24 |

**Table 3.** In column 2 – quantum numbers $\{K, L, l_x, l_y\}$ of hyperspherical harmonic in (($\alpha$-$\alpha$)-n) Jacobi system. The third column contains weights for $p$-wave component in ($\alpha$-n) subsystem for this harmonic.

From Table 3 we can conclude that at least two states can be formed in an "energy efficient" way, including alphas with a neutron predominantly in $p$-wave. They are easily identified. It is $^9$Be ground $3/2^-$state with structure {1 1 0 1} in ($\alpha$-$\alpha$)-n Jacobi system (can be compared with results of the three-cluster variational calculations [11]). And $5/2^-$state dominated by {3 2 2 1} with $5 - 10\%$ of {5 2 2 1} (see [97, 29] and our recent analysis in Section 3.6.2 [10]). If one needs it for some reason, these states can be considered as $^5$He+$\alpha$ without a contradiction with basic principles of physics.

The other negative parity states we can construct in the $^9$Be spectrum have $p$-wave contents on the level less then 50%. The $7/2^-$state at 6.8 MeV is most probably dominated with {3 3 2 1} amplitude (44% of $p$-wave). Highly excited states at 11.28 and 11.86 MeV, are assumed in Section 3.6.2 to have Halo Analog structure and decay via dominating {5 1 2 1} or {7 3 2 1} channels (23% and 24% of $p$-wave correspondingly). Generally, when we go higher up in excitation (higher $K$ numbers) the weights of negative and positive parity amplitudes in the subsystem $\alpha$-n have a tendency to become equal. It means that even if our suggestions about the structure of the highly excited states in $^9$Be are not correct, one can expect around 50% of WF to have even parity relative motion for $\alpha$-n. It gives the sequential analysis, assuming $^5$He+$\alpha$ as an intermediate step for the decay of such states, an accuracy $\pm 50\%$.

[10] Of course, analysis in Section 3.6.2 can not distinguish between $L$=2 and $L$=3, due to the quality of the experimental data. But, following [97], we think the higher $p$-wave contents for $L$=2 amplitudes is making this choice preferable.

## 3.7 $^6$Li$(0^+1) \rightarrow ^6$Li$(1^+0)$ M1 decay

**The spin currents** are recognized to dominate normally in the M1 transitions. The reason is very simple: "intrinsic" magnetic momenta of the nucleons are much more intensive then orbital (coefficient $K_p - K_n = 4.7$). The spin currents contribution to the M1 decay of the $^6$Li$(0^+1)$, 3.563 MeV state to the $^6$Li$(1^+0)$ ground state is closely connected with the $\beta$-decay matrix elements: as far as $^6$Li$(0^+1)$ is an isobaric analog state of $^6$He g.s. the sets of quantum numbers of the spin-radial components are the same and high geometrical identity of the radial WFs is promised by the strict calculations [44, 41, 12]. The reduced matrix element of the spin part of operator (2.16) for the studied transition is given by

$$M_{M1} = -\sqrt{\frac{2\pi}{qV}} \frac{\lambda q e}{4M} \left(K_p - K_n\right) \sum_{k=1}^{2} \left\langle J' \left\| \sigma_k \right\| J \right\rangle \left\langle T' T'_3 \left| \tau_k^0 \right| T T_3 \right\rangle$$

where ME of the isospin parts differs from the case of $\beta$-decay:

$$\left\langle T' T'_3 \left| \tau_k^0 \right| T T_3 \right\rangle = \left\langle 00 \left| \tau_k^0 \right| 10 \right\rangle = (-)^{k+1}$$

While reduced ME $\left\langle J' \left\| \sigma_k \right\| J \right\rangle$ have already been calculated in (3.1) :

$$\left\langle J' \left\| \sigma_k \right\| J \right\rangle = (-)^{k+1} \left( \sum_{\substack{K=0,2,\ldots \\ l=even}} \int \chi_{K01ll}^{Li(1^+)} \chi_{K00ll}^{Li(0^+)} d\rho - \tfrac{1}{\sqrt{3}} \sum_{\substack{K=2,4,\ldots \\ l=odd}} \int \chi_{K00ll}^{Li(1^+)} \chi_{K01ll}^{Li(0^+)} d\rho \right)$$

**The treatment of the orbital currents** is much more complicated in our formalism. To calculate the ME of the individual particle orbital momentum vector we need to have eigenfunctions of the one-particle orbital momentum. That is not exactly the case for the WF in the HH method. In the three-body WF only one particle (ordinary here referred as "third") would have a definite one-particle angular momentum. So the following steps are required:

1. Convert the three-body WF to the Jacobi system, where the particle of interest is "third". This is done using Raynal-Revai unitary transformation formalism discussed in the end of Section 2.2.5 .

2. Calculate ME of orbital momentum vector $l_y$

3. Renormalize the obtained value as far as eigenvalues of the $l_y$ operator differs from that of one-particle angular momentum operator

**Conversion.** The analysis of the quantum numbers and weights of the WF's harmonics shows that the $\alpha$-particle motion do not contribute the $M1$ ME significantly and $M1$ ME connected with proton motion is strongly dominated

by the transitions between harmonics which quantum numbers (in the notation $KLSl_xl_y$) are

$$\begin{array}{l} 20000(\text{ converted to } 20011) \to 21011(\text{ converted to } 21011) \\ 21111(\text{ converted to } 21111) \to 20100(\text{ converted to } 20111) \end{array}$$

where the first set of numbers represents the harmonic in the "native" Jacobi system $\alpha$-(N-N), while set in the brackets gives the quantum numbers of the significant for $M1$ transition harmonic obtained after the conversion to the nucleon Jacobi "eigensystem" N-($\alpha$-N).

To make the formalism more evident we will calculate the Raynal-Revai coefficients required for this conversion "by hands". The definitions of the normalized Jacobi coordinates $\mathbf{x}$ and $\mathbf{y}$ in all the three possible Jacobi systems are (note $A_1$=1, $A_2$=1, $A_3$=4):

$$\begin{array}{lll} 1) \quad \mathbf{x} = \dfrac{\mathbf{r}_2 - \mathbf{r}_1}{\sqrt{2}} & 2) \quad \mathbf{x} = \dfrac{2\mathbf{r}_1 - 2\mathbf{r}_3}{\sqrt{5}} & 3) \quad \mathbf{x} = \dfrac{2\mathbf{r}_3 - 2\mathbf{r}_2}{\sqrt{5}} \\ \mathbf{y} = \dfrac{\mathbf{r}_1 + \mathbf{r}_2 - 2\mathbf{r}_3}{\sqrt{3}} & \mathbf{y} = \dfrac{\mathbf{r}_1 + 4\mathbf{r}_3 - 5\mathbf{r}_2}{\sqrt{30}} & \mathbf{y} = \dfrac{\mathbf{r}_2 + 4\mathbf{r}_3 - 5\mathbf{r}_1}{\sqrt{30}} \end{array} \tag{3.11}$$

Let's now overview some simplest bilinear forms of this vectors:

- $\mathbf{x}^2 + \mathbf{y}^2 = \rho^2$ — we know this is hyperradius.
- $\mathbf{x}^2 - \mathbf{y}^2 = \mathcal{J}^{00}_{200}$ — the other simplest combination, which is scalar in general, as well as in respect with angular momenta of the subsystems.
- $2(\mathbf{xy}) = \mathcal{J}^{00}_{211}$ — this harmonic together with previous should transform through each other while changing Jacobi system.
- $[\mathbf{x} \times \mathbf{y}]_\mu = \mathcal{J}^{1\mu}_{211}$ — it is evident that this harmonic is not changing while conversion to other Jacobi system.

So harmonic $\mathcal{J}^{00}_{200}(1)$ in the other Jacobi system will become a sum (see definition (2.15) )

$$\mathcal{J}^{00}_{200}(1) = R^{00}_{00}\left(j \to 1; 20\right) \mathcal{J}^{00}_{200}(j) + R^{11}_{00}\left(j \to 1; 20\right) \mathcal{J}^{00}_{211}(j)$$

We see that in this case coefficients $R$ can be easily found directly using (3.11) and definitions of harmonics as bilinear forms.

$$\begin{array}{ll} R^{00}_{00}\left(2 \to 1; 20\right) = -1/5 & R^{11}_{00}\left(2 \to 1; 20\right) = -\sqrt{24}/5 \\ R^{00}_{00}\left(3 \to 1; 20\right) = -1/5 & R^{11}_{00}\left(3 \to 1; 20\right) = \sqrt{24}/5 \end{array}$$

**The reduced ME** of angular momentum vector operator can be found after this

$$\left\langle J' \left\| l_y(k) \right\| J \right\rangle = (-)^{k+1} \frac{\sqrt{24}}{5} (-)^{J+S+l_x+l_y} \hat{J}\hat{L}' \left\{ \begin{array}{ccc} J & S & L \\ L' & 1 & J' \end{array} \right\} \hat{L}\hat{l}'_y \left\{ \begin{array}{ccc} L & l_x & l_y \\ l'_y & 1 & L' \end{array} \right\} \times$$

$$\times \left\langle l'_y \left\| \hat{l}_y \right\| l_y \right\rangle \sum_{LS} \int \chi^{Li(1^+)}_{KLSl'_x l'_y}(\rho)\, \chi^{Li(0^+)}_{KLSl_x l_y}(\rho)\, d\rho$$

Note, this formula is valid only for $K = 2$ and $l_x = l_y = l'_x = l'_y = 1$ and hyperradial functions $\chi$ here depends on the quantum numbers in the "rotated" (N-($\alpha$-N)) system. The reduced ME of the orbital momentum operator is $\left\langle l' \left\| \hat{l} \right\| l \right\rangle = \sqrt{l(l+1)}\delta_{ll'}$ and finally we obtain (in this formula the hyperradial functions $\chi$ here depends on the quantum numbers in the "native" Jacobi system $\alpha$-(N-N) )

$$\langle J' \| l_y(k) \| J \rangle = (-)^{k+1} \frac{\sqrt{24}}{5} \left( \int \chi^{Li(1^+)}_{21011} \chi^{Li(0^+)}_{20000} d\rho + \frac{1}{\sqrt{3}} \int \chi^{Li(1^+)}_{20100} \chi^{Li(0^+)}_{21111} d\rho \right)$$

**The idea of renormalization** of angular momentum eigenvalues when we turn to Jacobi angular momenta is very simple: the rotational energy should have the same value. In the CMS this condition can be written (for the second and the third Jacobi systems)

$$\frac{\hat{l}^2}{r_j^2} = \frac{\hat{l}_y^2}{y_j^2} \quad ; \quad r_{2,3} = \frac{5}{6} y_{2,3} \quad \Rightarrow \quad \hat{l} = \frac{5}{6} \hat{l}_y$$

It also can be shown directly using the definition of the angular momentum

$$\hat{l} = [\mathbf{Y}\mathbf{P}_Y] \quad ; \quad \hat{l}_y = [\mathbf{y}\mathbf{p}_y]$$

$$\mathbf{Y} = \sqrt{\frac{A_1 + A_2}{(A_1 + A_2 + A_3)A_3}} \mathbf{y} \quad ; \quad \mathbf{P}_Y = \sqrt{\frac{(A_1 + A_2)A_3}{A_1 + A_2 + A_3}} \mathbf{p}_y \quad \Rightarrow$$

$$\Rightarrow \quad \hat{l} = \frac{A_1 + A_2}{A_1 + A_2 + A_3} \hat{l}_y$$

**The final expression** for ME and probability of M1 transition

$$\sum_{k=1}^{2} \langle J' \| \{\ldots\}_k \| J \rangle \langle T' T'_3 | \tau^0_k | T T_3 \rangle =$$

$$= 2(K_p - K_n) \left( \sum_{\substack{K=0,2,\ldots \\ l=even}} \int \chi^{Li(1^+)}_{K01ll} \chi^{Li(0^+)}_{K00ll} d\rho - \frac{1}{\sqrt{3}} \sum_{\substack{K=2,4,\ldots \\ l=odd}} \int \chi^{Li(1^+)}_{K00ll} \chi^{Li(0^+)}_{K01ll} d\rho \right) +$$
$$+ 2\frac{5}{6} \frac{\sqrt{24}}{5} \left( \int \chi^{Li(1^+)}_{21011} \chi^{Li(0^+)}_{20000} d\rho + \frac{1}{\sqrt{3}} \int \chi^{Li(1^+)}_{20100} \chi^{Li(0^+)}_{21111} d\rho \right)$$

$$W = \frac{e^2 \Delta E^3 (K_p - K_n)^2}{M^2} \times$$
$$\times \left| \left( \sum_{\substack{K=0,2,\ldots \\ l=even}} \int \chi^{Li(1^+)}_{K01ll} \chi^{Li(0^+)}_{K00ll} d\rho - \frac{1}{\sqrt{3}} \sum_{\substack{K=2,4,\ldots \\ l=odd}} \int \chi^{Li(1^+)}_{K00ll} \chi^{Li(0^+)}_{K01ll} d\rho \right) + \right.$$

$$+\frac{1}{K_p-K_n}\frac{\sqrt{24}}{6}\left(\int\chi^{Li(1^+)}_{21011}\chi^{Li(0^+)}_{20000}d\rho+\frac{1}{\sqrt{3}}\int\chi^{Li(1^+)}_{20100}\chi^{Li(0^+)}_{21111}d\rho\right)\Bigg|^2$$

## 3.8 $^6$Li$(0^+1)$ M1 transition to alpha+d continuum

The formula for the probability of the M1 transition can easily be obtained using (2.17) and our experience from Section 4.4 ( here $\langle\tau^0_k\rangle=\langle T'T'_3\,|\tau^0_k|\,TT_3\rangle$ ) :

$$dW=\left(\frac{2J'+1}{2J+1}\left|\frac{1}{k}\sum_{k=1}^{2}\langle J'\,\|\{\ldots\}_k\|\,J\rangle\,\langle\tau^0_k\rangle\right|^2\right)\frac{e^2\left(\Delta E-k^2/2M_R\right)^3}{12M^2}\,\frac{2}{\pi}\,k^2dk$$

$$dW=\left(\frac{2J'+1}{2J+1}\left|\sum_{k=1}^{2}\langle J'\,\|\{\ldots\}_k\|\,J\rangle\,\langle\tau^0_k\rangle\right|^2\right)\frac{\sqrt{2M_R}e^2\left(\Delta E-E\right)^3}{6\pi M^2}\,\frac{dE}{\sqrt{E}}$$

$$W=\frac{\sqrt{2M_R}e^2}{6\pi M^2}\int_0^{\Delta E}\frac{dE}{\sqrt{E}}\,B_{M1}(E)\cdot\left(\Delta E-E\right)^3$$

This spectrum have never been calculated completely, but was used for the evaluations of M1 transition to continuum as a possible background to the parity violating decay of $^6$Li$(0^+1)$, 3.563 MeV state. It was done in [P2]. The evaluation of the branching ratio for M1 transition to $^6$Li ground state and $\alpha$+d continuum, which is using experimental branching for $\beta$-decay, can be found in this paper as well.

## 3.9 Parity violating decay of $^6$Li$(0^+1)$ state

This process is studied in paper [P2]. The approximations done make this analysis rather simple and the description, given in the article is in this sense complete. There is probably one dark place I would like to explain here once more. This is the question how the M1 transition to the $\alpha$+d channel may be a background for the parity violating decay. Imagine two possible types of parity violating reactions involving $^6$Li $(0^+)$ state: fusion and decay (real experiment may look very complicated but finally will belong to one of this types). The nature of the background is illustrated in Figure 16 (a – for fusion and b – for decay cases).

In the fusion type experiment deuterons and alphas are brought in collision, looking for the yield of excited $^6$Li nuclei. As far as the beam has some energy spread width, the particles in the beam, which have energy lower then resonance one[11] would interact only in elastic channel, those few particles which energy is

[11]Resonance energy here is meant energy of $^6$Li $(0^+)$ state (3.563 MeV) mines the energy of $\alpha$+d threshold (1.475 MeV); $E_R$=2.088 MeV.

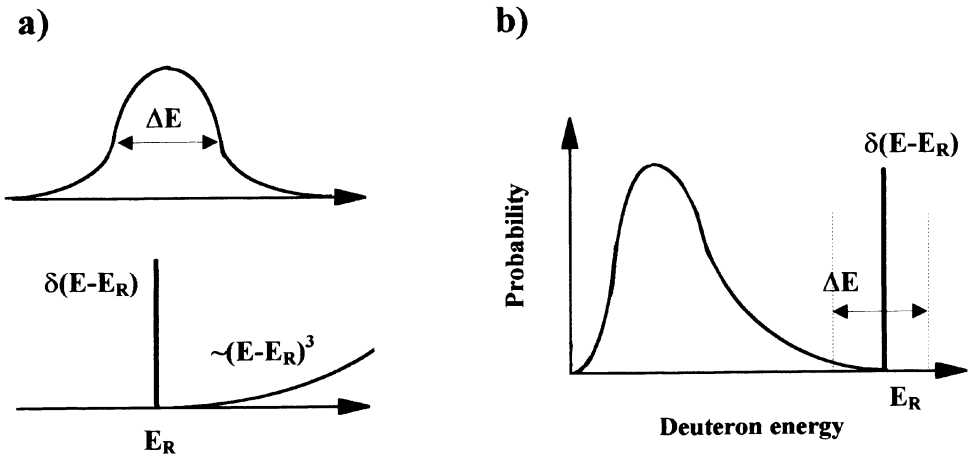


Figure 3.13: (a) is illustrating the possible source of the background in the fusion case. Upper picture gives the energy profile of the beam, lower schematically plots the probability of interaction via inelastic channel ($\delta$-function is connected with parity violating transition, continuous spectrum — with $\alpha$(d,$\gamma$)$^6$Li ($0^+$) reaction). (b) gives the schematic spectrum of deuterons ($\alpha$-particles) from the decay of $^6$Li ($0^+$) state (both via parity violating and electromagnetic channels). $\Delta$E in the both pictures is characteristic energy resolution of the experiment.

precisely resonance, get an opportunity to form $^6$Li ($0^+$) state via parity violating channel and finally those particles which energy is greater then resonance can also form $^6$Li ($0^+$) state throwing the energy excess with M1 quantum. Though the width of the beam may be rather small and the probability of forming $^6$Li ($0^+$) state via "M1" channel behaves like (E–$E_R$)$^3$, the intensities of weak and electromagnetic processes are incomparable, making "M1" channel serious competitor to parity violating channel.

In the decay experiments $^6$Li ($0^+$) state is populated (ordinary decaying via M1 transition to $^6$Li ground state) somehow and then you are looking for deuterons or alphas in the products of its decay. But if the excited $^6$Li nuclei have energy spreading or bin size for detection of deuterons (alphas) is large, then some number of particles from the decay $^6$Li ($0^+$)$\rightarrow$ $\alpha$+d+$\gamma$(M1) is registered together with particles from parity violating decay.

The conditions on the width of the beam for fusion type reaction and on the energy resolution for the decay type reaction are given in [P2].

# Chapter 4

# Achievements and Problems

*One can imagine extremely useful device:*
*a lavatory pan and a soup tureen in the same time...*
*Some concepts in science remind very much*
*this device in a household.*

*D.P. Grechukhin*

This part contains some problems in our field of science which I faced in the process of work and which were left unresolved in our articles as well as in the works of other authors. They are presented in more concentrated form and straightforward manner then in the articles. Of course, it makes the possibility of the erroneous statement much higher [1]. It should be taken into account reading this part. Understanding science as asking questions to the nature, this is really scientific part. And certainly it is the prospect for my further work in the field.

## 4.1 Achievements

This short section is given here to show what can be considered as our achievement in the field (to my opinion) in comparison with what is desirable to achieve (the subject of the following sections).

1. The reason why the probability of the $^6$He $\beta$-decay to the $\alpha$+d continuum is strongly suppressed in comparison with the decay to the $^6$Li g.s. was understood as a result of the developed halo structure of $^6$He, $^6$Li nuclei [P1].

2. The concept of the Halo Analog state was suggested to explain the concentration of the Gamow-Teller strength high in the spectrum of nuclei neighboring the halo nuclei. The location of such states 1–3 MeV below the

[1] "If we lock the door for delusion, how the truth would enter?" R. Descartes

mother state is simply understood taking into account that only deuteron-like correlation may give an energy gain in the spatially extended halo. Possible Halo Analog states were identified in $^8$Li, $^9$Be and $^{11}$Li, providing useful framework for understanding structure and reactions [P3,P4,P6,P8]. Existence of the HA states have already got some experimental confirmation [80, 92].

3. The $^8$He $\beta$-decay was studied as a tool probing nuclear structure of $^8$Li in the whole $\beta$-decay energy window [P4,P6].

4. The formalism for extracting the information about nuclear states from the three-body $\beta$-delayed decays is developed [P4]. This formalism is a reasonable alternative to the R-matrix approach which has a limited applicability in this case [P4,P8].

5. The method of taking into account binary correlations for the three-body "nonborromean" systems[2] in the framework of the hyperspherical harmonic approach was developed [P7]. Correct treatment of both two-body and three-body asymptotics in this method is essential for calculations of variety of processes, including those, which are important for astrophysical applications.

6. The experiments were proposed, which can clarify some of the questions listed below: $^6$Li($0^+$)($\gamma$d)$\alpha$ and $^6$Li($^6$He,$\alpha$)$^8$Li$^*$.

## 4.2 The decays of $^6$He,$^6$Li ($0^+$) states

### 4.2.1 Beta-decay and M1 transition to ground state

The experimental information about some transition can be used in two ways: to investigate the structure of the initial and final state if we exactly know the interaction and to study the interaction if we have a perfect knowledge of the structure. The recognized tool for the investigation of the weak interaction is the $\beta$-decay of neutron and $0^+ \to 0^+$ transitions. These two types of reactions are the only source of the information about constants $G_A$ and $G_V$. As far as $0^+ \to 0^+$ transitions belongs to the Fermi type and the $\beta$-decay of neutron has a mixed character (both Fermi and Gamow-Teller), hence the value of $G_A$ constant (or constant $\lambda = G_A/G_V$) can be obtained only in complicated experiments with polarized neutron. For a long time the Gamow-Teller transitions were not a proper source of information about weak interaction because of the poor knowledge about structure of the participating nuclei. Nowadays the situation have changed because of the intensive development of microscopic many-body models. The theory of the three-nucleon nuclei is very advanced, pretending the

[2]Three-body systems, having bound binary subsystems.

adequate description of practically all observables for $t$ and $^3$He. What can be told about heavier nuclei?

The life-time of the $^6$He, governed by the $\beta$-decay to the $^6$Li g.s., is known with a good precision: $t_{1/2} = 806.7 \pm 1.5$ ms [4]. To reproduce this value, for example, in the shell-model calculations the $\lambda$ value should be significantly renormalized (however see [16]). In the semi-microscopic approaches [70, 44, 46] and microscopic calculations [41, 42] this renormalization is shown to be unnecessary. The success of the models in describing of many other observables may make us think that the structure is described well. Is it correct? One of few problems here is the consistency of the matrix elements of the operator $\sigma$ extracted from the $\beta$-decay data and from the electromagnetic width of the $^6$Li $(0^+, T{=}1)$ state connected with M1 transition to $^6$Li g.s. For M1 transition this procedure (described, for example, in Section 3.7) is more complicated, but very similar results were obtained in two different three-cluster approaches: in our article [P2]

$$\langle\sigma\rangle_\beta = 3.26 \quad \langle\sigma\rangle_{M1} = 3.64$$

and in the article [70]

$$\langle\sigma\rangle_\beta = 3.18 \quad \langle\sigma\rangle_{M1} = 3.49$$

Two possible conclusions can be drawn:

1. The structure of the $0^+$ multiplet of A=6 nuclei is not understood well enough in all the works [71, 70, 44, 41, 12].

2. The experimental figure [4] obtained for the electromagnetic width of the $^6$Li $0^+$ state is erroneous (see experimental papers [83, 56, 23]).

Which of these statements is correct will show the further theoretical and experimental investigation of the A=6 systems.

### 4.2.2 Beta-decay and M1 transition to alpha+d continuum

The $\beta$-delayed deuteron emission was firstly observed in [85]. The improved figure for the branching ratio of the decay to continuum to the decay to $^6$He ground state was obtained in [33] with better experimental setup: $Br = (7.6 \pm 0.6) \times 10^{-6}$. The first attempt to study this process theoretically was done in [51] using a simple two-body model. The result was that if we fit the $\alpha$-"dineutron potential" to the binding energy of $^6$He and fit the $\alpha$-deuteron potential to get a state with the binding energy of $^6$Li then the branching ratio is **overestimated** by an order of magnitude. More advanced attempt to understand this process was semi-three-body studies of [P1], where the exact three-body WFs of $^6$He and $^6$Li were used, but a potential model WF for $\alpha$-d relative motion. The branching ratio is **overestimated** in these calculations 3–5 times. The reasons of difference with the results of [51] were explained as

1. Better accounting of NN correlations in [P1] and
2. Correct three-body asymptotics of the $^6$He and $^6$Li WFs used in [P1].

The process was studied in [42, 19] using microscopic WFs of RGM-like approaches. The branching ratio is **underestimated** in these calculations 5–50 times. The weak sides of the method, which could have caused this discrepancy with the experimental results, to my opinion can be found as follows:

1. The quality of the WF's asymptotics, which is of a great importance for the process, can be found questionable (as always, working with basis of square integrable functions).
2. The properties of the $\alpha$-d continuum are not so well studied in the models; phase shifts are obtained in $s$-wave and only up till 5 MeV.
3. The calculations were carried out with effective NN potential (like Minnesota force), implying $s$-wave deuteron and hence possibly omitting an important aspects of nuclear dynamics.

Generally speaking, the microscopic approaches have a serious advantage, as compared with thee-cluster methods. The WF is completely antisymmetric and other cluster rearrangements can be taken into account (T+T in $^6$He or T+$^3$He in $^6$Li WFs). However, this advantage is not so important for the particular reaction discussed, as it has highly peripheral character.

What about the experimental data, which have caused such a great theoretical interest? Are they reliable enough? The $\beta$-delayed deuteron spectrum in the article [33] is reliably obtained only for the CM energies larger then 300–400 keV [3], missing (according to the theoretical results) the peak. It can scarcely be improved in technics of the direct measurements of the charged particles (like [33]), but there exists an independent experiment, which is very interesting itself and can provide a cross-check (unfortunately model dependent) of the $\beta$-delayed data. The experiment, studying $^6$Li $0^+$, 3.563 MeV state M1 decay to $\alpha$+d continuum, is discussed in paper [P2]. The main point of this discussion is that these reactions ($^6$He $\beta$-decay and $^6$Li $0^+$ M1 transition to $\alpha$+d continuum) have the same final state and initial states have practically identical spatial structure: they differ only in the isotopic spin projection [44]. From theoretical point of view the M1 experiment has the following advantages and disadvantages:

- The strong side of the experiment is that in a contrary with lepton pairs in the $\beta$-decay experiments, the $\gamma$-quanta yielding M1 transition can be detected, hence giving an opportunity to recover the full kinematics of the reaction. Note that the low-energy part of the deuteron spectrum (0–400 keV), which is not available in the $\beta$-decay experiment, can be reliably obtained in M1 experiment measuring the $\gamma$-quanta (1.6–2.0 MeV).

[3] The end point of the deuteron $\beta$-delayed spectrum is at 2.032 MeV CM energy.

- The weak side of this experiment is the necessity to calculate the matrix elements of orbital current, to be able to compare its results with the $\beta$-decay experiment results. That is what I meant speaking about model dependent cross-check of the $\beta$-decay and M1 experiments.

To be able to study those processes theoretically we should have the exact WFs both of the nuclear-stable states of A=6 multiplet and of the $\alpha$+d continuum.

### 4.2.3 Parity violating transition

The parity violating transition of the $^6$Li $0^+$, 3.563 MeV state is recently studied in many experimental [100, 13, 15, 21, 87] and theoretical [86, 38, P2] works. The situation with theoretical studies is more or less clear. The articles [86, P2] predict the parity violating width of the $^6$Li $0^+$ state to be the same, within the order of magnitude $\Gamma_{PV} \sim (0.16-1.5)\times 10^{-8}$ eV and the precision of each model itself can be also estimated as an order of magnitude. The results of [38] are two orders of magnitude lower, then the characteristic value predicted in the other articles: $\Gamma_{PV} \sim 8 \times 10^{-11}$eV. It is argued in paper [P2] that the reason of this discrepancy is the lack of admixture L=0, S=1 component in the $^6$Li $0^+$ state WF used in [38]. In the absence of this component, the one-pion parity violating exchange, ordinary dominating the parity violating transitions, is suppressed according to the selection rules. While the weight of such admixture component in the $^6$He g.s. can be reliably extracted from the experimental data on the level of 9–15 %, the weight of this component in the $^6$Li $0^+$ state according to the experiment (M1 transition) seem to be close to zero, though the isobaric symmetry and strict calculations predict the same weight as in the $^6$He g.s. (see also the discussion in [P2] and in the Section 4.2.1 above). So, if the weight of the admixture component in the $^6$Li $0^+$ state is really lower then it is predicted in the calculations [71, 70, 44, 41, 12], then we should expect that parity violating width of this state is lower, then the predictions [86, P2] approaching the results of [38].

The precision of the best experiment [87] searching for the PV transition of the $^6$Li $0^+$ state is very high, putting the upper limit $\Gamma_{PV} < 6.5\times 10^{-7}$ eV. If the experimental precision is improved on 1.5–2 orders of magnitude and the parity violating decay is

- observed, then probably our understanding of the $^6$Li $0^+$ state structure is correct (see item 2 in the end of Section 4.2.1)
- not observed, then either our understanding of the $^6$Li $0^+$ state structure is not complete (see item 1 in the end of Section 4.2.1), or the understanding of the mechanism of parity violation in nuclei is not complete.

Though of a serious experimental and theoretical activity "in the field of parity violation", this effect was observed only in rather complicated polarization

experiments with rather complicated systems. The discovery of the parity violating transition of the $^6$Li $0^+$, 3.563 MeV state would allow to investigate parity violation in the process of the other kind (PV $\alpha$-decay), in the system allowing the accurate theoretical treatment. And the results of such investigation may have a serious impact on the understanding of other important features of the system.

## 4.3 $^8$He beta-decay

### 4.3.1 Low-energy neutrons

A serious amount of the low-energy neutrons observed in the experiment [26] is indicating $s$-wave behavior (instead of expected $p$-wave) of the $\beta$-decay matrix elements. It is argued in the paper [P4], Section 5 that this phenomenon may be connected with the forbidden $\beta$-decay of $^8$He to the states of negative parity in vicinity of the two-body thresholds in $^8$Li. Such states predicted theoretically in [89] and in [P4], have never been observed clearly in the other types of experiments. Existence and positions of negative parity states in the continuum of $^8$Li may have a serious impact on the theory of reactions with this nucleus which is important for example for astrophysical applications. To confirm or to reject this hypothesis the results of [26] for the low-energy neutrons should be confirmed and further theoretical investigation then performed.

### 4.3.2 High-energy tritons

The $\beta$-delayed triton spectrum from $^8$He decay was first reported in [31] and then re-measured with better experimental setup (see [33]). This spectrum is noted for serious amount of the high-energy tritons: the peak of the intensity is at $\sim$1.4 MeV, while the energy available for tritons is $\sim$3.8 MeV. This fact is even more amazing if we remind that this spectrum belongs to the three-body continuum (sharing of energy among many particles should decrease the peak energy). The high-energy tritons can be explained assuming rather narrow state with high $B_{GT}$ value a bit lower than the mother state (see fits [18, 33]). It is shown in the paper [P4] that if we apply the three-body formalism to the analysis of the experimental data, instead of standard R-matrix approach, the position of the state is obtained lower in excitation energy and the shape of the spectrum may be explained as governed by the three-body phase volume (not by the specific three-body correlations as it is implied by the R-matrix approach). The specific structure of the state, so called Halo Analog state (see also the discussion of the next section), is supposed in [P4] to explain the high $B_{GT}$ value.

The complete kinematics data about $\alpha$, T and neutron in this decay and independent information about position and width of the HA state in $^8$Li are desirable to resolve the problem. It is pointed out in [P4] that the possible independent experiment looking for the Halo Analog state may be $^6$Li($^6$He,$\alpha$)$^8$Li$^*$.

### 4.3.3 The beta-decay to $^6$Li+n+n continuum

The studies of this reaction have an exploratory character [P6]. The expected branching is very low and should be observed (if it is possible at all) in a very specific experiment for double-neutron emission in $^8$He $\beta$-decay. The theoretical conclusion also have a lot of "IFs". **If** the state, we found close to $^6$Li+n+n threshold, is really there and **if** its internal structure is really the HA structure (hence high $B_{GT}$). Then there is a chance to observe it in experiment, and it will give as an interesting information.

## 4.4 $^9$Li beta-decay

When one looks on the $\beta$-delayed particle spectra from $^9$Li decay, one feels that a great job has been done and it can be done better in the nearest future only with a great problems. When one looks in Section 3.6.1 how these spectra were assembled for analysis one feels that it is a maze...

What is the reason? The new method of analysis is proposed and it is very requiring in the sense of a quality and consistency of the data. Data, available for today, are meeting these requirements only in some aspects. The difficulties we faced analyzing these data are just consequence.

Concerning decay to the highly excited states (11.28, 11,81 MeV) in $^9$Be, similar to the case of $^8$He, we do not know the position of the state – there are two candidates and we do not know in which proportion they are populated. As a result, we try to use one harmonic approximation to extract position and width of the state instead of using the method full power to obtain better information about correlations in momentum space and $B_{GT}$ values. The other available experimental data about these states is not very helpful. If we believe that these states are the HA states then they should have a very similar spatial structure and a high deuteron spectroscopic factor.

1. *Both* states were observed in the deuteron transfer reaction $^7$Li($^3$He,p)$^9$Be [40], but only *upper* state in $^7$Li($^6$Li,$\alpha$)$^9$Be reaction [77].
2. Only *lower* state was observed in electron scattering $(e, e')$ ([7, 4] probably M1), while *upper* was clearly seen in photoabsorption measurements [52].
3. And so on ...

As we can not be supported by the nuclear reaction data, we have to hope for the $\beta$-decay data improvement. Fortunately it is possible for $^9$Li beta-decay: only one type of charged particles ($\alpha$) is emitted in the decay. The experimental setup, like used in [75], with two parallel detectors aside absorption foil would allow to get energy correlation spectra of alphas with a good confidence. Correlation spectra for charged particles, together with better neutron spectrum in a full energy range may make it possible to extract information about the 11.28 and 11.81 MeV states in $^9$Be not on a level of guess, but on the level of confidence.

## 4.5 $^{11}$Li beta-decay

### 4.5.1 Halo Analog state in $^{11}$Li

The term "Halo Analog state", introduced in the paper [P3], have caused a lot of discussions. Here we will try to understand what was the reason to introduce it. First of all, we remind the meaning of the well-known terms and then give the definition of the Halo Analog state:

> **Isobaric analog state** is the state with the same total isotopic spin and the same total angular momentum, but another zero component of the isotopic spin. Usually the spatial structure of all the nuclei belonging to the same isobaric chain is very similar. The relative position of two isobaric analog states is defined ($M_p - M_n + \Delta E_{Coulomb}$) — ordinary $\pm 1$ MeV. In the sense of the $\beta$-decay, the isobaric analog states may be connected only with Fermi transitions.
>
> **Gamow-Teller resonance** is ordinary understood not as a state, but as a series of states with a high $B_{GT}$ values. This condition means, that while the isobaric analog states belong to one isotopic multiplet, the Gamow-Teller resonance states belong to one spin-isospin SU(4) supermultiplet.
>
> **Halo Analog state** concept is based on the $\beta$-decay experiments, hence the Halo Analog state belong to the Gamow-Teller resonance states. But it is Gamow-Teller resonance state with very specific structure. If the mother state has a (neutron) halo structure, then the HA state would have very similar extended spatial structure, and spin-isospin structure defined by the fact that one of the halo neutrons is replaced with proton (the total angular momentum is, certainly, **J**(daughter)=**J**(mother)+**1** ).

Note that HA state is a "physical" state, which existence and distinct nature are connected with the remote, spatially separated from the core nature of the valence nucleons in the halo nuclei. Halo nuclei do not know what is happening with a core. The position of the HA state may be easily estimated basing on its "physical" nature. The energy difference of the mother and the HA state can be estimated according to the energy gain in the cluster structures, which can appear replacing one neutron in the mother state by a proton. The sparse character of the halo means that only deuteron-like correlation would be significant for the energy gain in the case of the HA state, which is hence approximately given by $(M_p - M_n + \Delta E_{Coulomb} - E_d) \sim 2$ MeV.

In the other words: all the states with the same spin-isospin Young tableau as the mother state would belong to the GTR states and only one of them with very peculiar halo structure would be called Halo Analog state. The necessity to introduce this term is that a strong concentration of the GT strength is observed

in the $\beta$-decays of all the investigated neutron halo nuclei ($^6$He, $^8$He, $^9$Li, $^{11}$Li) with energy about 2 MeV lower then mother state. This energy splitting is easily explained above suggesting that the energy gain of the state is connected with the binding energy of the deuteron. But to be able to gain this amount of energy we have to assume a very large size of the valence nucleon-nucleon correlation; here we return to the halo nature of the state.

The idea of the HA states is very intuitive and it is explaining some phenomenon in the halo nuclei, but the only HA state, which is really well studied now is the $^6$Li g.s. The information about such states in the other nuclei is quite poor: in $^8$Li HA state ($\sim$ 9 MeV) was observed only in $\beta$-decay; in $^9$Be the experimental data about possible HA states at 11.28, 11.81 MeV are controversial (see Section 4.4). For $^{11}$Be two recent experimental works appeared [80, 92], which can be interpreted as confirmation of the HA state concept.

### 4.5.2 Many-body beta-delayed decays of $^{11}$Li

Multiparticle $\beta$-delayed emission from the highly excited states in $^{11}$Be is another challenge for the analysis. There are two decay channels, which can be analyzed using procedures described in [P4,P8]: $\alpha$+$^6$He+n, 2$\alpha$+3n, which are most probably connected with the decay of $^9$Li-core. Because of various charged particles produced in the decay of $^{11}$Li only the high-energy part of spectrum is accessible for analysis. Nevertheless, it is interesting to study the interplay of five-body and three-body channels of the decay.

## 4.6 New method for calculations of the three-body "nonborromean" systems

This method [P7] pretends the adequate description of both two-body and three-body asymptotics for bound states of the nonborromean systems. Hence it pretends to be specially suited for description of processes, which have peripheral character and require exact knowledge of asymptotics. Two important results of our quite recent studies should be emphasized.

1. The convergence of radial characteristics is much slower than the energy convergence. The complete energy convergence may not mean convergence of WF in remote districts with a high precision if this is not guaranteed by analytically correct choice of the basis.

2. In the case of the Coulomb interaction the asymptotics is formed on a larger distance then we were able to imagine, requiring enormous basis for convergency.

These two aspects we would like to discuss for $^6$Li and $^8$B separately.

### 4.6.1 Properties of the $^6$Li ground state

The increase of the matter radius $\sim 0.1$ fm was found in these new calculations for $^6$Li, as compared with ordinary HH calculations. It is a significant addition if we are interested in the peripheral processes. If we look at convergence curves, then we see that energy convergence is very similar in both methods, but radial characteristics converge much faster in the new calculations. The reason is that in HH the "weight" of each individual harmonic number $K$ is defined by some characteristic distance $\rho_K$, where it give maximum contribution in energy. For $\rho > \rho_K$ HH machinery is "not very interested" in the correct asymptotic behavior. For nonborromean systems, formally, it is guaranteed by coupling of channels in the limit of their infinite number. In real HH calculations the individual harmonics with quantum numbers of binary channel rapidly achieve three-body borromean asymptotic behavior $\sim e^{-\varkappa\rho}/\rho^{5/2}$. In BC formalism individual harmonics automatically have correct asymptotics as they are obtained as a decomposition of analytically constructed binary function.

### 4.6.2 Properties of the $^8$B ground state

Using the realistic inter-cluster forces, adopted previously [88] for $^8$Li, it was possible to obtain binding energy of $^8$B with a good ($\sim$ 20 keV) precision. Radial characteristics, quadrupole and magnetic momenta were reproduced at least not worse than in microscopic calculations [41, 96]. The fact, that asymptotic normalization coefficients (ANC) are straightforwardly connected with cross sections of radioactive capture reactions in the limit of zero energy, was used in the works [81, 102] to obtain astrophysical factor $S_{17}(0)$. Value of $S_{17}$ factor is crucial for the solar neutrino problem. Using ANC value, based on our WF, the estimate $S_{17}(0)\sim$18 eV·b was obtained. That is in good agreement with the last "recommended" value $19^{+4}_{-2}$ eV·b [2].

It was found in paper [P7] that ANC is stabilizing on the distances $\sim$ 20-25 fm. That is in a sharp contrast with results of [81, 102], where stability was achieved at 5-7 fm. Cross check of this result is very difficult: RGM [41], GCM [50], or shell-model [102] based calculations simply can not penetrate that far. The physical reason of such slow stabilization is that real-life three-body Coulomb interaction ($\sim 1/\rho$) differs from two-body Coulomb ($\sim 1/Y$). This difference is quite slowly decreasing: $\sim 1/Y^3$. Compressibility of the dilute nuclear matter at large (20-25 fm) distances is very high and even such small perturbation may cause the deviation of WF from asymptotic behavior. The further investigation is required to clarify this important nuclear structure theory issue.

# Chapter 5

# Final remarks and acknowledgments

*Science can not be the terminal purpose of the humankind.*
*Only morality can be the terminal purpose...*

*N. Solov'yov*

*And two white snows have fallen this day.*
*Two white snows – the first one and the last one.*

*From a song*

After reading (or at least after looking through) this work one may have the feeling that the thesis deals with too different things and that the choice of the investigation subject was often accidental. To some extent it is true. The principal line for my work was studies of (two- and three-body) continuum of the three-body systems in the framework of the hyperspherical harmonic method. For different reasons only about "1/3" of this task was completed (consideration of binary correlations in the three-body bound state calculations [P7]). The most important of these reasons is that permanent communication with experimentalists always turns my attention to the necessity of qualitative understanding things, too complicated to be treated exactly. Among available interesting things the Author always tried to choose those, which are in his competence (the weaker process — the higher competence). He succeed in that not each time. Failed excursions as well as irrelevant to the main line investigations are not displayed in the thesis. But owing to the deviations from the principal line the problems were studied, which Author thought to be perspectiveless due to complexity ($\beta$-decays of $^{8}$He, $^{9}$Li, $^{11}$Li). In some cases ($^{8}$He, $^{9}$Li) processes were reasonably clarified (if not to everybody, then at least to the Author).

If the destiny is kind, it would be possible in the nearest years to study the two-body continuum of the three-body systems, and inelastic scattering ($2\to3$ processes). It would allow to make the next step in the studies of the problems,

connected with binary continuum of $^{6}$Li, $^{8}$Li, $^{8}$B, $^{11}$Be, discussed in this thesis. And may be it would allow to resolve some of them. Even the first results in this direction connected with the ground state of $^{8}$B were very interesting.

I would like to express gratitude to many people:

Professor Dmitriy Grechukhin, who left us not so long ago. He introduced me to the subject of nuclear physics, which was not popular among students at all: we were pacifists. His respective attitude to the students and soft pedagogical talent to a great extent defined the direction of my life.

My supervisor Mikhail Zhukov, whose care about me was much more then normal and not only in professional life.

Boris Danilin who taught me the basic skills and was always ready to assist with stupid problems, always arising in everyday's work.

Sometimes it is not simple to work with Natasha Shul'gina, but practically everything I've done, I've done in collaboration with her.

I always try to follow rigorous and demanding work style of Aleksey Barabanov. Unfortunately only try...

Permanent interest of Björn Jonson to my (sometimes may be not very minded) ideas was extremely stimulating. I've never heard "no" if I needed attention or help.

Hours spent with Göran Nyman discussing the details of experiments were the best possible school of "real life". As normal theoretical physicist I was not well (not at all) acquainted with the real life of experimentalists.

Jan Vaagen is an integral part of our collaboration. He is always very busy, but somehow do not forget about my existence.

I am not easily get used to people. I am grateful to everybody in the department for making this process painless.

Finally, I would like to thank all those who did not disturb me, and especially those who helped me, even if there was no special reason to do that.

---

*This fatty line means that I have nothing more to tell. At least in that work.*

*L. Grigorenko*

# Chapter 6

# Useful to know...

**Note:** the system of units used in the thesis is $\hbar = c = 1$ . All quantities in this system have dimensions like $[energy]^n$ (or $[length]^{-n}$— what you like better). To recalculate between quantities given in the units of energy and those given in the units of length you need only one coefficient, suitable both for nuclear and atomic physics:

$$\Xi = 197.327\ [\mathrm{MeV} \cdot \mathrm{fm}] = 197.327\ [\mathrm{eV} \cdot \mathrm{nm}]$$

The usage of this coefficient is the following: if you have some quantities $E(MeV)$ and $L(fm)$ then

$$E(fm^{-1}) = \frac{E(MeV)}{197.327} \quad ; \qquad L(MeV^{-1}) = \frac{L(fm)}{197.327}$$

Be attentive: the value inverse to the momentum of the particle is not wave length, but wave length over $2\pi$.

$$\frac{197.327}{P(MeV)} = \bar{\lambda}(fm) = \frac{\lambda(fm)}{2\pi} \quad ; \qquad \frac{1239.842}{P(MeV)} = \lambda(fm)$$

To convert from this system to SI the values in $MeV$ should be divided by Plank constant for energy, and also by speed of light for momenta

$$\begin{aligned} E(s^{-1}) &= E(MeV)/\hbar = 1.51927 \cdot 10^{21} \cdot E(MeV) \\ P(m^{-1}) &= P(MeV)/\hbar c = 5.06773 \cdot 10^{12} \cdot P(MeV) \\ \hbar &= h/2\pi = 6.58212 \cdot 10^{-22}\ [MeV \cdot s] \\ c &= 299792458.\ [m \cdot s^{-1}] \end{aligned}$$

The other few constants you need to feel yourself confident with this system of units are

| | |
|---|---|
| $\alpha = e^2 = \frac{1}{137.036}$ | Fine structure constant |
| $C_{coul} = 1.44001$ | Coulomb constant [MeV $\cdot$ fm] |
| $C_{cfg} = 20.7355$ | Centrifugal constant [MeV $\cdot$ fm$^2$] |
| $„\frac{(M_n+M_p)}{\hbar^2}" = \frac{1}{20.7355}$ | Constant in the Schrödinger equation [MeV$^{-1}$ $\cdot$ fm$^{-2}$] |
| $m_e = 0.510999$ | Electron mass [MeV] |
| $M_n = 939.5656$ | Neutron mass [MeV] |
| $M_p = 938.2723$ | Proton mass [MeV] |
| $E_d = 2.22457$ | Deuteron binding energy [MeV] |
| $k = 8.618 \cdot 10^{-5}$ | Bolzman constant [eV $\cdot$ K$^{-1}$] |
| $k^{-1} = 11604.$ | Inverse Bolzman constant [eV$^{-1}$ $\cdot$ K] |

The values $C_{coul}$ and $C_{cfg}$ are used in the following way:

$$U_{coul}(MeV) = \frac{C_{coul}\, Z_1 Z_2}{r(fm)} \quad ; \qquad U_{cfg}(MeV) = \frac{C_{cfg}\, l(l+1)\,(A_1+A_2)}{A_1 A_2\, r^2(fm)}$$

Coulomb parameter as a function of the C.M. energy

$$\eta(E) = \frac{\alpha Z_1 Z_2}{v} = 0.158112 \cdot Z_1 Z_2 \sqrt{\frac{A_1 A_2}{(A_1+A_2)\, E(MeV)}}$$

$$\psi''_{pl} + \left( p^2 - \frac{l(l+1)}{r^2} - \frac{2\eta p}{r} \right) \psi_{pl} = 0$$

Momentum and angular momentum operators

$$\hat{\mathbf{P}} = -i\,\nabla \quad ; \qquad \hat{\mathbf{L}} = \left[\mathbf{r}\,\hat{\mathbf{P}}\right] = -i\,[\mathbf{r}\,\nabla]$$

So plane wave normalized per one particle in a box volume $V$ is

$$|\mathbf{k}\rangle = \frac{\exp\{i\mathbf{P}\mathbf{r}\}}{\sqrt{V}}$$

Properties of the antisymmetric tensor

$$\varepsilon_{ikl}\varepsilon_{ikl} = 6\ ; \quad \varepsilon_{ikl}\varepsilon_{pkl} = 2\delta_{ip}\ ; \qquad \varepsilon_{ikl}\varepsilon_{pql} = \delta_{ip}\delta_{kq} - \delta_{iq}\delta_{kp}$$

$$\varepsilon_{ikl}\varepsilon_{pqt} = \begin{vmatrix} \delta_{ip} & \delta_{iq} & \delta_{it} \\ \delta_{kp} & \delta_{kq} & \delta_{kt} \\ \delta_{lp} & \delta_{lq} & \delta_{lt} \end{vmatrix}$$

# Chapter 7

# Jacobi coordinates and hyperspherical harmonics

The Jacobi coordinate systems have found a wide implementation in nuclear and atomic many-body problems because they are exploiting native, but hidden symmetry of the many-body free Hamiltonian (kinetic energy). For the general case of N particles it is the symmetry in respect with O(3N-3) group (here three degrees of freedom belong to center of mass motion of the system and it is of no interest to us). If we turn to the case of three particles, the symmetry of Hamiltonian in respect with $O(3)\otimes O(3)\otimes O(3)$ is evident. The use of Jacobi coordinates allows to deal only with $O(3)\otimes O(3)$ and isomorphism $O(3)\otimes O(3)\Longleftrightarrow O(6)$ leads to new quantum number — *hypermomentum* K. This quantum number appeared to be "good" (conserving) for 6-dimensional (collective) oscillator potential and free Hamiltonian. And as far as all the nuclear potentials are more or less "oscillator-like" (at least in some part of space) the bases build using the quantum number K should be well suited to the needs of computation. This implementation is done in the *hyperspherical harmonics* method.

## 7.1 Jacobi coordinates

are constructed in the following way: the first Jacobi vector is connecting two arbitrary particles; the second vector is connecting their center of mass with the third particle and so on. The last Jacobi vector is connecting center of mass of the whole system with the arbitrary point in the space, chosen as an origin and hence the momentum conjugated to this coordinate is ordinary conserved. For two particles the Jacobi system is unique. For three particles we have three possible systems. For $N\geq 4$ we have not only 4 systems obtained by the cyclical permutation of particles but also a set of topologically nonequivalent systems (having different graphs). The formulae connecting individual and Jacobi coordinates and individual and Jacobi coordinates momenta are the following

$(M = m_1 + m_2 + m_3)$:

$$\begin{cases} \mathbf{X} = & \mathbf{r}_1 - \mathbf{r}_2 \\ \mathbf{Y} = & \dfrac{m_1\mathbf{r}_1 + m_2\mathbf{r}_2}{m_1 + m_2} - \mathbf{r}_3 \\ \mathbf{R} = & \dfrac{m_1\mathbf{r}_1 + m_2\mathbf{r}_2 + m_3\mathbf{r}_3}{M} \end{cases} \qquad \begin{cases} \mathbf{r}_1 = & \mathbf{R} + \dfrac{m_3}{M}\mathbf{Y} + \dfrac{m_2}{m_1 + m_2}\mathbf{X} \\ \mathbf{r}_2 = & \mathbf{R} + \dfrac{m_3}{M}\mathbf{Y} - \dfrac{m_1}{m_1 + m_2}\mathbf{X} \\ \mathbf{r}_3 = & \mathbf{R} - \dfrac{m_1 + m_2}{M}\mathbf{Y} \end{cases}$$

$$\begin{cases} \mathbf{P}_x = & \dfrac{m_1\mathbf{p}_1 - m_2\mathbf{p}_2}{m_1 + m_2} \\ \mathbf{P}_y = & \dfrac{m_3(\mathbf{p}_1 + \mathbf{p}_2) - (m_1 + m_2)\mathbf{p}_3}{M} \\ \mathbf{P}_R = & \mathbf{p}_1 + \mathbf{p}_2 + \mathbf{p}_3 \end{cases} \qquad \begin{cases} \mathbf{p}_1 = & \dfrac{m_1}{M}\mathbf{P}_R + \dfrac{m_1}{m_1 + m_2}\mathbf{P}_y + \mathbf{P}_x \\ \mathbf{p}_2 = & \dfrac{m_2}{M}\mathbf{P}_R + \dfrac{m_2}{m_1 + m_2}\mathbf{P}_y - \mathbf{P}_x \\ \mathbf{p}_3 = & \dfrac{m_3}{M}\mathbf{P}_R - \mathbf{P}_y \end{cases}$$

This transformations keep two important bilinear forms (the phase of the plane wave and kinetic energy) diagonal (see speculations about hidden symmetry above)

$$\mathbf{p}_1\mathbf{r}_1 + \mathbf{p}_2\mathbf{r}_2 + \mathbf{p}_3\mathbf{r}_3 = \mathbf{P}_x\mathbf{X} + \mathbf{P}_y\mathbf{Y} + \mathbf{P}_R\mathbf{R}$$

$$\frac{\mathbf{p}_1^2}{2m_1} + \frac{\mathbf{p}_2^2}{2m_2} + \frac{\mathbf{p}_3^2}{2m_3} = \frac{m_1 + m_2}{2m_1m_2}\mathbf{P}_x^2 + \frac{M}{2(m_1 + m_2)m_3}\mathbf{P}_y^2 + \frac{1}{2M}\mathbf{P}_R^2$$

The Jacobians of the transformations are all unity

$$\frac{D\left(\mathbf{r}_1\mathbf{r}_2\mathbf{r}_3\right)}{D\left(\mathbf{RYX}\right)} = \frac{D(\mathbf{p}_1\mathbf{p}_2\mathbf{p})}{D(\mathbf{P}_R\mathbf{P}_y\mathbf{P}_x)} = 1$$

## 7.2 Normalized Jacobi coordinates

are introduced to simplify the *hyperspherical harmonics* method variables and to unify them for different sets of masses $m_1$, $m_2$, $m_3$. To keep the correct dimensions for the coordinates and momenta the mass numbers $A_1$, $A_2$, $A_2$ ($A = A_1 + A_2 + A_3$) are used instead of masses.

$$\begin{cases} \mathbf{x} = & \sqrt{\dfrac{A_1A_2}{A_1 + A_2}}\left(\mathbf{r}_1 - \mathbf{r}_2\right) \\ \mathbf{y} = & \sqrt{\dfrac{(A_1 + A_2)A_3}{A}}\left(\dfrac{A_1\mathbf{r}_1 + A_2\mathbf{r}_2}{A_1 + A_2} - \mathbf{r}_3\right) \\ \mathbf{r} = & \dfrac{A_1\mathbf{r}_1 + A_2\mathbf{r}_2 + A_3\mathbf{r}_3}{\sqrt{A}} \end{cases}$$

$$\begin{cases} \mathbf{r}_1 = & \dfrac{\mathbf{r}}{\sqrt{A}} + \sqrt{\dfrac{A_3}{A(A_1 + A_2)}}\mathbf{y} + \sqrt{\dfrac{A_2}{(A_1 + A_2)A_3}}\mathbf{x} \\ \mathbf{r}_2 = & \dfrac{\mathbf{r}}{\sqrt{A}} + \sqrt{\dfrac{A_3}{A(A_1 + A_2)}}\mathbf{y} - \sqrt{\dfrac{A_2}{(A_1 + A_2)A_3}}\mathbf{x} \\ \mathbf{r}_3 = & \dfrac{\mathbf{r}}{\sqrt{A}} - \sqrt{\dfrac{A_1 + A_2}{AA_3}}\mathbf{y} \end{cases}$$

$$\begin{cases} \mathbf{p}_x = & \sqrt{\dfrac{A_1+A_2}{A_1A_2}}\dfrac{A_1\mathbf{p}_1 - A_2\mathbf{p}_2}{A_1+A_2} \\ \mathbf{p}_y = & \sqrt{\dfrac{A}{(A_1+A_2)A_3}}\dfrac{A_3(\mathbf{p}_1+\mathbf{p}_2)-(A_1+A_2)\mathbf{p}_3}{A} \\ \mathbf{p}_r = & \dfrac{\mathbf{p}_1+\mathbf{p}_2+\mathbf{p}_3}{\sqrt{A}} \end{cases}$$

$$\begin{cases} \mathbf{p}_1 = & \dfrac{A_1}{\sqrt{A}}\mathbf{p}_r + A_1\sqrt{\dfrac{A_3}{A(A_1+A_2)}}\mathbf{p}_y + \sqrt{\dfrac{A_1A_2}{A_1+A_2}}\mathbf{p}_x \\ \mathbf{p}_2 = & \dfrac{A_2}{\sqrt{A}}\mathbf{p}_r + A_2\sqrt{\dfrac{A_3}{A(A_1+A_2)}}\mathbf{p}_y - \sqrt{\dfrac{A_1A_2}{A_1+A_2}}\mathbf{p}_x \\ \mathbf{p}_3 = & \dfrac{A_3}{\sqrt{A}}\mathbf{p}_r - \sqrt{\dfrac{(A_1+A_2)A_3}{A}}\mathbf{p}_y \end{cases}$$

As in the previous case the transformations conserve two bilinear forms diagonal

$$\mathbf{p}_1\mathbf{r}_1 + \mathbf{p}_2\mathbf{r}_2 + \mathbf{p}_3\mathbf{r}_3 = \mathbf{p}_x\mathbf{x} + \mathbf{p}_y\mathbf{y} + \mathbf{p}_r\mathbf{r}$$

$$\frac{\mathbf{p}_1^2}{2m_1} + \frac{\mathbf{p}_2^2}{2m_2} + \frac{\mathbf{p}_3^2}{2m_3} = \frac{\mathbf{p}_r^2}{2m} + \frac{\mathbf{p}_y^2}{2m} + \frac{\mathbf{p}_x^2}{2m} =$$

where $m$ is a nucleon mass taken to be equal for neutrons and protons. The Jacobians of the transformations are:

$$\frac{D\left(\mathbf{r}_1\mathbf{r}_2\mathbf{r}_3\right)}{D(\,\mathbf{r}\,\mathbf{y}\,\mathbf{x}\,)} = \left(\frac{D(\mathbf{p}_1\mathbf{p}_2\mathbf{p}_3)}{D(\mathbf{p}_r\mathbf{p}_y\mathbf{p}_x)}\right)^{-1} = \left(A_1A_2A_3\right)^{-3/2}$$

## 7.3 Hyperspherical harmonics

both in the coordinate and momentum spaces are defined using collective variables $\rho$ and $\theta_\rho$ ($\varkappa$ and $\theta_\varkappa$):

$$\rho = \sqrt{x^2+y^2} \quad ; \qquad \theta_\rho = \arctan(x/y)$$

$$\varkappa = \sqrt{p_x^2+p_y^2} = \sqrt{2mE} = \sqrt{2m(E_x+E_y)}$$

$$\theta_\varkappa = \arctan\left(\sqrt{E_x/E_y}\right) = \arctan\left(p_x/p_y\right)$$

Variable $\rho$ is invariant in respect with rotations in the space and permutations of particles. We can also write it in explicitly symmetric form using relative distances between the particles $\mathbf{r}_{ij}$:

$$\rho^2 = \frac{A_1A_2A_3}{A}\left(\frac{\mathbf{r}_{12}^2}{A_3} + \frac{\mathbf{r}_{23}^2}{A_1} + \frac{\mathbf{r}_{31}^2}{A_2}\right)$$

In the work we use two "types" of the hyperspherical harmonics: function $\mathcal{J}^{LM_L}_{Kl_xl_y}$, which is pure coordinate and function $\mathcal{L}^{JM}_{KLSl_xl_y}$, which contains also spin coupling and internal WF of the clusters.

$$\mathcal{J}^{JM}_{Kl_xl_y}(\Omega) = \psi_K^{l_xl_y}(\theta)\ \left[Y_{l_x}\otimes Y_{l_y}\right]_{JM}$$

$$\mathcal{L}^{JM}_{KLSl_xl_y}(\Omega) = \psi_K^{l_xl_y}(\theta)\left[\left[Y_{l_x}\otimes Y_{l_y}\right]_{LM_L}\otimes\Psi_{SM_S}\right]_{JM} \tag{7.1}$$

where $\Psi_{SM_S}$ contains WFs of clusters coupled in the total angular momentum $S$ ; $\Omega$ is $\Omega\rho = \{\theta\rho, \hat{x}, \hat{y}\}$ or $\Omega_\varkappa = \{\theta_\varkappa, \hat{p}_x, \hat{p}_y\}$ ; $\psi_K^{l_xl_y}(\theta)$ can be expressed by means of the Jacobi polynomials:

$$\psi_K^{l_xl_y}(\theta) = N_K^{l_xl_y}(\sin\theta)^{l_x}(\cos\theta)^{l_y}P^{l_x+1/2,l_y+1/2}_{\frac{K-l_x-l_y}{2}}(\cos 2\theta)$$

$$N_K^{l_xl_y} = \sqrt{\frac{2(n!)(K+2)(n+l_x+l_y+1)!}{\Gamma(n+l_x+3/2)\Gamma(n+l_y+3/2)}} \quad ; \qquad n = \frac{K-l_x-l_y}{2}$$

The normalization conditions for the functions $\psi_K^{l_xl_y}(\theta)$ are:

$$\int_0^{\pi/2}\psi_K^{l_xl_y}(\theta)\,\psi_{K'}^{l'_xl'_y}(\theta)\,\sin^2\theta\,\cos^2\theta\,d\theta = \delta_{KK'}\delta_{l_xl'_x}\delta_{l_yl'_y}$$

### 7.3.1 Some lowest harmonics

| Positive parity | Negative parity |
|---|---|
| $\psi_0^{00}(\theta) = \frac{4}{\sqrt{\pi}}$ | $\psi_1^{10}(\theta) = \frac{8}{\sqrt{2\pi}}\sin\theta$ |
| $\psi_2^{00}(\theta) = \frac{8}{\sqrt{\pi}}\cos 2\theta$ | $\psi_1^{01}(\theta) = \frac{8}{\sqrt{2\pi}}\cos\theta$ |
| $\psi_2^{11}(\theta) = \frac{8}{\sqrt{3\pi}}\sin 2\theta$ | $\psi_3^{10}(\theta) = \frac{8}{\sqrt{6\pi}}(4\cos 2\theta+1)\sin\theta$ |
| $\psi_2^{20}(\theta) = \frac{16}{\sqrt{5\pi}}\sin^2\theta$ | $\psi_3^{12}(\theta) = \frac{32}{\sqrt{6\pi}}\cos^2\theta\sin\theta$ |
| $\psi_2^{02}(\theta) = \frac{16}{\sqrt{5\pi}}\cos^2\theta$ | $\psi_3^{01}(\theta) = \frac{8}{\sqrt{6\pi}}(4\cos 2\theta-1)\cos\theta$ |
| $\psi_4^{00}(\theta) = \frac{4}{\sqrt{\pi}}(1+2\cos 4\theta)$ | $\psi_3^{21}(\theta) = \frac{32}{\sqrt{6\pi}}\cos\theta\sin^2\theta$ |
| $\psi_4^{11}(\theta) = \frac{8}{\sqrt{2\pi}}\sin 4\theta$ | $\psi_5^{10}(\theta) = \frac{8}{\sqrt{3\pi}}(2+2\cos 2\theta+3\cos 4\theta)\sin\theta$ |
| $\psi_4^{20}(\theta) = \frac{32}{\sqrt{70\pi}}(5\cos 2\theta+2)\sin^2\theta$ | $\psi_5^{12}(\theta) = \frac{32}{\sqrt{30\pi}}(6\cos 2\theta-1)\cos^2\theta\sin\theta$ |
| $\psi_4^{02}(\theta) = \frac{32}{\sqrt{70\pi}}(5\cos 2\theta-2)\cos^2\theta$ | $\psi_5^{10}(\theta) = \frac{8}{\sqrt{3\pi}}(2-2\cos 2\theta+3\cos 4\theta)\cos\theta$ |
| $\psi_6^{00}(\theta) = \frac{8}{\sqrt{\pi}}(\cos 2\theta+\cos 6\theta)$ | $\psi_5^{21}(\theta) = \frac{32}{\sqrt{30\pi}}(6\cos 2\theta+1)\cos\theta\sin^2\theta$ |

# Chapter 8

# Special functions

## 8.1 Spherical functions

**Definition**

$$Y_{lm}(\theta,\varphi) = \sqrt{\frac{2l+1}{4\pi}\frac{(l-|m|)!}{(l+|m|)!}}\, P_l^{|m|}(\cos\theta)\, e^{im\varphi}$$

$$Y_{l0}(\theta,\varphi) = \sqrt{\frac{2l+1}{4\pi}}\, P_l(\cos\theta)$$

this definition, known as "Condon and Shortley", is used in the thesis. The other widely used definition is one of Edmonds, Fano and Racah. The difference is the phase coefficient $i^l$. From the physical point of view the function calibrated in EFR have the advantage that conjugation is equivalent to reflection of time:

$$Y_{lm}^* = (-)^{l-m} Y_{l-m}$$

**Normalization and orthogonality**

$$\int Y_{lm}^*(\hat{r})\, Y_{l'm'}(\hat{r})\, d\Omega_r = \delta_{ll'}\, \delta_{mm'}$$

$$\sum_{l,m} Y_{lm}^*(\hat{r})\, Y_{lm}(\hat{r}') = \delta(\hat{r},\hat{r}')$$

$$\sum_{m} Y_{lm}^*(\hat{r})\, Y_{lm}(\hat{r}) = \frac{2l+1}{4\pi}$$

$$P_l(\cos\widehat{rr}') = \frac{4\pi}{2l+1}\sum_{m=-l}^{l} Y_{lm}^*(\hat{r})\, Y_{lm}(\hat{r}')$$

**Symmetries**

$$Y_{lm} = (-)^{-m} Y_{l-m}^* \quad ; \qquad Y_{lm}^* = (-)^{-m} Y_{l-m} \quad ; \qquad Y_{lm}(-\hat{r}) = (-)^l Y_{lm}(\hat{r})$$

**Formulae**

Expansions of product

$$Y_{Pq}Y_{lm} = \sum_{LM} \frac{\hat{P}\hat{l}}{\sqrt{4\pi}\hat{L}} C^{L0}_{l0P0} C^{LM}_{lmPq} Y_{LM} \tag{8.1}$$

$$Y_{l_1m_1}Y_{l_2m_2}Y_{l_3m_3} = \sum_{LML'M'} \frac{\hat{l}_1\hat{l}_2\hat{l}_3}{4\pi\hat{L}} C^{L'0}_{l_10l_20} C^{L0}_{L0l_30} C^{L'M'}_{l_1m_1l_2m_2} C^{LM}_{L'M'l_3m_3} Y_{LM}$$

Plane wave expansion

$$e^{i\mathbf{kr}} = 4\pi \sum_{l=0}^{\infty} \sum_{m=-l}^{l} i^l \, j_l(kr) \, Y^*_{lm}(\hat{r}) Y_{lm}(\hat{k})$$

Summation theorem can be obtained as consequence of plane wave expansion

$$\begin{aligned}(\mathbf{r}-\mathbf{r}')^l Y_{lm}(\widehat{r-r'}) \;\; &= \;\; \sum_{LM} (-)^L \left( \tfrac{4\pi(2l+1)!}{(2L+1)!(2l-2L+1)!} \right)^{1/2} C^{lm}_{(l-L)(m-M)LM} \\ &\quad \times r^{(l-L)} Y_{(l-L)(m-M)}(\hat{r}) \;\cdot\; (r')^L Y_{LM}(\hat{r}')\end{aligned}$$

The multipole expansion of the Coulomb factor for $|\mathbf{r}| > |\mathbf{r}'|$ (otherwise $\mathbf{r} \leftrightarrow \mathbf{r}'$ should be replaced)

$$\frac{1}{|\mathbf{r}-\mathbf{r}'|} = \sum_{l,m} \frac{4\pi}{2l+1} \frac{1}{r} \left( \frac{r'}{r} \right)^l Y^*_{lm}(\hat{r}) \, Y_{lm}(\hat{r}')$$

**Special cases**

$$\begin{aligned} Y_{00} &= \tfrac{1}{\sqrt{4\pi}} & Y_{20} &= \sqrt{\tfrac{5}{16\pi}}(3\cos^2\theta - 1) \\ Y_{10} &= \sqrt{\tfrac{3}{4\pi}} \cos\theta & Y_{2\pm1} &= \mp\sqrt{\tfrac{15}{8\pi}} \sin\theta\cos\theta \, e^{\pm i\varphi} \\ Y_{1\pm1} &= \mp\sqrt{\tfrac{3}{8\pi}} \sin\theta \, e^{\pm i\varphi} & Y_{2\pm2} &= \sqrt{\tfrac{15}{32\pi}} \sin^2\theta \, e^{\pm 2i\varphi} \end{aligned}$$

**Connection with other functions**

Expressions for some spherical functions via spherical components of the unity vector $\mathbf{n}_i$, $i = -1, 0, 1$ ( $n_0 = \cos\theta$ ; $n_{\pm1} = \mp\frac{1}{\sqrt{2}} \sin\theta e^{\pm i\varphi}$)

$$\begin{aligned} Y_{00} &= \tfrac{1}{\sqrt{4\pi}} & Y_{33} &= \sqrt{\tfrac{35}{8\pi}} n_1 n_1 n_1 \\ Y_{1\lambda} &= \sqrt{\tfrac{3}{4\pi}} n\lambda & Y_{32} &= \sqrt{\tfrac{35}{8\pi}} \sqrt{3} n_0 n_1 n_1 \\ Y_{22} &= \sqrt{\tfrac{15}{8\pi}} n_1 n_1 & Y_{31} &= \sqrt{\tfrac{35}{8\pi}} \sqrt{\tfrac{3}{5}} (n_{-1} n_1 n_1 + 2 n_0 n_0 n_1) \\ Y_{21} &= \sqrt{\tfrac{15}{8\pi}} \sqrt{2} n_0 n_1 & Y_{30} &= \sqrt{\tfrac{35}{8\pi}} \sqrt{\tfrac{2}{5}} (n_0 n_0 n_0 + 3 n_{-1} n_0 n_1) \\ Y_{20} &= \sqrt{\tfrac{15}{8\pi}} \sqrt{\tfrac{2}{3}} (n_0 n_0 + n_{-1} n_1) & Y_{3-1} &= \sqrt{\tfrac{35}{8\pi}} \sqrt{\tfrac{3}{5}} (n_{-1} n_{-1} n_1 + 2 n_{-1} n_0 n_0) \\ Y_{2-1} &= \sqrt{\tfrac{15}{8\pi}} \sqrt{2} n_{-1} n_0 & Y_{3-2} &= \sqrt{\tfrac{35}{8\pi}} \sqrt{3} n_{-1} n_{-1} n_0 \\ Y_{2-2} &= \sqrt{\tfrac{15}{8\pi}} n_{-1} n_{-1} & Y_{3-3} &= \sqrt{\tfrac{35}{8\pi}} n_{-1} n_{-1} n_{-1} \end{aligned}$$

**Expressions via vectors for correlation calculations**

$$
\begin{aligned}
(4\pi)^{3/2}C^{00}_{1k1p}Y^*_{00}(\hat{a})Y_{1k}(\hat{b})Y_{1p}(\hat{c}) &= -\sqrt{3}(\hat{b}\,\hat{c})\\
(4\pi)^{3/2}C^{1m}_{1k00}Y^*_{1m}(\hat{a})Y_{1k}(\hat{b})Y_{00}(\hat{c}) &= 3(\hat{a}\;\hat{b})\\
i(4\pi)^{3/2}C^{1m}_{1k1p}Y^*_{1m}(\hat{a})Y_{1k}(\hat{b})Y_{1p}(\hat{c}) &= -\frac{3\sqrt{6}}{2}(\hat{a}\,[\hat{b}\,\hat{c}])\\
i(4\pi)^{3/2}C^{2m}_{1k2p}Y^*_{2m}(\hat{a})Y_{1k}(\hat{b})Y_{2p}(\hat{c}) &= -\frac{15\sqrt{2}}{2}(\hat{a}\,[\hat{b}\,\hat{c}])(\hat{a}\;\hat{c})\\
i(4\pi)^{3/2}C^{1m}_{2k2p}Y^*_{1m}(\hat{a})Y_{2k}(\hat{b})Y_{2p}(\hat{c}) &= \frac{3\sqrt{30}}{2}(\hat{a}\,[\hat{b}\,\hat{c}])(\hat{b}\;\hat{c})\\
i(4\pi)^{3/2}C^{3m}_{2k2p}Y^*_{3m}(\hat{a})Y_{2k}(\hat{b})Y_{2p}(\hat{c}) &= \frac{3\sqrt{70}}{4}(\hat{a}\,[\hat{b}\,\hat{c}])\left\{(\hat{b}\;\hat{c})-5(\hat{a}\;\hat{b})(\hat{a}\;\hat{c})\right\}\\
(4\pi)^{3/2}C^{2m}_{1k1p}Y^*_{2m}(\hat{a})Y_{1k}(\hat{b})Y_{1p}(\hat{c}) &= \frac{\sqrt{30}}{2}\left\{3(\hat{a}\;\hat{b})(\hat{a}\;\hat{c})-(\hat{b}\;\hat{c})\right\}\\
(4\pi)^{3/2}C^{1m}_{1k2p}Y^*_{1m}(\hat{a})Y_{1k}(\hat{b})Y_{2p}(\hat{c}) &= \frac{3\sqrt{2}}{2}\left\{(\hat{a}\;\hat{b})-3(\hat{a}\;\hat{c})(\hat{b}\;\hat{c})\right\}\\
(4\pi)^{3/2}C^{3m}_{1k2p}Y^*_{3m}(\hat{a})Y_{1k}(\hat{b})Y_{2p}(\hat{c}) &= \frac{3\sqrt{7}}{2}\left\{5(\hat{a}\;\hat{c})^2(\hat{a}\;\hat{b})-2(\hat{a}\;\hat{c})(\hat{b}\;\hat{c})-(\hat{a}\;\hat{b})\right\}\\
(4\pi)^{3/2}C^{2m}_{2k2p}Y^*_{2m}(\hat{a})Y_{2k}(\hat{b})Y_{2p}(\hat{c}) &= \frac{5\sqrt{70}}{14}\left\{3\left[(\hat{a}\;\hat{b})^2+(\hat{a}\;\hat{c})^2+(\hat{b}\;\hat{c})^2\right]\right.\\
&\quad \left.-9(\hat{a}\;\hat{b})(\hat{b}\;\hat{c})(\hat{a}\;\hat{c})-2\right\}\\
(4\pi)^{3/2}C^{2m}_{1k3p}Y^*_{2m}(\hat{a})Y_{1k}(\hat{b})Y_{3p}(\hat{c}) &= \frac{3\sqrt{5}}{2}\left\{(\hat{b}\;\hat{c})+2(\hat{a}\;\hat{b})(\hat{a}\;\hat{c})-5(\hat{a}\;\hat{c})^2(\hat{b}\;\hat{c})\right\}
\end{aligned}
$$

## 8.2 Bessel functions

**Definition**

$$j_n(r)=\sqrt{\frac{\pi}{2r}}J_{n+1/2}(r)=r^n\left(-\frac{d}{rdr}\right)^n\frac{\sin r}{r}\quad;\qquad n_n(r)=(-)^{n+1}j_{-(n+1)}(r)$$

Function $j_n$ for negative and positive $n$ can be found in the following way:

$$
\begin{aligned}
j_n(r) &= f_n(r)\sin(r)+(-)^{n+1}f_{-(n+1)}(r)\cos(r)\\
f_{n+1} &= (2n+1)\frac{f_n}{r}-f_{n-1}\\
f_{-1} &= 0\quad;\qquad f_0=\frac{1}{r}\quad;\qquad f_1=\frac{1}{r^2}
\end{aligned}
$$

**Asymptotics**

$$
\begin{aligned}
j_n(r\to 0) &= \frac{r^n}{1\cdot 3\cdot\ldots\cdot(2n+1)} & n_n(r\to 0) &= -\frac{1\cdot 3\cdot\ldots\cdot(2n-1)}{r^{n+1}}\\
j_n(r\to\infty) &= \frac{\sin(r-\pi n/2)}{r} & n_n(r\to\infty) &= -\frac{\cos(r-\pi n/2)}{r}
\end{aligned}
$$

**Equation and recurrent relations**

Here $f_n = \left\{ j_n, n_n, h_n^{(1)}, h_n^{(2)} \right\}$

$$f_n'' + \frac{2}{r} f_n' + \left[ 1 - \frac{n(n+1)}{r^2} \right] f_n = 0$$

$$\begin{aligned} n f_{n-1} - (n+1) f_{n+1} &= (2n+1) \frac{d}{dr} f_n \\ \frac{(n+1)}{r} f_n + \frac{d}{dr} f_n &= f_{n-1} \\ \frac{n}{r} f_n - \frac{d}{dr} f_n &= f_{n+1} \end{aligned}$$

**Special cases**

$$\begin{aligned} j_0 &= \frac{\sin r}{r} \qquad j_1 = \frac{\sin r}{r^2} - \frac{\cos r}{r} \qquad j_2 = \left( \frac{3}{r^3} - \frac{1}{r} \right) \sin r - \frac{3}{r^2} \cos r \\ j_3 &= \left( \frac{15}{r^4} - \frac{6}{r^2} \right) \sin r - \left( \frac{15}{r^3} - \frac{1}{r} \right) \cos r \\ j_4 &= \left( \frac{105}{r^5} - \frac{45}{r^3} + \frac{1}{r} \right) \sin r - \left( \frac{105}{r^4} - \frac{10}{r^2} \right) \cos r \\ j_5 &= \left( \frac{945}{r^6} - \frac{420}{r^4} + \frac{15}{r^2} \right) \sin r - \left( \frac{945}{r^5} - \frac{105}{r^3} + \frac{1}{r} \right) \cos r \\ n_0 &= -\frac{\cos r}{r} \qquad n_1 = -\frac{\cos r}{r^2} - \frac{\sin r}{r} \qquad n_2 = -\left( \frac{3}{r^3} - \frac{1}{r} \right) \cos r - \frac{3}{r^2} \sin r \end{aligned}$$

## 8.3 Legendre polynomials

**Definition**

$$P_l(x) = \frac{1}{2^l l!} \frac{d^l}{dx^l} (x^2 - 1)^l \quad ; \qquad P_l^m(x) = (1 - x^2)^{m/2} \frac{d^m}{dx^m} P_l(x)$$

**Normalization**

$$\int_{-1}^{1} \left[ P_l^m(x) \right]^2 dx = \frac{2}{2l+1} \frac{(l+m)!}{(l-m)!}$$

**Special cases**

$$\begin{aligned} P_0 &= 1 \qquad P_1 = x \qquad P_2 = \frac{3x^2 - 1}{2} \qquad P_3 = \frac{5x^3 - 3x}{2} \\ P_4 &= \frac{35x^4 - 30x^2 + 3}{8} \qquad P_5 = \frac{63x^5 - 70x^3 + 15x}{8} \end{aligned}$$

# Chapter 9

# Algebra of spin-tensors

This is the Wigner-Eckart theorem, which brings the angular momentum theory to the hearts of the nuclear and atomic physicists:

$$\langle l'm' \left| T_{Pq} \right| lm \rangle = C^{l'm'}_{lmPq} \langle l' \left\| T_p \right\| l \rangle \tag{9.1}$$

Taking the things pragmatically, it allows not to take care of the magnetic quantum numbers calculating matrix elements. All the rest in this Section only allows to use this theorem in a full swing.

To make use of the expression (9.1) the wave functions should be in the representation with definite total angular momentum (how it is done in the continuum, see Sections 2.1.2, 2.1.3 and 2.2.5). Operator $T_{Pq}$ should be in a spin-tensor form with coupling corresponding to that of wave functions. It is achieved using expressions like (9.4) and (9.6).

## 9.1 Cyclic covariant vectors

Here $\mathbf{n}$ is a unity vector. The expressions for cyclic covariant vectors via Cartesian vectors and vice versa are:

$$\begin{cases} \mathbf{n}_+ = -\dfrac{\mathbf{n}_x + i\mathbf{n}_y}{\sqrt{2}} \\ \mathbf{n}_0 = \mathbf{n}_z \\ \mathbf{n}_- = \dfrac{\mathbf{n}_x - i\mathbf{n}_y}{\sqrt{2}} \end{cases} \qquad \begin{cases} \mathbf{n}_x = \dfrac{\mathbf{n}_- - \mathbf{n}_+}{\sqrt{2}} \\ \mathbf{n}_y = i\dfrac{\mathbf{n}_- + \mathbf{n}_+}{\sqrt{2}} \\ \mathbf{n}_z = \mathbf{n}_0 \end{cases}$$

The contravariant vector is complex conjugated to covariant. The connection of cyclic vectors with spherical functions is very simple

$$r_\lambda = \sqrt{\frac{4\pi}{3}}\, r\, Y_{1\lambda}(\hat{r}) \quad ; \qquad Y_{1\lambda}(\hat{r}) = \sqrt{\frac{3}{4\pi}}\, \frac{r_\lambda}{r}$$

The vector operations can be expressed using cyclic vectors and spherical functions in the following way:

$$(\mathbf{a}\cdot\mathbf{b}) = \sum_{\lambda=-1}^{1} a_\lambda b^*_\lambda = \sum_{\lambda=-1}^{1} (-)^\lambda a_\lambda b_{-\lambda} = -\,\hat{1}\, C^{00}_{1\lambda 1v} a_\lambda b_v = -\tfrac{4\pi ab}{\sqrt{3}} \left[ Y_1(\hat{a}) \otimes Y_1(\hat{b}) \right]_{00} \tag{9.2}$$

$$[\mathbf{a}\times\mathbf{b}]_\lambda = (-i)\sqrt{2}\, C^{1\lambda}_{1\mu 1v} a_\mu b_v = (-i)\, \frac{4\pi\sqrt{2}}{3} ab \left[ Y_1(\hat{a}) \otimes Y_1(\hat{b}) \right]_{1\lambda}$$

$$(\mathbf{a}\cdot[\mathbf{b}\times\mathbf{c}]) = i\, \frac{4\pi\sqrt{8\pi}}{3} abc \left[ Y_1(\hat{a}) \otimes \left[ Y_1(\hat{b}) \otimes Y_1(\hat{c}) \right]_1 \right]_{00}$$

## 9.2 Sigma-matrixes

**Cartesian**

$$\sigma_x = \begin{pmatrix} 0 & 1 \\ 1 & 0 \end{pmatrix} \qquad \sigma_y = \begin{pmatrix} 0 & -i \\ i & 0 \end{pmatrix} \qquad \sigma_z = \begin{pmatrix} 1 & 0 \\ 0 & -1 \end{pmatrix}$$

**Spherical**

$$\sigma_1 = \begin{pmatrix} 0 & -\sqrt{2} \\ 0 & 0 \end{pmatrix} \qquad \sigma_0 = \begin{pmatrix} 1 & 0 \\ 0 & -1 \end{pmatrix} \qquad \sigma_{-1} = \begin{pmatrix} 0 & 0 \\ \sqrt{2} & 0 \end{pmatrix}$$

**Commutation rules**

$$\sigma_i\sigma_k = \delta_{ik} + i\varepsilon_{ikl}\sigma_l \qquad \Rightarrow$$

$$\begin{array}{ll} \{\sigma_i\sigma_k\} = 2\delta_{ik} & \Rightarrow \qquad (\boldsymbol{\sigma}\cdot\mathbf{a})^2 = a^2 \\ [\sigma_i\sigma_k] = 2i\varepsilon_{ikl}\sigma_l & \end{array}$$

***τ*** **– matrixes**,
as they are defined in the nuclear physics, have nonzero matrix elements with unity absolute value.

$$\tau_+ = \begin{pmatrix} 0 & -1 \\ 0 & 0 \end{pmatrix} \qquad \tau_0 = \begin{pmatrix} 1 & 0 \\ 0 & -1 \end{pmatrix} \qquad \tau_- = \begin{pmatrix} 0 & 0 \\ 1 & 0 \end{pmatrix}$$

The $\sigma$ matrixes are providing the connection between manifolds of real vectors and complex matrixes 2×2; together with unity matrix — between manifolds of real 4-vectors and 2×2 matrixes.

$$A = \mathbf{I}\cdot a_0 + (\boldsymbol{\sigma}\cdot\mathbf{a})$$

$$a_0 = Sp(A) \quad ; \qquad a_i = Sp(\sigma_i A)$$

## 9.3 Clebsch-Gordan coefficients

**Definition**

Clebsch-Gordan coefficients (CGC) are defined as the expansion coefficients of the direct product for two presentation of some group over the other presentations of the same group.

$$\Psi_{l_1 m_1} \otimes \Psi_{l_2 m_2} = \sum_{JM} C^{JM}_{l_1 m_1 l_2 m_2} \Psi_{JM}$$

I used here the notations from angular momentum theory as mainly the rotation group (O(3) or SU(2) ) representations are used in physics. According to normalization and orthogonality of CGC, they supply a simple method for construction of the WF with definite angular momenta.

$$\Psi_{JM} = C^{JM}_{l_1 m_1 l_2 m_2} \Psi_{l_1 m_1} \Psi_{l_2 m_2}$$

**Conditions of triangle**

$C^{c\gamma}_{a\alpha b\beta} = 0$, if the condition of triangle for numbers $(a, b, c)$ is not satisfied.

**Normalization and orthogonality**

$$\sum_{m_1 m_2} C^{JM}_{l_1 m_1 l_2 m_2} C^{J'M'}_{l_1 m_1 l_2 m_2} = \delta_{JJ'}\delta_{MM'}$$

$$\sum_{JM} C^{JM}_{l_1 m_1 l_2 m_2} C^{JM}_{l_1 m'_1 l_2 m'_2} = \delta_{m_1 m'_1}\delta_{m_2 m'_2}$$

$$\sum_{m_1 m_2} C^{l_2 m_2}_{l_1 m_1 JM} C^{l_2 m_2}_{l_1 m_1 J'M'} = \frac{2l_2+1}{2J+1}\delta_{JJ'}\delta_{MM'}$$

**Symmetries**

| | |
|---|---|
| $C^{c\gamma}_{a\alpha b\beta} = (-)^{a+b-c} C^{c-\gamma}_{a-\alpha b-\beta}$ | changing signs |
| $C^{c\gamma}_{a\alpha b\beta} = (-)^{a+b-c} C^{c\gamma}_{b\beta a\alpha}$ | transposing lower indexes |
| $C^{c\gamma}_{a\alpha b\beta} = (-)^{a-\alpha}\frac{\hat{c}}{\hat{b}} C^{b-\beta}_{a\alpha c-\gamma} = (-)^{b+\beta}\frac{\hat{c}}{\hat{a}} C^{a-\alpha}_{c-\gamma b\beta} =$ | transposing upper with lower |
| $= (-)^{a-\alpha}\frac{\hat{c}}{\hat{b}} C^{b\beta}_{c\gamma a-\alpha} = (-)^{b+\beta}\frac{\hat{c}}{\hat{a}} C^{a\alpha}_{b-\beta c\gamma}$ | cyclical permutation |

**Special cases**

$$C^{a\alpha}_{b\beta 00} = C^{a\alpha}_{00 b\beta} = \delta^{a,b}_{\alpha,\beta} \quad ; \qquad C^{00}_{a\alpha b\beta} = \frac{(-)^{a-\alpha}}{\hat{a}}\delta^{a,b}_{\alpha,-\beta}$$

$$C^{a\alpha}_{a\alpha 10} = \frac{\alpha}{\sqrt{a(a+1)}}$$

$$C^{c0}_{a010} = \begin{cases} \sqrt{\frac{a+1}{2a+1}} & c = a+1 \\ 0 & c = a \\ -\sqrt{\frac{a}{2a+1}} & c = a-1 \end{cases}$$

"parity symbol": $C^{c0}_{a0b0} \neq 0$ if $a+b+c$ is even

**Connections with the other functions**

$$\begin{pmatrix} a & b & c \\ \alpha & \beta & \gamma \end{pmatrix} = \frac{(-)^{a-b-\gamma}}{\hat{c}} C^{c-\gamma}_{a\alpha b\beta}$$

## 9.4 6J symbols

**Definition**

$$\begin{Bmatrix} a & b & c \\ d & e & f \end{Bmatrix} = \frac{(-)^{a+b+e+d}}{\hat{a}\hat{d}} \sum_{\alpha\beta\gamma\delta\varepsilon} C^{f\varphi}_{a\alpha e\varepsilon} C^{a\alpha}_{c\gamma b\beta} C^{f\varphi}_{d\delta b\beta} C^{d\delta}_{c\gamma e\varepsilon}$$

This definition provides useful formulae for calculation of reduced matrix elements

$$\sum_{\alpha\beta\delta} C^{c\gamma}_{a\alpha b\beta} C^{e\varepsilon}_{d\delta b\beta} C^{d\delta}_{a\alpha f\varphi} = (-)^{c+b+f+d} \hat{c}\hat{d} \begin{Bmatrix} c & b & a \\ d & f & e \end{Bmatrix} C^{e\varepsilon}_{c\gamma f\varphi} \qquad (9.3)$$

and for recoupling of angular WFs

$$\begin{aligned} [[a \otimes b]_e \otimes d]_c &= \sum_{\mathbf{f}} (-)^{a+b+c+d} \hat{e}\,\hat{\mathbf{f}} \begin{Bmatrix} a & b & e \\ d & c & \mathbf{f} \end{Bmatrix} [a \otimes [b \otimes d]_{\mathbf{f}}]_c \qquad (9.4) \\ [a \otimes [b \otimes d]_e]_c &= \sum_{\mathbf{f}} (-)^{a+b+c+d} \hat{e}\,\hat{\mathbf{f}} \begin{Bmatrix} d & b & e \\ a & c & \mathbf{f} \end{Bmatrix} [[a \otimes b]_{\mathbf{f}} \otimes c]_c \end{aligned}$$

**Conditions of triangle**

$$\begin{Bmatrix} a & b & e \\ d & c & f \end{Bmatrix} = 0$$

if the condition of triangle for any set of numbers $(a,b,e)$, $(d,c,e)$, $(d,b,f)$, $(a,c,f)$ is not satisfied. In the graphical form these conditions are

$$\begin{Bmatrix} * & * & * \\ & & \end{Bmatrix} \quad \begin{Bmatrix} & & * \\ * & * & \end{Bmatrix} \quad \begin{Bmatrix} & * & \\ * & & * \end{Bmatrix} \quad \begin{Bmatrix} * & & \\ & * & * \end{Bmatrix}$$

Note, that all these conditions can be obtained from the first one applying the symmetry rules.

Let us introduce triangle condition symbol

$$\Delta_{abc} = \begin{cases} 1 & \text{if } (a,b,c) \text{ satisfy condition of triangle} \\ 0 & \text{if not} \end{cases}$$

**Normalization and orthogonality**

$$\sum_{\mathbf{e}} \hat{\mathbf{e}}^2 \hat{f}^2 \begin{Bmatrix} a & b & \mathbf{e} \\ d & c & f \end{Bmatrix} \begin{Bmatrix} a & b & \mathbf{e} \\ d & c & f' \end{Bmatrix} = \delta_{ff'} \Delta_{acf} \Delta_{bdf}$$

**Symmetries**

1. Invariant in respect with the transposition of any two columns.
2. Invariant in respect with the transposition of **any two** elements in the top row with **corresponding two** elements of the bottom row.

**Special cases**

$$\begin{Bmatrix} a & b & c \\ 0 & d & f \end{Bmatrix} = \frac{(-)^{a+b+c}}{\hat{b}\hat{c}} \delta_{bf} \delta_{cd} \Delta_{abc}$$

**Connections with other functions**

$$\begin{Bmatrix} a & b & e \\ d & c & f \end{Bmatrix} = (-)^{a+b+c+d} W(abcd; ef)$$

where $W(abcd; ef)$ is Rakah's W-function.

## 9.5 9J symbols

**Definition**

$$\begin{Bmatrix} a & b & c \\ d & e & f \\ g & h & i \end{Bmatrix} = \sum_{\mathbf{k}} (-)^{2\mathbf{k}} (2\mathbf{k}+1) \begin{Bmatrix} a & d & g \\ h & i & \mathbf{k} \end{Bmatrix} \begin{Bmatrix} b & e & h \\ d & \mathbf{k} & f \end{Bmatrix} \begin{Bmatrix} c & f & i \\ \mathbf{k} & a & b \end{Bmatrix}$$

The following formulae are useful for calculations of the reduced matrix elements

$$\left\langle [j_1' \otimes j_2']_{j'} \| [\mathbf{k_1} \otimes \mathbf{k_2}]_{\mathbf{k}} \| [j_1 \otimes j_2]_j \right\rangle = \hat{j}_1' \hat{j}_2' \hat{j} \hat{\mathbf{k}} \begin{Bmatrix} j_1 & j_2 & j \\ \mathbf{k_1} & \mathbf{k_2} & \mathbf{k} \\ j_1' & j_2' & j' \end{Bmatrix} \langle j_1' \| \mathbf{k_1} \| j_1 \rangle \times \\ \times \langle j_2' \| \mathbf{k_2} \| j_2 \rangle \qquad (9.5)$$

and for recoupling of the angular WFs

$$[[l_1 \otimes l_2]_L \otimes [S_1 \otimes S_2]_S]_J = \sum_{j_1 j_2} \hat{L}\,\hat{S}\,\hat{j}_1\,\hat{j}_2 \left\{ \begin{array}{ccc} l_1 & l_2 & L \\ S_1 & S_2 & S \\ j_1 & j_2 & J \end{array} \right\} \Big[[l_1 \otimes S_1]_{j_1} \otimes [l_2 \otimes S_2]_{j_2}\Big]_J \tag{9.6}$$

**Conditions of triangle**

should be satisfied in each column and each row of the 9J symbol.

**Normalization and orthogonality**

$$\sum_{\mathbf{h},\mathbf{i}} \hat{c}^2 \hat{f}^2 \hat{\mathbf{h}}^2 \hat{\mathbf{i}}^2 \left\{ \begin{array}{ccc} a & b & c \\ d & e & f \\ \mathbf{h} & \mathbf{i} & j \end{array} \right\} \left\{ \begin{array}{ccc} a & b & c' \\ d & e & f' \\ \mathbf{h} & \mathbf{i} & j \end{array} \right\} = \delta_{cc'}\delta_{ff'}$$

**Symmetries**

1. Invariant in respect with the matrix transposition.

2. Invariant in respect with even[1] transposition of the rows (columns).

3. If the transposition of rows (columns) is odd then the 9-J symbol is multiplied to $(-)^p$, $p = \sum_{kl} J_{kl}$ —the sum of all the 9 angular momenta in the symbol.

**Special cases**

$$\left\{ \begin{array}{ccc} 0 & e & e \\ f & d & b \\ f & c & a \end{array} \right\} = \left\{ \begin{array}{ccc} e & 0 & e \\ c & f & a \\ d & f & b \end{array} \right\} = \left\{ \begin{array}{ccc} f & f & 0 \\ d & c & e \\ b & a & e \end{array} \right\} = \left\{ \begin{array}{ccc} f & b & d \\ 0 & e & e \\ f & a & c \end{array} \right\} =$$

$$\left\{ \begin{array}{ccc} a & f & c \\ e & 0 & e \\ b & f & d \end{array} \right\} = \left\{ \begin{array}{ccc} b & a & e \\ f & f & 0 \\ d & c & e \end{array} \right\} = \left\{ \begin{array}{ccc} e & d & c \\ e & b & a \\ 0 & f & f \end{array} \right\} = \left\{ \begin{array}{ccc} c & e & d \\ a & e & b \\ f & 0 & f \end{array} \right\} =$$

$$\left\{ \begin{array}{ccc} a & b & e \\ c & d & e \\ f & f & 0 \end{array} \right\} = \frac{(-)^{b+c+e+f}}{\hat{e}\hat{f}} \left\{ \begin{array}{ccc} a & b & e \\ d & c & f \end{array} \right\}$$

[1]The transposition is **even** if it can be presented as a sequence of even number of elementary transpositions. The transposition is **odd** if the number of requiring elementary transpositions is odd.

## 9.6 Reduced matrix elements

### 9.6.1 Operators $\mathbf{Y}_{lm}$, r, $\ell$, sigma

**Spherical functions**

This expression is easily obtained using formula (8.1)

$$\langle l' \| Y_P \| l \rangle = \frac{\hat{P}\hat{l}}{\hat{l}'\sqrt{4\pi}} C^{l'0}_{l0P0}$$

**Operator r**

$$(\mathbf{r})_\nu = \sqrt{\frac{4\pi}{3}} r Y_{1\nu}(\hat{r})$$

$$\langle l' \| r \| l \rangle = \sqrt{\frac{4\pi}{3}} \frac{r}{C^{l'm'}_{lm1\mu}} \int Y^*_{l'm'} Y_{1\mu} Y_{lm} do = \sqrt{\frac{4\pi}{3}} \frac{r}{C^{l'm'}_{lm1\mu}} \int Y_{l'm'} \sum_{LM} \frac{\hat{1}\hat{l}}{\hat{L}\sqrt{4\pi}} \times$$

$$\times C^{L0}_{l010} C^{LM}_{lm1\mu} Y_{LM} do = \left(\delta^{Mm'}_{Ll'}\right) = r \frac{\hat{l}}{\hat{l}'} C^{l'0}_{l010} = \begin{pmatrix} \sqrt{\frac{l+1}{2l+3}} & l'=l+1 \\ -\sqrt{\frac{l}{2l-1}} & l'=l-1 \end{pmatrix} r$$

**Operator $\ell$**

$$\langle l' \| L \| l \rangle = \frac{1}{C^{l'm}_{lm10}} \langle l'm | L_0 | lm \rangle = \frac{m}{C^{l'm}_{lm10}} \delta_{ll'} = \delta_{ll'} \sqrt{l(l+1)}$$

$$C^{lm}_{lm10} = \frac{m}{\sqrt{l(l+1)}}$$

**Operator $\boldsymbol{\sigma}$**

The reduced ME of the spin 1/2 WFs is

$$\langle 1/2 \| \sigma \| 1/2 \rangle = \frac{1}{C^{\frac{1}{2}\frac{1}{2}}_{\frac{1}{2}\frac{1}{2}10}} \langle 1/2, 1/2 | \sigma_0 | 1/2, 1/2 \rangle = \frac{1}{C^{\frac{1}{2}\frac{1}{2}}_{\frac{1}{2}\frac{1}{2}10}} = \sqrt{3}$$

$$C^{\frac{1}{2}\frac{1}{2}}_{\frac{1}{2}\frac{1}{2}10} = \frac{1/2}{\sqrt{1 \cdot 3/4}} = \frac{1}{\sqrt{3}}$$

The reduced ME of one-particle operator $\sigma$ between WFs of two particles spin 1/2 coupled in total spin S is

$$\langle S' \| \sigma_k \| S \rangle = \begin{bmatrix} (-)^S, k=1 \\ (-)^{-S'}, k=2 \end{bmatrix} \cdot \frac{\hat{1}}{2} \hat{S} \begin{Bmatrix} S & \frac{1}{2} & \frac{1}{2} \\ \frac{1}{2} & 1 & S' \end{Bmatrix} \langle 1/2 \| \sigma \| 1/2 \rangle =$$

$$= \left[ \begin{array}{c} (-)^{S} \\ (-)^{-S'} \end{array} \right]_{,k=2}^{,k=1} \cdot \sqrt{6}\hat{S} \left\{ \begin{array}{ccc} S & \frac{1}{2} & \frac{1}{2} \\ \frac{1}{2} & 1 & S' \end{array} \right\} \tag{9.7}$$

This is obtained in the following way:

$$\langle S'M' \left|(\sigma_1)_\mu\right| SM\rangle = C^{S'M'}_{\frac{1}{2}m'_1\frac{1}{2}m'_2} C^{SM}_{\frac{1}{2}m_1\frac{1}{2}m_2} \langle m'_1 \left|(\sigma_1)_\mu\right| m_1\rangle \langle m'_2 \mid m_2\rangle =$$

$$= C^{SM_S}_{\frac{1}{2}m_1\frac{1}{2}m_2} C^{S'M'_S}_{\frac{1}{2}m'_1\frac{1}{2}m_2} C^{\frac{1}{2}m'_1}_{\frac{1}{2}m_1 1\mu} \langle 1/2 \left\|\sigma\right\| 1/2\rangle =$$

$$= (-)^S \hat{S}\frac{\hat{1}}{2} \left\{ \begin{array}{ccc} S & \frac{1}{2} & \frac{1}{2} \\ \frac{1}{2} & 1 & S' \end{array} \right\} C^{S'M'_S}_{SM_S 1\mu} \langle 1/2 \left\|\sigma\right\| 1/2\rangle$$

### 9.6.2 Operator nabla

$$\vec{P} = -i\vec{\nabla}$$

Operator $\nabla$ in the spin-tensor form is

$$\nabla_\mu = \sqrt{\frac{4\pi}{3}} D_{l'l} Y_{1\mu}(\hat{r})$$

where

$$D_{l'l} = \left( \frac{d}{dr} + \frac{l(l+1) - l'(l'+1) + 2}{2r} \right)$$

So, RME of the operator $\nabla$ can be expressed via RME of operator $\mathbf{r}$:

$$\langle l' \left\|\nabla\right\| l\rangle = \langle l' \left\|r\right\| l\rangle \frac{D_{l'l}}{r} = C^{l'0}_{l010} \frac{\hat{l}}{\hat{l}'} \left( \frac{d}{dr} + \frac{l(l+1) - l'(l'+1) + 2}{2r} \right) =$$

$$= \delta_{l',l+1} \sqrt{\frac{l+1}{2l+3}} \left( \frac{d}{dr} - \frac{l}{r} \right) - \delta_{l',l-1} \sqrt{\frac{l}{2l-1}} \left( \frac{d}{dr} + \frac{l+1}{r} \right)$$

Note, that expressions in the bracket are in a spirit of recurrence formulae for spherical Bessel functions:

$$\left\{ \begin{array}{l} kj_{l+1}(kr) = -\left( \frac{d}{dr} - \frac{l}{r} \right) j_l(kr) \\ kj_{l-1}(kr) = \left( \frac{d}{dr} + \frac{l+1}{r} \right) j_l(kr) \end{array} \right.$$

This is the trivial result connected with the fact that spherical Bessel functions are eigenfunctions of the momentum operator

$$D_{l'l}\, j_l(kr) = -k \left( \delta_{l',l+1}\, j_{l+1}(kr) \sqrt{\frac{l+1}{2l+3}} + \delta_{l',l-1}\, j_{l-1}(kr) \sqrt{\frac{l}{2l-1}} \right)$$

$$\left\{ \begin{array}{l} D_{l+1,l}\, j_l(kr) = -k\, j_{l+1}(kr) \sqrt{\frac{l+1}{2l+3}} \\ D_{l-1,l}\, j_l(kr) = -k\, j_{l-1}(kr) \sqrt{\frac{l}{2l-1}} \end{array} \right.$$

### 9.6.3 Three different particles. (SS) potential

**System 1**

$$\left\langle \left[[l'_x l'_y]_{L'}[[S_2 S_3]_{S'_x} S_1]_{S'}\right]_J \| (SS) \| \left[[l_x l_y]_L [[S_2 S_3]_{S_x} S_1]_S\right]_J \right\rangle =$$

$$= \frac{1}{2}\left[S_x(S_x+1) - S_2(S_2+1) - S_3(S_3+1)\right] \delta_{l_x l'_x} \delta_{l_y l'_y} \delta_{LL} \delta_{S_x S'_x} \delta_{SS'}$$

**System 2,3**

In system 2 ME is

$|S_1 - S_3| \le S_p \le S_1 + S_3$

$$\langle \ldots \| (SS) \| \ldots \rangle = \sum_{S_p} \hat{S}'_x \hat{S}_x \hat{S}_p^2 \left\{ \begin{array}{ccc} S_2 & S_3 & S_x \\ S_1 & S & S_p \end{array} \right\} \left\{ \begin{array}{ccc} S_2 & S_3 & S'_x \\ S_1 & S & S_p \end{array} \right\} \times$$

$$\times \frac{1}{2}\left[S_p(S_p+1) - S_1(S_1+1) - S_3(S_3+1)\right] \delta_{l_x l'_x} \delta_{l_y l'_y} \delta_{LL} \delta_{SS'}$$

In system 3 the ME is obtained exchanging $S_2 \leftrightarrow S_3$ for ME in system 2

### 9.6.4 Three different particles. (LS) potential

**System 1**

$|l_x - S_x| \le j_x \le l_x + S_x \; ; \quad |l_y - S_1| \le j_y \le l_y + S_y$

$$\left\langle \left[[l'_x l'_y]_{L'}[[S_2 S_3]_{S'_x} S_1]_{S'}\right]_J \| (LS) \| \left[[l_x l_y]_L [[S_2 S_3]_{S_x} S_1]_S\right]_J \right\rangle = \sum_{j_x j_y} \hat{L}\hat{S}\hat{L}'\hat{S}'\hat{j}_x^2 \hat{j}_y^2 \times$$

$$\times \left\{ \begin{array}{ccc} l_x & l_y & L \\ S_x & S_1 & S \\ j_x & j_y & J \end{array} \right\} \left\{ \begin{array}{ccc} l_x & l_y & L' \\ S_x & S_1 & S' \\ j_x & j_y & J \end{array} \right\} \frac{[j_x(j_x+1) - l_x(l_x+1) - S_x(S_x+1)]}{2} \delta_{l_x l'_x} \delta_{l_y l'_y} \delta_{S_x S'_x}$$

**System 2,3**

The angular part of the WF is considered to be converted to the proper Jacobi system, so $l_x$ is angular momentum for particles 1,3 in system 2 and for particles 1,2 in system 3. In system 2 ME is

$|l_x - S_x| \le j_x \le l_x + S_x \; ; \quad |l_y - S_1| \le j_y \le l_y + S_y \; ; \quad |S_1 - S_3| \le S_p \le S_1 + S_3$

$$\langle \ldots \| (LS) \| \ldots \rangle = \sum_{j_x j_y S_p} \hat{L}\hat{S}\hat{S}_x \hat{L}'\hat{S}'\hat{S}'_x \hat{j}_x^2 \hat{j}_y^2 \hat{S}_p^2 \left\{ \begin{array}{ccc} S_2 & S_3 & S_x \\ S_1 & S & S_p \end{array} \right\} \left\{ \begin{array}{ccc} S_2 & S_3 & S'_x \\ S_1 & S & S_p \end{array} \right\} \times$$

$$\times \left\{ \begin{array}{ccc} l_x & l_y & L \\ S_p & S_2 & S \\ j_x & j_y & J \end{array} \right\} \left\{ \begin{array}{ccc} l_x & l_y & L' \\ S_p & S_2 & S' \\ j_x & j_y & J \end{array} \right\} \frac{[j_x(j_x+1) - l_x(l_x+1) - S_p(S_p+1)]}{2} \delta_{l_x l'_x} \delta_{l_y l'_y}$$

In system 3 the ME is obtained exchanging $S_2 \leftrightarrow S_3$ for ME in system 2.

### 9.6.5 Tensor operator

$$\hat{S}_{12} = 3(\sigma_1\hat{r})(\sigma_2\hat{r}) - (\sigma_1\sigma_2)$$

To calculate RME for WFs in LS coupling we have to convert this expression to the spin-tensor form with the same coupling. Using (9.2)

$$\hat{S}_{12} = 3\frac{4\pi}{3}\hat{1}^2\,[[\sigma_1 \otimes Y_1]_0 \otimes [\sigma_2 \otimes Y_1]_0]_{00} + \hat{1}[\sigma_1\sigma_2]_{00}$$

After recoupling

$$[[\sigma_1 \otimes Y_1]_0 \otimes [\sigma_2 \otimes Y_1]_0]_{00} = \sum_L \frac{\hat{L}}{3}\,[[Y_1 \otimes Y_1]_L \otimes [\sigma_1 \otimes \sigma_2]_L]_{00} =$$

and expansion of spherical functions product

$$= -\tfrac{1}{4\pi\sqrt{3}}[\sigma_1\sigma_2]_{00} + \sqrt{\tfrac{10}{3}}\frac{1}{\sqrt{4\pi}\hat{2}}\,[Y_2 \otimes [\sigma_1 \otimes \sigma_2]_2]_{00}$$

we see that term with zero angular momentum disappear and

$$\hat{S}_{12} = \sqrt{4\pi}\sqrt{6}\;\;[Y_2 \otimes [\sigma_1 \otimes \sigma_2]_2]_{00}$$

RME of this expression is obtained trivially:

$\langle JL'S' \|\, \hat{S}_{12} \,\| JLS\rangle =$

$= \sqrt{4\pi}\sqrt{6}\,\langle [L' \otimes [1/2 \otimes 1/2]_{S'}]_J \|\, [Y_2 \otimes [\sigma_1 \otimes \sigma_2]_2]_0 \,\| [L \otimes [1/2 \otimes 1/2]_S]_J\rangle =$

$$= 2\sqrt{30}(-)^{L+S'+J}\,\hat{L}\hat{S}'\hat{S}\begin{Bmatrix} S & L & J \\ L' & S' & 2 \end{Bmatrix}\begin{Bmatrix} 1/2 & 1/2 & S \\ 1 & 1 & 2 \\ 1/2 & 1/2 & S' \end{Bmatrix} C^{L'0}_{L020}\,\langle 1/2 \,\|\sigma\|\, 1/2\rangle^2$$

### 9.6.6 Three different particles. Tensor potential

**System 1**

$|l_x - S_x| \le j_x \le l_x + S_x\;; \quad |l_y - S_1| \le j_y \le l_y + S_y$

$$\left\langle \left[[l'_x l'_y]_{L'}[[S_2S_3]_{S'_x}S_1]_{S'}\right]_J \|(LS)\| \,[[l_xl_y]_L[[S_2S_3]_{S_x}S_1]_S]_J \right\rangle =$$

$$= 6\sqrt{30}\sum_{j_xj_y}(-)^{l_x+S'_x+j_x}\hat{L}\hat{S}\hat{L}'\hat{S}'\hat{j}_x^2\hat{j}_y^2\hat{l}_x\hat{S}'_x\hat{S}_x\begin{Bmatrix} l_x & l_y & L \\ S_x & S_1 & S \\ j_x & j_y & J \end{Bmatrix}\begin{Bmatrix} l_x & l_y & L' \\ S_x & S_1 & S' \\ j_x & j_y & J \end{Bmatrix}\times$$

$$\times\begin{Bmatrix} S_x & l_x & j_x \\ l'_x & S'_x & 2 \end{Bmatrix}\begin{Bmatrix} 1/2 & 1/2 & S_x \\ 1 & 1 & 2 \\ 1/2 & 1/2 & S'_x \end{Bmatrix} C^{l'_x0}_{l_x020}\,\delta_{l_yl'_y}$$

**System 2,3**

The angular part of the WF is considered to be converted to the proper Jacobi system, so $l_x$ is angular momentum for particles 1,3 in system 2 and for particles 1,2 in system 3. In system 2 ME is

$|l_x - S_x| \le j_x \le l_x + S_x$ ; $|l_y - S_1| \le j_y \le l_y + S_y$ ; $|S_1 - S_3| \le S_p, S'_p \le S_1 + S_3$

$$\langle \ldots \| \, (LS) \, \| \ldots \rangle = 6\sqrt{30} \sum_{j_x j_y S_p S'_p} (-)^{l_x + S'_p + j_x} \hat{L}\hat{S}\hat{S}_x \hat{L}'\hat{S}'\hat{S}'_x \hat{j}_x^2 \hat{j}_y^2 \hat{l}_x \hat{S}_p^2 \hat{S}_p'^2 \times$$

$$\times \left\{ \begin{array}{ccc} S_2 & S_3 & S_x \\ S_1 & S & S_p \end{array} \right\} \left\{ \begin{array}{ccc} S_2 & S_3 & S'_x \\ S_1 & S & S'_p \end{array} \right\} \left\{ \begin{array}{ccc} S_p & l_x & j_x \\ l'_x & S'_p & 2 \end{array} \right\} \times$$

$$\times \left\{ \begin{array}{ccc} l_x & l_y & L \\ S_p & S_2 & S \\ j_x & j_y & J \end{array} \right\} \left\{ \begin{array}{ccc} l_x & l_y & L' \\ S'_p & S_2 & S' \\ j_x & j_y & J \end{array} \right\} \left\{ \begin{array}{ccc} 1/2 & 1/2 & S_p \\ 1 & 1 & 2 \\ 1/2 & 1/2 & S'_p \end{array} \right\} C^{l'_x 0}_{l_x 020} \, \delta_{l_y l'_y}$$

In system 3 the ME is obtained exchanging $S_2 \leftrightarrow S_3$ for ME in system 2.

# Chapter 10

# Relativism

## 10.1 Kinematics

The metric tensor is $g_{ij} = g^{ij} = diag(1, -1, -1, -1)$. Momentum and energy arise from Lagrangian $L$ by means of $E = \mathbf{pv} - L$ , $\mathbf{p} = \frac{\partial L}{\partial \mathbf{v}}$.

| Ordinary units | Units $\hbar = c = 1$ |
|---|---|
| $L = -mc^2\sqrt{1 - v^2/c^2}$ | $L = -m\sqrt{1 - v^2}$ |
| $E = \dfrac{mc^2}{\sqrt{1 - v^2/c^2}}$ | $E = \dfrac{m}{\sqrt{1 - v^2}}$ |
| $\mathbf{p} = \dfrac{m\mathbf{v}}{\sqrt{1 - v^2/c^2}}$ | $\mathbf{p} = \dfrac{m\mathbf{v}}{\sqrt{1 - v^2}}$ |
| $E^2 = c^2\mathbf{p}^2 + c^4m^2$ | $E^2 = \mathbf{p}^2 + m^2$ |

$$p_\mu = (E, \mathbf{p}) = \frac{m}{\sqrt{1 - v^2}}(1, \mathbf{v})$$

$$v_\mu = \frac{dr_\mu}{ds} = \frac{1}{\sqrt{1 - v^2}}(1, \mathbf{v})$$

definition: $\quad ds^2 = r^\mu r_\mu \qquad ds = \sqrt{dt^2 - dr^2} = dt\sqrt{1 - v^2} \qquad \Rightarrow$

$v^\mu v_\mu = 1 \qquad \Rightarrow \qquad w^\mu v_\mu = 0 \qquad$ (where 4-acceleration $w^\mu = \dfrac{dv^\mu}{ds}$)

For calculation of cross–sections in relativistic case the relative velocity should be defined.

$$p_1^\mu p_{2\mu} = E_1E_2 - (\mathbf{p}_1 \cdot \mathbf{p}_2) = \langle \text{in the rest system of particle 1} \rangle = E_2m_1 = \frac{m_1m_2}{\sqrt{1 - v^2}}$$

$$\Rightarrow \qquad v_{rel} = \sqrt{1 - \left(\frac{m_1m_2}{p_1^\mu p_{2\mu}}\right)^2} = \frac{\sqrt{(\mathbf{v}_1 - \mathbf{v}_2)^2 - [\mathbf{v}_1 \times \mathbf{v}_2]^2}}{1 - (\mathbf{v}_1 \cdot \mathbf{v}_2)}$$

## 10.2 Lorenz transformations

The system $K'$ is moving relative to system $K$ with velocity $v$ **collinear** with axis $x$ . The contravariant coordinates are transformed like

$$\begin{pmatrix} x^0 \\ x^1 \end{pmatrix} = \gamma \begin{pmatrix} 1 & v \\ v & 1 \end{pmatrix} \begin{pmatrix} x^{0\prime} \\ x^{1\prime} \end{pmatrix} \quad ; \qquad \gamma = \frac{1}{\sqrt{1-v^2}}$$

In the vector form

$$\begin{cases} x^0 = \gamma \left( x^{0\prime} + (\mathbf{v}\mathbf{x}') \right) \\ \mathbf{x} = \gamma \left( \mathbf{v} x^{0\prime} + \dfrac{(\mathbf{v}\mathbf{x}')}{v^2}\mathbf{v} \right) + \dfrac{1}{v^2}\left[\mathbf{v}[\mathbf{x}'\mathbf{v}]\right] \end{cases}$$

Let us show that the transformation of covariant coordinates are done by matrix with "inverse direction of velocity":

$$x^i = T^i_j x^{j\prime} \quad ; \qquad x_i = g_{ij} T^j_k g^{kp} x'_p$$

$$gTg = \begin{pmatrix} 1 & 0 \\ 0 & -1 \end{pmatrix} \begin{pmatrix} 1 & v \\ v & 1 \end{pmatrix} \begin{pmatrix} 1 & 0 \\ 0 & -1 \end{pmatrix} = \begin{pmatrix} 1 & -v \\ -v & 1 \end{pmatrix}$$

The Newton's law (connection between force and acceleration) is not simple in relativism

$$\mathbf{a} = \frac{d\mathbf{v}}{dt} \quad ; \qquad \mathbf{f} = \frac{d\mathbf{p}}{dt} = \frac{m}{\sqrt{1-v^2}}\frac{d\mathbf{v}}{dt} + \frac{m}{\left(1-v^2\right)^{3/2}}\left(\mathbf{v}\frac{d\mathbf{v}}{dt}\right)\mathbf{v}$$

Projection on the parallel and transverse directions gives

$$\begin{cases} \mathbf{f}_{\shortparallel} = m\gamma^3 \mathbf{a}_{\shortparallel} \\ \mathbf{f}_{\perp} = m\gamma \mathbf{a}_{\perp} \end{cases} \qquad \begin{cases} \mathbf{f}_{\shortparallel} = \mathbf{f}'_{\shortparallel} \\ \mathbf{f}_{\perp} = \gamma^{-1}\mathbf{f}'_{\perp} \end{cases} \tag{10.1}$$

In some sense it is possible to speak about "longitudinal" $m\gamma^3$ and "transverse" $m\gamma$ masses. Transformations of force and acceleration in the vector form are

$$\begin{cases} \mathbf{a} = \dfrac{(1-v^2)^{3/2}}{v^2}\left\{(\mathbf{v}\mathbf{a}')\mathbf{v} + \gamma\left[\mathbf{v}[\mathbf{a}'\mathbf{v}]\right]\right\} \\ \mathbf{f} = \dfrac{(\mathbf{v}\mathbf{f}')}{v^2}\mathbf{v} + \dfrac{1}{v^2\gamma}\left[\mathbf{v}[\mathbf{f}'\mathbf{v}]\right] \end{cases}$$

Transformation for the electromagnetic field:

$$\begin{cases} E_x = & E'_x \\ E_y = & \gamma(E'_y + vH'_z) \\ E_z = & \gamma(E'_z - vH'_y) \end{cases} \qquad \begin{cases} H_x = & H'_x \\ H_y = & \gamma(H'_y - vE'_z) \\ H_z = & \gamma(H'_z + vE'_y) \end{cases}$$

$$\begin{matrix} \mathbf{E}_{\shortparallel} = \mathbf{E}'_{\shortparallel} & \mathbf{E}_{\perp} = \gamma(\mathbf{E}'_{\perp} + [\mathbf{H}'_{\perp}\mathbf{v}]) \\ \mathbf{H}_{\shortparallel} = \mathbf{H}'_{\shortparallel} & \mathbf{H}_{\perp} = \gamma(\mathbf{H}'_{\perp} - [\mathbf{E}'_{\perp}\mathbf{v}]) \end{matrix} \tag{10.2}$$

in the vector form :

$$\begin{cases} \mathbf{E} = \gamma(\mathbf{E}' + [\mathbf{H}'\mathbf{v}]) + (1-\gamma)\dfrac{(\mathbf{E}'\mathbf{v})}{v^2}\mathbf{v} \\ \mathbf{H} = \gamma(\mathbf{H}' - [\mathbf{E}'\mathbf{v}]) + (1-\gamma)\dfrac{(\mathbf{H}'\mathbf{v})}{v^2}\mathbf{v} \end{cases}$$

Formula for Lorenz force can be obtained as "relativistic effect" from the Coulomb law. For that purpose we should boost from the frame $K$ (where particle is moving and there are fields $\mathbf{E}$, $\mathbf{H}$ ) to the frame $K'$ where particle is in rest

$$\mathbf{f}'_{\shortparallel} = e\mathbf{E}'_{\shortparallel} \qquad \mathbf{f}'_{\perp} = e\mathbf{E}'_{\perp}$$

Substituting (10.2) and (10.1) (in (10.2) should be done exchange $\mathbf{E} \leftrightarrow \mathbf{E}'$ and also $v \to -v$ as the direction of boost from $K'$ which is moving to $K$ which is in rest is negative due to definition in the beginning of section) one can obtain normal expression for Lorenz force:

$$\mathbf{f} = e\left\{\mathbf{E} + [\mathbf{v}\mathbf{H}]\right\}$$

## 10.3 Gamma-matrixes

**Dirac representation**

$$\gamma_0 = \begin{pmatrix} 1 & 0 \\ 0 & -1 \end{pmatrix} \qquad \boldsymbol{\gamma} = \begin{pmatrix} 0 & \boldsymbol{\sigma} \\ -\boldsymbol{\sigma} & 0 \end{pmatrix} \qquad \gamma_5 = i\,\gamma_1\gamma_2\gamma_3\gamma_0 = -\begin{pmatrix} 0 & 1 \\ 1 & 0 \end{pmatrix}$$

$$\sigma^{\mu\nu} = (\gamma^\mu\gamma\nu - \gamma\nu\gamma\mu)$$

Here $\gamma_5$ is given in the notation of Okun',

**Weyl ("split") representation**

$$\gamma_0 = \begin{pmatrix} 0 & 1 \\ 1 & 0 \end{pmatrix} \qquad \boldsymbol{\gamma} = \begin{pmatrix} 0 & -\boldsymbol{\sigma} \\ \boldsymbol{\sigma} & 0 \end{pmatrix} \qquad \gamma_5 = \begin{pmatrix} i & 0 \\ 0 & -i \end{pmatrix}$$

**Commutation rules and the rest**

$$\{\gamma^\mu\gamma^\nu\} = 2\eta^{\mu\nu} \qquad \{\gamma^\mu\gamma^5\} = 0$$
$$\gamma^{0+} = \gamma^0 \qquad \boldsymbol{\gamma}^+ = -\boldsymbol{\gamma} \qquad \gamma^{5+} = \gamma^5$$
$$(\gamma^\mu a_\mu)^2 = a^\mu a_\mu \qquad (\boldsymbol{\gamma}\mathbf{a})^2 = -\mathbf{a}^2$$

$$Sp\,1 = 4 \qquad Sp\,\gamma^\mu = 0 \qquad Sp\,\gamma^5 = 0 \qquad Sp\,\gamma^0\gamma^\mu = 0 \qquad Sp\,\gamma^\mu\gamma^\nu = 4\eta^{\mu\nu}$$

$$Sp\,\gamma^\alpha\gamma^\beta\gamma^\gamma\gamma^\delta = 4\left(\eta^{\alpha\beta}\eta^{\gamma\delta} + \eta^{\alpha\delta}\eta^{\beta\gamma} - \eta^{\alpha\gamma}\eta^{\beta\delta}\right) \qquad Sp\,\gamma^5\gamma^\alpha\gamma^\beta\gamma^\gamma\gamma^\delta = 4i\varepsilon^{\alpha\beta\gamma\delta}$$

$$\gamma^\mu\hat{A}\gamma_\mu = -2\hat{A} \qquad \gamma^\mu\hat{A}B\gamma_\mu = 4\,(AB) \qquad \gamma^\mu\hat{A}\hat{B}\hat{C}\gamma_\mu = -2\hat{C}\hat{B}\hat{A}$$
$$\gamma^\mu\hat{A}\hat{B}\hat{C}\hat{D}\gamma_\mu = 2(\hat{D}\hat{A}\hat{B}\hat{C} + \hat{C}\hat{B}\hat{A}\hat{D})$$

# Chapter 11

# Some numerical methods

## 11.1 Differentiation

First derivative

$$\begin{aligned} f'(0) &= \frac{-3f(0)+4f(h)-f(2h)}{2h} = \frac{f(-2h)-4f(-h)+3f(0)}{2h} = \\ &= \frac{f(-3h)-27f(-h)+27f(h)-f(3h)}{48h} = \\ &= \frac{2f(-2h)-16f(-h)+16f(h)-2f(2h)}{24h} = \\ &= \frac{-50f(0)+96f(h)-72f(2h)+32f(3h)-6f(4h)}{24h} = \end{aligned}$$

Second derivative

$$\begin{aligned} f''(0) &= \frac{f(-h)-2f(0)+f(h)}{h^2} = \\ &= \frac{-f(-2h)+16f(-h)-30f(0)+16f(h)-f(2h)}{12h^2} \end{aligned}$$

## 11.2 Integration

Standard trapezoidal, Simpson extended and "3/8" formulae

$$\int_a^b f(x)dx \quad ; \quad f(a)=f_0 \quad ; \quad f(b)=f_n \quad ; \quad n=\frac{b-a}{h}+1$$

$\forall n$ $\quad h\left[\frac{(f_0+f_n)}{2}+(f_1+\ldots+f_{n-1})\right]$

odd $n$ $\quad \frac{h}{3}\left[(f_0+f_n)+4(f_1+\ldots+f_{n-1})+2(f_2+\ldots+f_{n-2})\right]$

even $n$ $\quad \frac{3h}{8}\left[(f_0+f_n)+3(f_1+f_2+f_4+f_5+\ldots)+2(f_3+f_6+f_9+\ldots)\right]$

Formulae with "highest accuracy" (exact for polynomials $2N+1$ power)

$$\int_{-1}^{1} f(x)dx = \sum_{k=1}^{N} A_k^{(n)} f(x_k^{(n)}) \quad ; \quad P_n(x_k^{(n)}) = 0 \quad ; \quad A_k^{(n)} = \frac{2}{nP_{n-1}(x_k^{(n)})P_n'(x_k^{(n)})}$$

$$\int_{-1}^{1} \frac{f(x)dx}{\sqrt{1-x^2}} = \frac{\pi}{N} \sum_{k=1}^{N} f\left(\cos \pi \tfrac{2k-1}{N}\right)$$

$$\int_{-1}^{1} f(x)\sqrt{1-x^2}dx = \frac{\pi}{N+1} \sum_{k=1}^{N} \sin^2\left(\tfrac{\pi k}{N+1}\right) f\left(\cos \tfrac{\pi k}{N+1}\right)$$

$$\int_{-1}^{1} f(x)\sqrt{\tfrac{1-x}{1+x}}dx = \frac{4\pi}{2N+1} \sum_{k=1}^{N} \sin^2\left(\tfrac{\pi k}{2N+1}\right) f\left(\cos \tfrac{2\pi k}{2N+1}\right)$$

# Chapter 12

# Differential operators

$$\nabla(\mathbf{AB}) = (\mathbf{A}\boldsymbol{\nabla})\mathbf{B}+(\mathbf{B}\boldsymbol{\nabla})\mathbf{A} + \mathbf{A}\times\mathrm{rot}\mathbf{B} + \mathbf{B}\times\mathrm{rot}\mathbf{A}$$
$$\mathrm{div}(\mathbf{A}\times\mathbf{B}) = \mathbf{B}\,\mathrm{rot}\mathbf{A} - \mathbf{A}\,\mathrm{rot}\mathbf{B}$$
$$\mathrm{rot}(\varphi\times\mathbf{A}) = \varphi\,\mathrm{rot}\mathbf{A}+(\boldsymbol{\nabla}\varphi)\times\mathbf{A}$$
$$\mathrm{rot}(\mathbf{A}\times\mathbf{B}) = (\mathbf{B}\boldsymbol{\nabla})\mathbf{A} - (\mathbf{A}\boldsymbol{\nabla})\mathbf{B}-\mathbf{B}\,\mathrm{div}\mathbf{A} + \mathbf{A}\,\mathrm{div}\mathbf{B}$$
$$\mathrm{div}\mathbf{A}(\varphi) = \frac{\partial\mathbf{A}}{\partial\varphi}(\boldsymbol{\nabla}\varphi) \quad ; \quad \mathrm{rot}\mathbf{A}(\varphi) = (\boldsymbol{\nabla}\varphi)\times\frac{\partial\mathbf{A}}{\partial\varphi}$$
$$(\mathbf{A}\boldsymbol{\nabla})\mathbf{B}(\varphi) = (\mathbf{A}\boldsymbol{\nabla}\varphi)\frac{\partial\mathbf{B}}{\partial\varphi}$$

## 12.1 Cylindrical system

**Operator $\nabla$**

$$\nabla = \mathbf{e}_r\frac{\partial}{\partial r} + \mathbf{e}_\varphi\frac{\partial}{r\partial\varphi} + \mathbf{e}_z\frac{\partial}{\partial z}$$

**Operator $\Delta$**

$$\Delta = \frac{1}{r}\frac{\partial}{\partial r}\left(r\frac{\partial}{\partial r}\right) + \frac{1}{r^2}\frac{\partial^2}{\partial\varphi^2} + \frac{\partial^2}{\partial z^2}$$

**Operator div**

$$\mathrm{div}\mathbf{A} = \frac{1}{r}\frac{\partial}{\partial r}(rA_r) + \frac{1}{r}\frac{\partial A_\varphi}{\partial\varphi} + \frac{\partial A_z}{\partial z}$$

**Operator rot**

$$\mathrm{rot}\mathbf{A} = \mathbf{e}_r\left(\frac{1}{r}\frac{\partial A_z}{\partial\varphi} - \frac{\partial A_\varphi}{\partial z}\right) + \mathbf{e}_\varphi\left(\frac{\partial A_r}{\partial z} - \frac{\partial A_z}{\partial r}\right) + \mathbf{e}_z\frac{1}{r}\left(\frac{\partial}{\partial r}(rA_\varphi) - \frac{\partial A_r}{\partial\varphi}\right)$$

**Operator $\Delta$ with vector argument**

$$\Delta\mathbf{A} = \nabla\,\mathrm{div}\,\mathbf{A} - \mathrm{rot}\,\mathrm{rot}\,\mathbf{A} = \mathbf{e}_r\left(\Delta A_r - \frac{A_r}{r^2} - \frac{2}{r^2}\frac{\partial A_\varphi}{\partial\varphi}\right)$$
$$+\mathbf{e}_\varphi\left(\Delta A_\varphi - \frac{A_\varphi}{r^2} + \frac{2}{r^2}\frac{\partial A_r}{\partial\varphi}\right) + \mathbf{e}_z\Delta A_z$$

## 12.2 Spherical system

**Operator $\nabla$**

$$\nabla = \mathbf{e}_r \frac{\partial}{\partial r} + \mathbf{e}_\theta \frac{\partial}{r\partial\theta} + \mathbf{e}_\varphi \frac{1}{r\sin\theta}\frac{\partial}{\partial\varphi}$$

**Operator $\Delta$**

$$\Delta = \frac{1}{r^2}\frac{\partial}{\partial r}\left(r^2\frac{\partial}{\partial r}\right) + \frac{1}{r^2\sin\theta}\frac{\partial}{\partial\theta}\left(\sin\theta\frac{\partial}{\partial\theta}\right) + \frac{1}{r^2\sin^2\theta}\frac{\partial^2}{\partial\varphi^2}$$

**Operator div**

$$\mathrm{div}\mathbf{A} = \frac{1}{r^2}\frac{\partial}{\partial r}\left(r^2 A_r\right) + \frac{1}{r\sin\theta}\frac{\partial}{\partial\theta}\left(\sin\theta A_\theta\right) + \frac{1}{r\sin\theta}\frac{\partial A_\varphi}{\partial\varphi}$$

**Operator rot**

$$\begin{aligned}\mathrm{rot}\mathbf{A} &= \mathbf{e}_r \frac{1}{r\sin\theta}\left(\frac{\partial}{\partial\theta}\left(\sin\theta A_\varphi\right) - \frac{\partial A_\theta}{\partial\varphi}\right) \\ &\quad + \mathbf{e}_\theta \frac{1}{r}\left(\frac{1}{\sin\theta}\frac{\partial A_r}{\partial\varphi} - \frac{\partial}{\partial r}\left(rA_\varphi\right)\right) + \mathbf{e}_\varphi \frac{1}{r}\left(\frac{\partial}{\partial r}\left(rA_\theta\right) - \frac{\partial A_r}{\partial\theta}\right)\end{aligned}$$

**Operator $\Delta$ with vector argument**

$$\begin{aligned}\Delta\mathbf{A} &= \nabla\ \mathrm{div}\ \mathbf{A} - \mathrm{rot}\ \mathrm{rot}\ \mathbf{A} = \\ &= \mathbf{e}_r\left(\Delta A_r - \frac{2}{r^2}\left[A_r + \frac{1}{\sin\theta}\frac{\partial}{\partial\theta}\left(\sin\theta A_\theta\right) + \frac{1}{\sin\theta}\frac{\partial A_\varphi}{\partial\varphi}\right]\right) + \\ &\quad + \mathbf{e}_\theta\left(\Delta A_\theta + \frac{2}{r^2}\left[\frac{\partial A_r}{\partial\theta} - \frac{A_\theta}{2\sin^2\theta} - \frac{\cos\theta}{\sin^2\theta}\frac{\partial A_\varphi}{\partial\varphi}\right]\right) \\ &\quad + \mathbf{e}_\varphi\left(\Delta A_\varphi + \frac{2}{r^2\sin\theta}\left[\frac{\partial A_r}{\partial\varphi} + \cot\theta\frac{\partial A_\theta}{\partial\varphi} - \frac{A_\varphi}{2\sin^2\theta}\right]\right)\end{aligned}$$

## 12.3 Hyperspherical system

$$\Delta = \frac{\partial^2}{\partial\rho^2} + \frac{5}{\rho}\frac{\partial}{\partial\rho} - \frac{1}{\rho^2}\hat{K}^2$$

$$\hat{K}^2 = -\frac{\partial^2}{\partial\theta^2} - 4\cot 2\theta\frac{\partial}{\partial\theta} + \frac{1}{\cos^2\theta}\hat{l}_x^2 + \frac{1}{\sin^2\theta}\hat{l}_y^2$$

# Bibliography


[1] Abramowitz, M., and Stegun, I. A. *Handbook of mathematical functions.* Dover, New-York, 1968.

[2] Adelberger, E. G., et al. "Solar fusion rates".
*Submitted to Rev. Mod. Phys.* (1997).

[3] Ajzenberg-Selove, F. "Energy levels of light nuclei A=16-17".
*Nucl. Phys. A 460* (1986), 1.

[4] Ajzenberg-Selove, F. "Energy levels of light nuclei A=5-10".
*Nucl. Phys. A 490* (1988), 1.

[5] Ajzenberg-Selove, F. "Energy levels of light nuclei A=11-12".
*Nucl. Phys. A 506* (1990), 1.

[6] Ajzenberg-Selove, F. "Energy levels of light nuclei A=13-15".
*Nucl. Phys. A 523* (1991), 1.

[7] Ajzenberg-Selove, F., and Lauritsen, M. "Energy levels of light nuclei A=5-10". Earlier version of [4].
*Nucl. Phys. A 227* (1974), 1.

[8] Al-Khalili, J. S., and Tostevin, J. A. "Matter radii of light halo nuclei". Reexamination of RMS matter radii for $^8B$, $^{11}$Li, $^{11}$Be.
*Phys. Rev. Lett. 76* (1996), 3903.

[9] Alburger, D. E. "$\beta$-decay of Li$^9$". First detailed experimental work.
*Phys. Rev. 132* (1963), 328.

[10] Anne, R., et al. "Exclusive and restricted inclusive reactions involving the $^{11}$Be one-neutron halo". Neutron distributions in coincidence with $^{10}$Be. Dissociation cross sections for reaction ($^{11}$Be,$^{10}$Be+X).
*Nucl. Phys. A 575* (1994), 125.

[11] Arai, K., Ogawa, Y., Suzuki, Y., and Varga, K. "Structure of the mirror nuclei $^9$Be and $^9$B in a microscopic cluster model". Ground states. Poles of S-matrix. Attempt to explaine beta decay of $^9$Li.
*Phys. Rev. C 54* (1996), 132.

[12] Arai, K., Suzuki, Y., and Varga, K. "Neutron-proton halo structure of the 3.563-MeV $0^+$ state in $^6$Li". RGM calculations for $^6$He, $^6$Li g.s. and $^6$Li $0^+$ states.
*Phys. Rev. C 51* (1995), 2488.

[13] Artemov, K. P., et al. "Study of Li$^6$ decay from excited states". [Yad. Fiz. 14 (1972) 1105]. Parity violation in $^6$Li $0^+$. Experiment.
*Sov. J. Nucl. Phys. 14* (1972), 615.

[14] Bang, J. M., and Thompson, I. J. "Three-body calculations for $^{11}$Li".
*Phys. Lett. B 279* (1992), 201.

[15] Barette, J., et al. "Search for the parity-forbidden heavy-particle width $\Gamma'_{\alpha d}$ of the $E_x$=3.562 MeV state in $^6$Li". Parity violation in $^6$Li $0^+$. Experiment.
*Nucl. Phys. A 238* (1975), 176.

[16] Barker, F. C. "Intermediate coupling shell-model calculations for light nuclei". Calculations for $^6$He, $^6$Li, $^7$Li, $^7$Be, $^8$Be, $^9$Li, $^9$Be, $^9$B. Experimental width of $^6$Li $0^+$ state is reproduced. States around 11-12 MeV in $^9$Be, $^9$B are discussed.
*Nucl. Phys. 83* (1966), 418.

[17] Barker, F. C. Development of R-matrix formalism for $\beta$-delayed decays.
*Aust. J. Phys. 22* (1969), 293.

[18] Barker, F. C., and Warburton, E. K. "The beta-decay of $^8$He". R-matrix fits for neutron and triton beta-delayed spectra.
*Nucl. Phys. A 487* (1988), 269.

[19] Baye, D., Suzuki, Y., and Descouvemont, P. "Evidence for halo in quenching of $^6$He $\beta$-decay into $\alpha$ and deuteron.". $^6$He beta decay to $\alpha$+d.
*Prog. Theor. Phys. 91* (1994), 2.

[20] Baz', A. I., Zel'dovich, Y. B., and Perelomov, A. M. *Scattering, reactions and decays in nonrelativistic quantum mechanics.* Nauka, Moscow, 1971.

[21] Bellotti, E., et al. "An experiment on the isospin-changing parity violation involving hadrons in nuclei". Parity violation in $^6$Li $0^+$. Experiment.
*Nuovo Cimento A 29* (1975), 106.

[22] Berestetskiy, V. B., Lifshitz, E. M., and Pitaevskiy, L. P. *Quantum electrodynamics*, vol. 4 of *Theoretical Physics.* Nauka, Moscow, 1989.

[23] Bergstrom, J. C., Auer, I. P., and Hicks, R. S. "Electroexcitation of the $0^+$ (3.562 MeV) level of $^6$Li and its application to the reaction $^6$Li$(\gamma, \pi^+)^6$He.". M1 transition in $^6$Li; attempt of comparative analysis together with the $^6$He beta-decay data.
*Nucl. Phys. A 251* (1975), 401.

[24] Bertsch, G. F., and Esbensen, H. "Pair corelations near the neutron drip line". Calculations for $^{11}$Li, $^{12}$Be, $^{14}$Be using three-body Green's function method.
*Annals Phys. 209* (1991), 327.

[25] Biedenharn, L. C., and Louck, J. D. *Angular momentum in quantum physics.* Addison-Wesley, Reading, Massachusetts, 1981.

[26] Björnstad, T., et al. "The decay of $^{8}$He". Neutron and $\gamma$ emission measurements. Feeding to the 0.98 MeV state in $^{8}$Li was found 84 %, due to $P_n$ ∼16 %.
*Nucl. Phys. A 366* (1981), 461.

[27] Blatt, J. M., and Weisskopf, V. F. *Theoretical nuclear physics.* Springer-Verlag, New York, 1979.

[28] Blin-Stoyle, R. J. *Fundumental interaction and the nucleus.* Addison-Wesley, Amsterdam, 1973.

[29] Bochkarev, O. V., et al. "Three-body decay of the $5/2^-$ state of the $^{9}$Be and $^{9}$B isotopic doublet". Studies of the three-body decaying states in $^{9}$Be and $^{9}$B.
*Sov. J. Nucl. Phys. (Yad. Phys.) 52* (1990), 1525.

[30] Bohm, A. *Quantum Mechanics: foundation and application.* Springer-Verlag, 1986.

[31] Borge, M. J. G., et al. "Beta-delayed triton emission in the decay of $^{8}$He". The beta decay of $^{8}$He to $\alpha$+T+n. Tritons are measured.
*Nucl. Phys. A 460* (1986), 373.

[32] Borge, M. J. G., et al. "Super allowed beta decay of nuclei at the drip-line". General discussion of the halo nuclei beta-decay: $^{6}$He, $^{8}$He, $^{9}$Li, $^{11}$Li.
*Z. Phys. A 340* (1991), 255.

[33] Borge, M. J. G., et al. "Study of charged particles emited in the $\beta$-decay of $^{6,8}$He". The decay of$^{6}$He to $\alpha$+d. The decay of $^{8}$He to $\alpha$+T+n.
*Nucl. Phys. A 560* (1993), 664.

[34] Borge, M. J. G., et al. "Hunting halo structure out by $\beta$-decay". In *ENAM-95 Proceedings (Int. Conf. on Exotic Nuclei and Atomic Masses)* (Arles, France, 1995), Editions Frontieres, p. 285.

[35] Borge, M. J. G., et al. "Probing the $^{11}$Li halo structure through $\beta$-decay into the $^{11}$Be*(18 MeV) state". Beta-decay of $^{11}$Li to $^{10}$Be+n, $^{9}$Be+2n, $^{6}$He+$\alpha$+n, 2$\alpha$+3n channels via halo analogue 18 MeV state. Estimates. Experiment.
*Nucl. Phys. A 613* (1997), 199.

[36] Borge, M. J. G., et al. A long paper about new $^{9,11}$Li data.
*in preparation* (1998).

[37] Brown, G. E., and Jackson, A. D. *The nucleon–nucleon interaction.* North-Holland, Amsterdam, 1976.

[38] Burov, V. V., et al. "Calculation of the parity-forbidden decay width of $^6$Li$^*(J^\pi = 0^+, T = 1; E^* = 3.56$ MeV)$\rightarrow \alpha$+d". Parity violation in $^6$Li $0^+$. Theory.
*J. Phys. G: Nucl. Phys 10* (1984), L21.

[39] Chen, Y. S., et al. "Decay modes of $^9$Li states in $^9$Be". Branchings reported for the 0, 2.43, 2.78 MeV states are 65, 32, 3 %.
*Nucl. Phys. A 146* (1970), 136.

[40] Cocke, C. L. "Level structure in $^9$Be and $^6$Li from $^7$Li($^3$He,p)$^9$Be and $^7$Li($^3$He,$\alpha$)$^6$Li". Clearly distinguished states at 2.43, 3.04, 11.9 MeV in $^9$Be.
*Nucl. Phys. A 110* (1968), 321.

[41] Csótó, A. "Proton skin of $^8$B in a microscopic model". Three-cluster RGM calculations.
*Phys. Lett. B 315* (1993), 24.

[42] Csótó, A., and Baye, D. "Microscopic description of the beta delayed deuteron emission from $^6$He". $^6$He beta decay to $\alpha$+d.
*Phys. Rev. C 49* (1994), 818.

[43] Csótó, A., and Lovas, R. G. "Dynamical microscopic three-cluster description of $^6$Li".
*Phys. Rev. C 46* (1992), 576.

[44] Danilin, B. V., et al. "Dynamical multicluster model for electroweak and charge-exchange reactions.". Three-body calculations for $^6$He, $^6$Li. EM formfactors, M1 transition, $\beta$-decay.
*Phys. Rev. C 43* (1991), 2835.

[45] Danilin, B. V., et al. "New models of the halo excitation in the $^6$He nucleus". Charge-exchange, inelastic cross-sections and different responce functions in the continuum of $^6$He.
*Phys. Rev. C 55* (1997), R577.

[46] Danilin, B. V., and Shulgina, N. B. Different models for $^6$He beta decay.
*Izv. Acad. Nauk SSSR, Ser. Fiz. 5* (1991), 908.

[47] Danilin, B. V., and Zhukov, M. V. "Resonance 3$\rightarrow$3 scattering and structure of the excited states of A=6 nuclei". Continuum calculations for A=6 nuclei.
*Phys. At. Nucl. 56* (1993), 460.

[48] Davidov, A. S. *Theory of atomic nucleus.* Nauka, Moscow, 1958.

[49] Descouvemont, P. "Halo structure of $^{14}$Be in a microscopic $^{12}$Be+n+n cluster model".
*Phys. Rev. C 52* (1995), 704.

[50] Descouvemont, P., and Baye, D. "The $^{7}$Be(p,$\gamma$)$^{8}$B reaction in a microscopic three-cluster model". Discrete spectrum and two-body continuum for $^{8}$Li, $^{8}$B. In reality, two-body calculations with folding forces.
*Nucl. Phys. A 487* (1988), 420.

[51] Descouvemont, P., and Leclercq-Willain, K. "Beta-delayed deuteron emission of $^{6}$He in a potential model". Two-body model for the $^{6}$He beta decay to $\alpha$+d.
*J. Phys. G 18* (1992), L99.

[52] Dolbilkin, B. S., et al. "Cross section of photoabsorption by Be$^{9}$ nuclei in the giant dipole resonance region". Measurements between 10-29 MeV. Resonance structures observed at 11.8, 14.8, 21 MeV.
*Sov. J. Nucl. Phys. 9* (1969), 534.

[53] Dubbers, D., Mampe, W., and Dohner, J. "Determination of the weak coupling constants from free-neutron decay". Values of $g_A$ and $g_V$. Constrains for axial-vector constant from different types of data.
*Europhys. Lett. 11* (1990), 195.

[54] Dzibuti, R. I., and Krupennikova, N. B. *Hyperspherical function method in the few-body quantum mechanics.* Mecniereba, Tbilisi, 1984.

[55] Efros, V. D., and Zhukov, M. V. "N-$^{4}$He scattering as 5 body problem". Application of interpolation approach.
*Phys. Lett. B 37* (1971), 18.

[56] Eigenbrod, F. "Investigation of the first four excited levels of $^{6}$Li by electron scattering.". Detailed information both theoretical and experimental about electromagnetic transitinns in $^{6}$Li.
*Z. Physik 228* (1969), 337.

[57] Eisenberg, J. M., and Greiner, W. *Excitation mechanisms of the nucleus. Electromagnetic and weak interactions.*, vol. 2 of *Nuclear Theory.* North-Holland, Amsterdam-London, 1970.

[58] Eskandrian, A., Lehman, D. R., and Parke, W. C. "Inelastic ($1^{+} \rightarrow 0^{+}$) electromagnetic form factor of $^{6}$Li from three-body model". WFs were obtained with separable potentials in earlier works.
*Phys. Rev. C 39* (1989), 1685.

[59] Fedorov, D. V., Jensen, A. S., and Riisager, K. "Three-body halos. II. From two- to three-body asymptotics". General discussion.
*Phys. Rev. C 50* (1994), 2372.

[60] Filippov, G. F., et al.
*Sov. J. Part. Nucl. 25* (1994), 1347.

[61] Funada, S., Kameyama, H., and Sakuragi, Y. "Halo structure and the soft dipole mode of the $^6$He nucleus in the $\alpha$+n+n cluster model". Direct variational method on the square integrable basis.
*Nucl. Phys. A 575* (1994), 93.

[62] Gaarde, C., et al. "The $^{48}$Ca($^3$He,$t$)$^{48}$Sc reaction at 66 and 70 MeV". Reaction mechanism and Gamow-Teller strength.
*Nucl. Phys. A 334* (1980), 248.

[63] Gaarde, C., et al. "Gamow-Teller and M1 resonances". (p,n), (p,p′) reactons on heavy nuclei. Gamow-Teller sum rule. Collective M1 resonances.
*Nucl. Phys. A 396* (1983), 127.

[64] Gradshteyn, I. S., and Ryzhik, I. M. *Table of integrals series and products.* Academic Press, 1980.

[65] Hamermesh, M. *Group theory and its application to physical problems.* Dover, New York, 1989.

[66] Hansen, P. G., Jensen, A. S., and Jonson, B. "Nuclear halos". Review.
*Ann. Rev. Nucl. Part. Sci. 45* (1995), 591.

[67] Jucys, A., and Bandzaitis, A. *Angular momentum theory in quantum mechanics.* Mintis, Vilnius, 1965.

[68] Kobayashi, T. "Nuclear structure experiments on $^{11}$Li". Density distributions for $^6$He, $^8$He, $^{11}$Li are discussed along with experiment.
*Nucl. Phys. A 553* (1993), 465c.

[69] Korsheninnikov, A. A., Danilin, B. V., and Zhukov, M. V.
*Nucl. Phys. A 599* (1993), 208.

[70] Kukulin, V. I., et al. "Detailed calculations of the cluster structure of the light nuclei in a three-body model". Calculations for $^6$He, $^6$Li, $^6$Be. The structure of $2^+$ and $1^+$ (!) states was also obtained.
*Nucl. Phys. A 586* (1995), 151.

[71] Kukulin, V. I., Krasnopol'sky, V. M., Voronchev, V. I., and Sazonov, P. B. "Detailed study of the cluster structure of light nuclei in a three-body model". The spectrum of low-lying states of nuclei with A=6.
*Nucl. Phys. A 453* (1986), 365.

[72] Landau, L. D., and Lifshitz, E. M. *Field Theory*, vol. 2 of *Theoretical Physics*. Nauka, Moscow, 1988.

[73] Landau, L. D., and Lifshitz, E. M. *Quantum Mechanics*, vol. 3 of *Theoretical Physics*. Nauka, Moscow, 1988.

[74] Lane, A. M., and Tomas, R. G. "R-matrix theory of nuclear reactions".
*Rev. Mod. Phys. 30* (1958), 257.

[75] Langeven, M., Detraz, C., Guillemaud, D., and Naulin, F. "$\beta$-delayed charged particles from $^{9}$Li and $^{11}$Li". Branchings for different branches of beta-decay for $^{9}$Li and $^{11}$Li. First detailed data in the whole energy window.
*Nucl. Phys. A 366* (1981), 449.

[76] Macefield, B. E. F. "States of $^{9}$Be from the $\beta$ decay of $^{9}$Li". Neutron spectra were measured; states at 2.43, 3. MeV were observed.
*Nucl. Phys. A 131* (1969), 250.

[77] Mendelson, R. A., Norbeck, J. E., and Carlson, R. R. "Be$^{9}$ states from the reaction Li$^{7}$(Li$^{6}$, $\alpha$)Be$^{9}$". Clearly observed states 0.00, 2.43, 3.04, 11.9 MeV.
*Phys. Rev. 135* (1964), B1319.

[78] Merkuriev, S. P. Asymptotic of the three-body problem in coordinate space.
*Sov. J. Nucl. Phys. 19* (1974), 447.

[79] Moshinsky, M. *The harmonic oscillator in modern physics: from atoms to quarks*. Gordon and Breach, New-York-London-Paris, 1969.

[80] Mukha, I., et al. "Observation of the $^{11}$Li($\beta$d) decay". The deuteron branching is estimated to be more than $10^{-4}$.
*Phys. Lett. B 367* (1996), 65.

[81] Mukhamedzhanov, A. M., and Timofeyuk, N. K. "Astrophysical S-factor for the reaction $^{7}$Be+p$\rightarrow^{8}$B+$\gamma$". [Pis'ma Zh. Eksp. Teor. Fis., 51 (1990) 247].
*JETP Lett. 51* (1990), 282.

[82] Nyman, G., et al. "The beta decay of $^{9}$Li to levels in $^{9}$Be: a new look". New analysis of the $^{9}$Li beta decay data. Formulae for the sequential decay R-matrix analysis.
*Nucl. Phys. A 510* (1990), 189.

[83] Rasmussen, V. K., and Swann, C. P. "Gamma ray widths in C$^{13}$, Li$^{6}$, and P$^{31}$". The M1 transition in $^{6}$Li was discussed among other things.
*Phys. Rev. 183* (1969), 918.

[84] Raynal, J., and Revai, J. "Transformation coefficients in the hyperspherical approach to the three-body problem". Explicit form and connection with Talmi-Moshinsky coefficients. Generating function for hyperspherical harmonics.
*Nuovo Cimento A 68* (1970), 612.

[85] Riisager, K., et al. "First observation of the beta-delayed deuteron emission.". $^{6}$He beta decay to $\alpha$+d. Experiment.
*Phys. Lett. B 235* (1990), 30.

[86] Robertson, R. G. H., and Brown, B. A. "Estimate of the parity-violating $\alpha$-decay width of the $0^+$ T=1 state of $^{6}$Li". Parity violation in $^{6}$Li $0^+$. Theory.
*Phys. Rev. C 28* (1983), 443.

[87] Robertson, R. G. H., et al. "Upper limit on the isovector parity-violating decay width of the $0^+$ T=1 state of $^{6}$Li". Parity violation in $^{6}$Li $0^+$. Experiment.
*Phys. Rev. C 29* (1984), 755.

[88] Shul'gina, N. B., et al. "Three-body structure of $^{8}$Li and $^{7}$Li(n,$\gamma$)$^{8}$Li reaction".
*Nucl. Phys. A 597* (1996), 197.

[89] Stöwe, H., and Zahn, W. "Microscopic calculations for the $^{8}$Li system". RGM calculations for dicrete spectrum and two-body continuum of $^{8}$Li.
*Nucl. Phys. A 289* (1977), 317.

[90] Tanihata, I. "Neutron halo nuclei". Review.
*J. Phys. G 22* (1996), 157.

[91] Tanihata, I., et al. "Measurement of interaction cross section using isotope beams of Be and B and isospin dependence of nuclei radii". Tables of the interaction cross sections and RMS radii for nuclei from $^{4}$He till $^{12}$C.
*Phys. Lett. B 206* (1988), 592.

[92] Teranishi, T., et al. "Isobaric analog state of $^{11}$Li".
*Phys. Lett. B 407* (1997), 110.

[93] Thompson, I. J., and Zhukov, M. V. "Structure and reactions of the $^{12,14}$Be nuclei". Three-body approach.
*Phys. Rev. C 53* (1996), 708.

[94] Tosaka, Y., and Suzuki, Y. "Structure of $^{11}$Li in the cluster-orbital shell model for the $^{9}$Li+n+n system".
*Nucl. Phys. 512* (1990), 46.

[95] Varga, K., Suzuki, Y., and Ohbayasi, Y. "Microscopic multicluster description of neutron-rich helium isotopes". Calculations of the $^{6,8}$He ground

states. Spatial correlation densities. The beta-decay of $^6$He to $\alpha$+d.
*Phys. Rev. C 50* (1994), 189.

[96] Varga, K., Suzuki, Y., and Tanihata, I. "Microscopic four-cluster description of the mirror nuclei $^9$Li and $^9$C". Stochastic variational method (version of RGM) is used to obtain characteristics of $^7$Li, $^7$Be $^8$Li, $^8$B, $^9$Li, $^9$C.
*Phys. Rev. C 52* (1995), 3013.

[97] Vasil'ev, O. Y., Korsheninnikov, A. A., Mukha, I. G., and Chulkov, L. V. "Observation of the kinematic focusing of the products of the three-particle decay of $^9$Be$(5/2^-)$". An attemt to extract additional quantum numbers for $^9$Be$(5/2^-)$ state.
*JETP Lett. 49* (1989), 622.

[98] Vostrikov, A. N., and Zhukov, M. V. "Theoretical study of the photodisintegration of $^3$H". Two-body and three-body continuum are treated simultaneously.
*Sov. J. Nucl. Phys. 34* (1981), 344.

[99] Warshalovich, D. A., Moskalev, A. N., and Hersonskiy, V. K. *Quantum theory of angular momentum.* Nauka, Moskow, 1975.

[100] Wilkinson, D. H. "Parity conservation in strong interaction: introduction and the reaction He$^4$(d,$\alpha$)Li$^6$". Parity violation in $^6$Li $0^+$. Experiment.
*Phys. Rev. 109* (1958), 1603.

[101] Wurzer, J., and Hofman, H. M. "Structure of the helium isotopes $^4$He–$^8$He". RGM calculations.
*Phys. Rev. C 55* (1996), 688.

[102] Xu, H. M., et al. "Overall normalization of the astrophysical S-factor and the nuclear vertex constant for $^7$Be(p,$\gamma$)$^8$B reactions". Estimates of Asymptotic Normalization Coefficient for $^8$B in shell-model calculations.
*Phys. Rev. Lett. 73* (1994), 2027.

[103] Zakhar'ev, B. N., Pustovalov, V. V., and Efros, V. D. "The three-body problem. The $K$-harmonic method in problems involving the continuum spectrum.". General formalism. d+n at zero energy.
*Sov. J. Nucl. Phys. 8* (1968), 234.

[104] Zhigunov, V. P., and Zakhar'ev, B. N. *Strong channel coupling methods in the quantum scattering theory.* Atomizdat, Moscow, 1974.

[105] Zhukov, M. V., and Efros, V. D. "Reactions in the systems of several nucleons". Interpolation approach.
*Sov. J. Nucl. Phys. 14* (1971), 577.

[106] Zhukov, M. V., et al. "Bound state properties of the borromean halo nuclei: $^{6}$He and $^{11}$Li.". Three-body calculations of $^{6}$He and $^{11}$Li. Review.
*Phys. Rep. 231* (1993), 153.

[107] Zhukov, M. V., and Jonson, B. "Particle momentum distributions in an analytical three-body approach".
*Nucl. Phys. A 589* (1995), 1.

[108] Zhukov, M. V., and Thompson, I. J. "Existence of proton halos near the drip line". Calculations of $^{17}$Ne as $^{15}$O+2p.
*Phys. Rev. C 52* (1995), 3505.